AD-A091 480   NAVAL ACADEMY ANNAPOLIS MD   F/G 13/13
               WAVE FORCE AND STRUCTURE RESPONSE: A COMPARISON OF THEORETICAL --ETC(U)
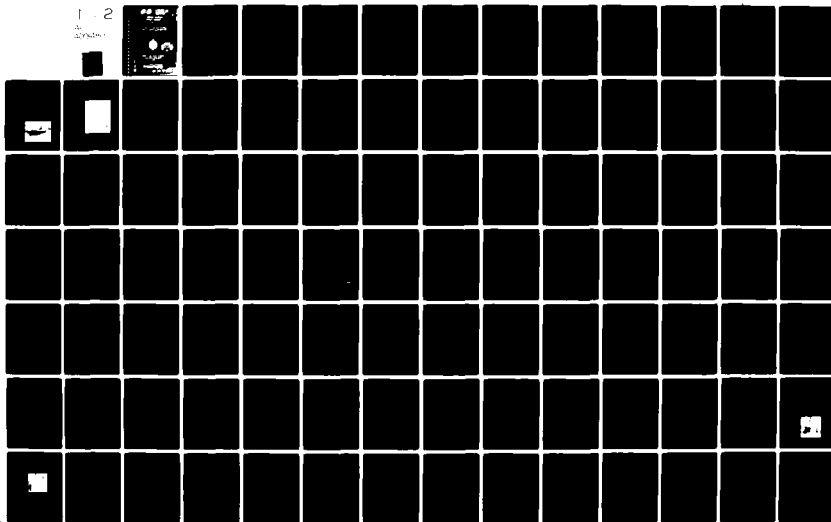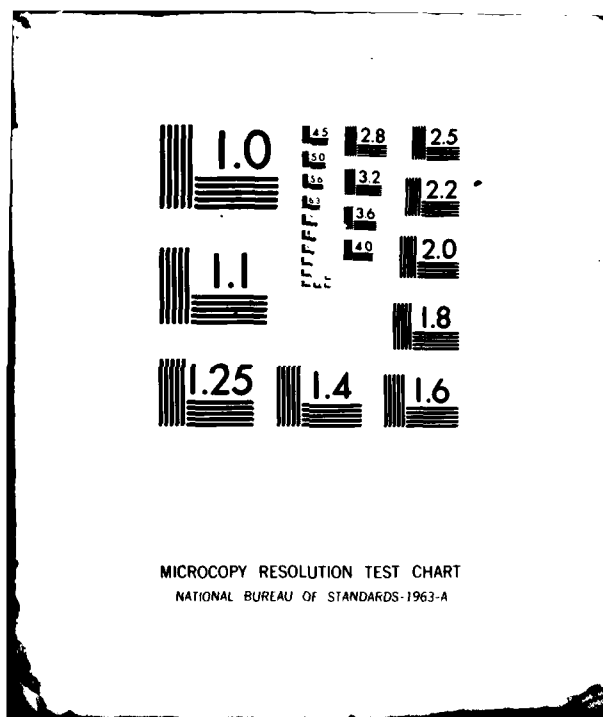   JUN 80   M H ROLFES
UNCLASSIFIED   USNA-TSPR-108   NL

MICROCOPY RESOLUTION TEST CHART
NATIONAL BUREAU OF STANDARDS-1963-A

(14) USNA-TSPR-1081

REPORT DOCUMENTATION PAGE	READ INSTRUCTIONS BEFORE COMPLETING FORM
1. REPORT NUMBER U.S.N.A. - TSPR; no. 108 (1980)	2. GOVT ACCESSION NO. AD-A091480	3. RECIPIENT'S CATALOG NUMBER
4. TITLE (and Subtitle) WAVE FORCE AND STRUCTURE RESPONSE; a Comparison of Theoretical and Experimental results Using Regular and Irregular Waves.	5. TYPE OF REPORT & PERIOD COVERED Final, 1979-1980
	6. PERFORMING ORG. REPORT NUMBER
7. AUTHOR(s) Marc Henry Rolfes	8. CONTRACT OR GRANT NUMBER(s)
9. PERFORMING ORGANIZATION NAME AND ADDRESS United States Naval Academy, Annapolis.	10. PROGRAM ELEMENT, PROJECT, TASK AREA & WORK UNIT NUMBERS
11. CONTROLLING OFFICE NAME AND ADDRESS United States Naval Academy, Annapolis.	12. REPORT DATE 5 June 1980
	13. NUMBER OF PAGES 107
14. MONITORING AGENCY NAME & ADDRESS(if different from Controlling Office)	15. SECURITY CLASS. (of this report) UNCLASSIFIED
	15a. DECLASSIFICATION/DOWNGRADING SCHEDULE

16. DISTRIBUTION STATEMENT (of this Report)

This document has been approved for public release;
its distribution is UNLIMITED.

17. DISTRIBUTION STATEMENT (of the abstract entered in Block 20, if different from Report)

This document has been approved for public release;
its distribution is UNLIMITED.

18. SUPPLEMENTARY NOTES

Accepted by the U. S. Trident Scholar Committee.

19. KEY WORDS (Continue on reverse side if necessary and identify by block number)

Wave force
Structure response
Ocean waves
Offshore structures

20. ABSTRACT (Continue on reverse side if necessary and identify by block number)

An 18 foot tall jacket type structure was tested for three dimentional forces and deck deflections using regular and irregular waves of up to 2.5 feet in height. Theoretical studies for both regular and irregular wave forces are presented in conjunction with experimental results. In addition, a similar comparison for deck deflection and frequency response is presented in this report. Results indicate base shear, lift force, and overturning moment calculations using the range of hydrodynamic coefficients recommended by the

OVER !

DD FORM 1473 1 JAN 73   EDITION OF 1 NOV 65 IS OBSOLETE
S/N 0102-014-6601 |

245600

20.

CONTINUED

American Petroleum Institute are in general agreement with experimentally determined values for wave frequencies between 0.3 and 0.8 Hz. Deck deflection measurements were significantly greater than those calculated using standard structural matrix techniques. The difference is concluded to be the result of inadequate analytical description of the test structure joints using a rigid joint analysis.

0 - 0

WAVE FORCE AND STRUCTURE RESPONSE:

a comparison of theoretical and
experimental results using regular
and irregular waves

A Trident Scholar Project Report

by

Midshipman Marc H. Rolfes, 1/C
U. S. Naval Academy
Annapolis, Maryland

Thomas H. Dawson

Associate Professor Thomas H. Dawson,
Naval Systems Engineering Department

Accepted for Trident Scholar Committee

Chairman

5 June 1980

Date

ABSTRACT

An 18 foot tall jacket type structure was tested for three dimen-
sional forces and deck deflections using regular and irregular waves
of up to 2.5 feet in height. Theoretical studies for both regular
and irregular wave forces are presented in conjunction with experi-
mental results. In addition, a similar comparison for deck deflec-
tion and frequency response is presented in this report.

Results indicate base shear, lift force, and overturning moment
calculations using the range of hydrodynamic coefficients recommended
by the American Petroleum Institute are in general agreement with
experimentally determined values for wave frequencies between 0.3
and 0.8 Hz. Deck deflection measurements were significantly greater
than those calculated using standard structural matrix techniques.
The difference is concluded to be the result of inadequate analytical
description of the test structure joints using a rigid joint analysis.

TABLE OF CONTENTS

NOMENCLATURE

A	wave amplitude
C	wave celerity
C_D	drag coefficient
C_M	inertia coefficient
D	member diameter
E	modulus of elasticity
F	total force
F_o	magnitude of forcing function
H	wave height
H_s	significant wave height
I	moment of inertia
K	member stiffness
K'	effective spring constant
L	wave length
M	total moment
M'	effective mass
S_F	force spectral density
S_M	moment spectral density
S_η	wave spectral density
T	wave period
T_F	force transfer function
T_M	moment transfer function
U	deck deflection
a_{nx}	water particle acceleration in the x direction normal to member
a_{ny}	water particle acceleration in the y direction normal to member
a_{nz}	water particle acceleration in the z direction normal to member
a_x	water particle acceleration in x direction
a_z	water particle acceleration in z direction
c_x	x angle relationship of member orientation
c_y	y angle relationship of member orientation
c_z	z angle relationship of member orientation
f	force per unit length

f_m frequency of peak energy

f_x force per unit length in the x direction

f_y force per unit length in the y direction

f_z force per unit length in the z direction

g   gravitational constant

h   water depth

k   wave number

ℓ member length

u   horizontal water particle velocity

u_{rms} *root mean square of horizontal water particle velocity*

w   vertical water particle velocity

u_n horizontal water particle velocity normal to member

w_n vertical water particle velocity normal to member

x   member phasing distance

z   depth below the still-water level

α tower orientation measured clockwise from tank axis

ϵ phase angle

ζ damping ratio

η water level displacement from still-water level

θ angle from +x axis to member axis

ν resultant water particle velocity

ρ density of water

ϕ angle from +z axis to member axis

ω *angular frequency*

SIGN CONVENTION
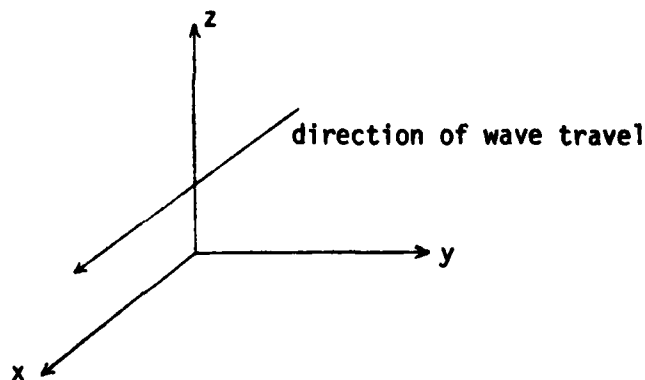
INTRODUCTION

For over 30 years the offshore oil industry has been employing fixed offshore structures for use in the recovery of natural gas and oil reserves. In addition, military and defense requirements have also required use of fixed offshore structures for many years. For example, the offshore 'Texas Towers' of the early 1950s formed part of the early warning system used by the United States and the Navy's air combat maneuvering range off the coast of North Carolina utilizes fixed offshore structures for instrumentation and flight monitoring purposes.

Because of the importance and increasingly wide use of these structures, major advances in their analysis and design have occured over the past 10 or 15 years. At present, the Cognac Platform off the coast of Louisiana in the Gulf of Mexico holds the record as the tallest offshore platform. This 1,265 foot platform, which is located in 1,025 feet of water, is taller than the Empire State Building. When under full production in 1983, Cognac is expected to deliver a daily peak production of 50,000 barrels of oil and 150,000,000 cubic feet of natural gas.

Wind, wave, and current loadings must be considered in the analysis and design of fixed offshore structures. Of these applied loads, wave loading is by far the most important and least understood. The most common approach in determining wave loading is to assume a regular

design wave of height and period representative of extreme storm conditions. Calculations are then based upon this wave for structure analysis and design. A second approach is to represent storm conditions using a simplified random wave model and determine the wave forces and structure response in a statistical sense.

While both of these methods are presently employed in offshore work, the foundations on which the analyses rest are still subject to some questions. For example, both methods employ a simplified wave force formulation known as the Morison equation which assumes simply that forces due to water velocity and acceleration are additive at any instant in time. Other questions such as its applicability to various structural member orientations as well as the proper choice of hydrodynamic coefficients indicate the uncertainties still associated with offshore structure design.

As a result, extensive theoretical analysis of offshore structures has occured over the past few years, yet the associated empirical data has been limited. Work has been done on wave forces on individual members as well as limited work on small scale structures in the 5 to 6 foot height range, but facilities are generally unavailable for subjecting larger models to both regular and irregular waves of the proper magnitude and period representative of storm conditions. Limited results have also been reported on field measurements of actual offshore platforms. Although these tests are realistic for the given sea state, they lack the control of waves offered by wave generation in the laboratory.

The present study was undertaken to investigate current techniques for determination of wave force and structure response under controlled laboratory conditions. The study is divided into 3 areas:

- wave forces using regular waves;

- wave forces using irregular waves;

- structural analysis using both deck deflections and

frequency response.

Experimental Objective

Experimentally, the objective of this study was to measure the base shear, lift force, overturning moment, and deck deflection on an off-shore platform test structure using both regular and irregular waves. These values are representative of those required for actual structure design and analysis and were used for comparison with associated theoretical results.

Testing was accomplished using the U.S. Naval Academy Towing Tank, which measures 380 feet in length, 26 feet in width, and has a nominal water depth of 16 feet. The wave generation system is capable of generating regular waves ranging from 0.1 Hz to 1.2 Hz and wave heights of up to 3 feet. The system is also capable of generating periodic random wave spectra of user-defined specifications. All measurements were made on a real time basis, converted to digital format, and placed on magnetic tape.

Test Structure

The model was designed and built using thin-walled 6061-T6 aluminum tubing and is shown in Figures 1 and 2. The main support piles consisted of 2.0 inch diameter tubing of 0.049 inch wall thickness and all cross bracing was of 1.0 inch tubing of 0.035 inch wall thickness. The design of the test structure was governed by 3 restrictions:

- the design was to contain representative member bracing of actual offshore platforms while remaining simple enough to be analyzed within the scope of this project;

- member bracing was to leave the structure flexible enough for desired frequency response and deck deflection measurements under the given wave loadings;

- the fundamental frequency of the structure was to be altered by use of added deck weight to bring the structure response into the range for dynamic amplification.

The structure was fixed to a base assembly which allowed 360 degrees rotation of the model.

The instrumentation utilized included 12 4-inch variable-reluctance modular force gauges for three dimensional force determination, 4 high frequency sonic transducers for deck displacement measurements, and 2 resistance-type wave probes for wave measurements. A 60-second computer data acquisition using a sampling rate of 51.2 Hz was done on the Hydromechanics Laboratory Digital PDP/11 computer system for each test run. On each run 17 data channels were acquired, and a representative 10-second sample for regular waves and 20-second sample for irregular waves was truncated from all data files for placement on magnetic tape. Additional test structure specifications and instrumentation information is given in Appendix A and sample experimental data is given in Appendix B.
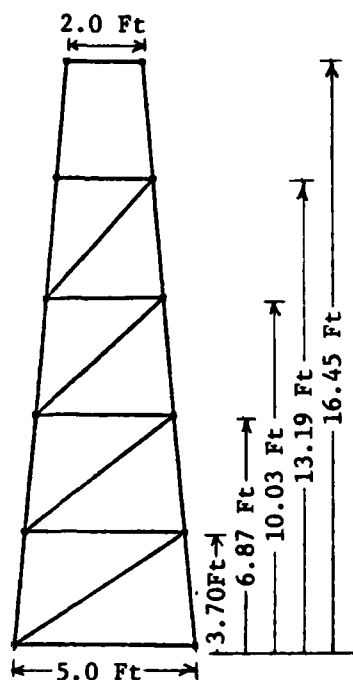
Principle Dimensions

FIGURE 1   Above Water View

FIGURE 2   Under Water Set-Up

SECTION I: REGULAR WAVE STUDY

Numerous regular wave theories have been proposed ranging from a simple linear theory developed by Airy in 1845 to more complex non-linear theories such as Stokes' 5th Order or Dean's Stream Function which have been developed over the past 20 years. Due to the dynamic characteristics of wave properties as a function of water depth, each of these theories approximates the solution in series form and hence has a region where it gives best results. Thus, it is important to determine the type of waves expected to act on an offshore structure so the proper wave theory may be chosen.

Figure 3 shows a regular wave moving at a celerity C in water of depth h. The wave height H and length L are as shown and the ratio of
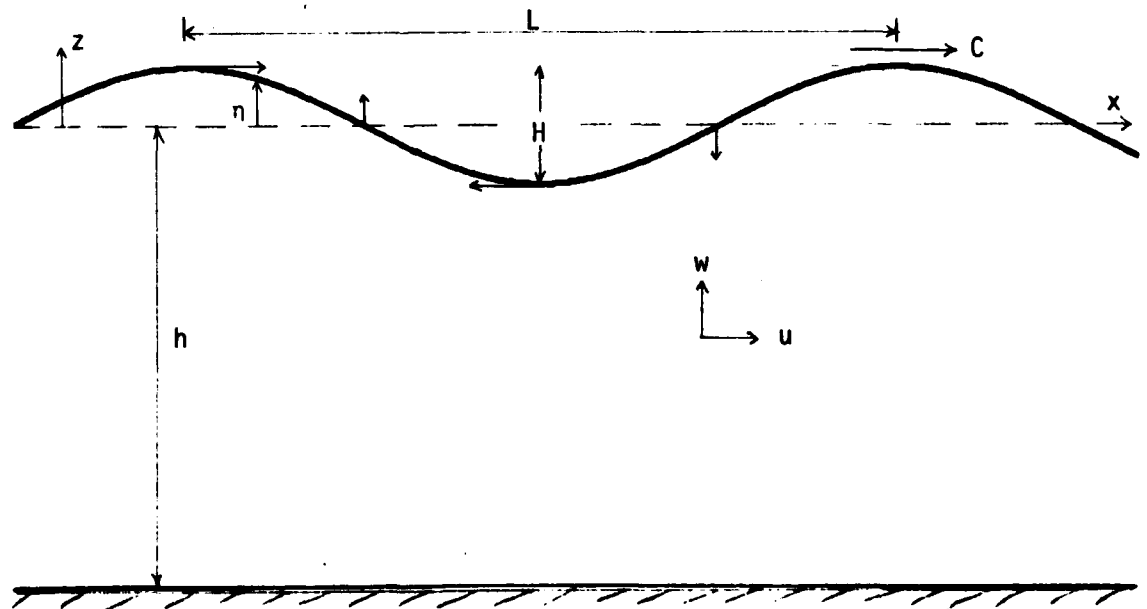
FIGURE 3 Definition Sketch for Regular Waves

H/L is defined as the wave slope. The wave period T is related to the
wave length and celerity by C=L/T. The water particle velocity compo-
nents at any instant are u and w and the water surface displacement
from the still-water level (SWL) at any point is η.

The arrows at the wave crest, trough, and still-water lines indi-
cate the directions of water particle motion at the surface. These
motions cause a water particle to move in a clockwise orbit as the
wave travels from left to right. The water particle velocities and
orbit sizes decrease with increasing depth as shown in Figure 4c. The
depth at which the velocity is negligible is L/2. A deep water wave
is defined when $h/L \geq 1/2$, transitional wave when $1/2 < h/L < 1/20$ and a
shallow water wave when $0 < h/L \leq 1/20$. As a deep water wave travels toward
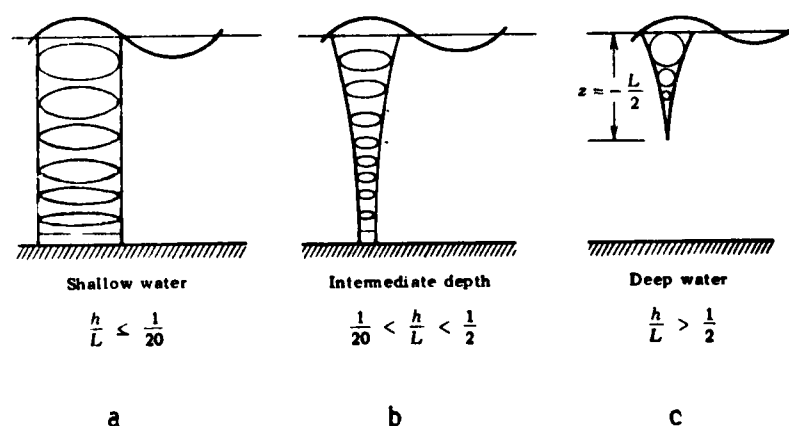shore, its properties are altered as are its particle orbits as shown
in Figures 4a and 4b.

Shallow water	Intermediate depth	Deep water
$\frac{h}{L} \leq \frac{1}{20}$	$\frac{1}{20} < \frac{h}{L} < \frac{1}{2}$	$\frac{h}{L} > \frac{1}{2}$
a	b	c

FIGURE 4 Variation of water particle orbits with depth

Linear Theory

Linear wave theory was developed by G. B. Airy and is significant because of its ease of application as well as its large range of applicability. Linear theory assumes a sinusoidal wave form whose amplitude is small in comparison with its wave length and the water depth. Referring to Figure 3, the free surface displacement from the still-water level is described by:

$$\eta = H/2 \, \cos(kx - \omega t) \tag{1}$$

and the horizontal and vertical velocity components (u,w) of the water motion at position (x,z) and time t are expressible as:

$$u = \frac{\pi H}{T} \, \frac{\cosh k(h+z)}{\sinh kh} \, \cos(kx - \omega t) \tag{2}$$

$$w = \frac{\pi H}{T} \, \frac{\sinh k(h+z)}{\sinh kh} \, \sin(kx - \omega t) \tag{3}$$

The associated acceleration components are given by differentiation with respect to time of equations (2) and (3). The wave number k and period T are given in terms of the wave angular frequency ω, and the wave length L by:

$$T = \frac{2\pi}{\omega} \; , \quad k = \frac{2\pi}{L} \tag{4}$$

The wave length L is expressible in terms of the wave period and water depth as:

$$L = \frac{gT^2}{2\pi} \, \tanh \frac{2\pi h}{L} \tag{5}$$

In deep water, however, $\tanh \frac{2\pi h}{L}$ approaches unity and the wave length can then be expressed as:

$$L_o = \frac{gT^2}{2\pi} \tag{6}$$

Although linear theory assumes a simple sinusoidal wave form of small amplitude, the agreement between theory and measured values in deep water is very good. Wiegel (1964) showed that linear theory predicts the velocities within the range of experimental error for values of h/L as low as 0.10 for waves of appreciable steepness. For a more complete description of linear theory, see McCormick (1973) or Ippen (1966).

Stokes' 2nd Order Theory

As the steepness of the wave increases, nonlinearities become significant in the surface displacement and in the velocity and acceleration profiles. To account for these nonlinearities, Stokes (1880) developed a wave theory in series form and calculated second and third order corrections to the Airy theory. In deep water the limited corrections employed by Stokes are generally applicable but De (1955) showed that Stokes' theory should not be used for depth to wave length ratios less than about 0.125. A more complete discussion of Stokes' 2nd order theory is presented by Wiegel (1964) and a brief summary of the applicable equations for the 2nd order theory is given below.

In expanding to 2nd order, the relation between wave length and period is the same as for the linear theory, namely equation (5). The expression for the free surface is:

$$\eta = \frac{H}{2} \cos (kx - \omega t) + \frac{\pi H^2}{8L} \frac{\cosh kh(2 + \cosh 2kh)}{\sinh^3 kh} \cos 2(kx - \omega t) \qquad (7)$$

which indicates that the mean level of the wave surface lies above the still-water level (i.e., the wave peaks more than it troughs). This

is consistent with experimental data which indicate the crests are steeper and the troughs are flatter than those predicted by linear theory.

The components of water particle velocities at any point (x,z) and time t in the water are given by:

$$u = \frac{\pi H}{T} \frac{\cosh k(h+z)}{\sinh kh} \cos (kx-\omega t) + \frac{3}{4} \left(\frac{\pi H}{T}\right)\left(\frac{\pi H}{L}\right) \frac{\cosh 2k(h+z)}{\sinh^4 kh} \cos 2(kx-\omega t) \quad (8)$$

$$w = \frac{\pi H}{T} \frac{\sinh k(h+z)}{\sinh kh} \sin (kx-\omega t) + \frac{3}{4} \left(\frac{\pi H}{T}\right)\left(\frac{\pi H}{L}\right) \frac{\sinh 2k(h+z)}{\sinh^4 kh} \sin 2(kx-\omega t) \quad (9)$$

and differentiation with respect to time yields the water particle accelerations at any point (x,z).

Experimental Waves

The regular waves chosen for this project were of constant 1/20 slope and were of frequencies from 0.3 Hz to 1.0 Hz in 0.1 Hz increments. This corresponds to a range of deep water wave lengths from 5.1 feet to 56.9 feet. Sorensen (1978) shows that no appreciable error will be incurred if deep water is assumed for h/L ratios as low as 0.3. Hence, with the lowest h/L ratio being 0.28, deep water was assumed for all theoretical analyses. The choice of the wave slope of 1/20 was made in an attempt to model storm waves. Although storm waves may reach slope values as high as 1/10 in the Gulf of Mexico, the practical limit of the wave generation system, keeping wave distortion negligible, was a slope of 1/20.

As shown in Figure 5, Stokes' 2nd order theory is appropriate for
constant 1/20 slope waves with periods ranging from 1 to 3.33 seconds
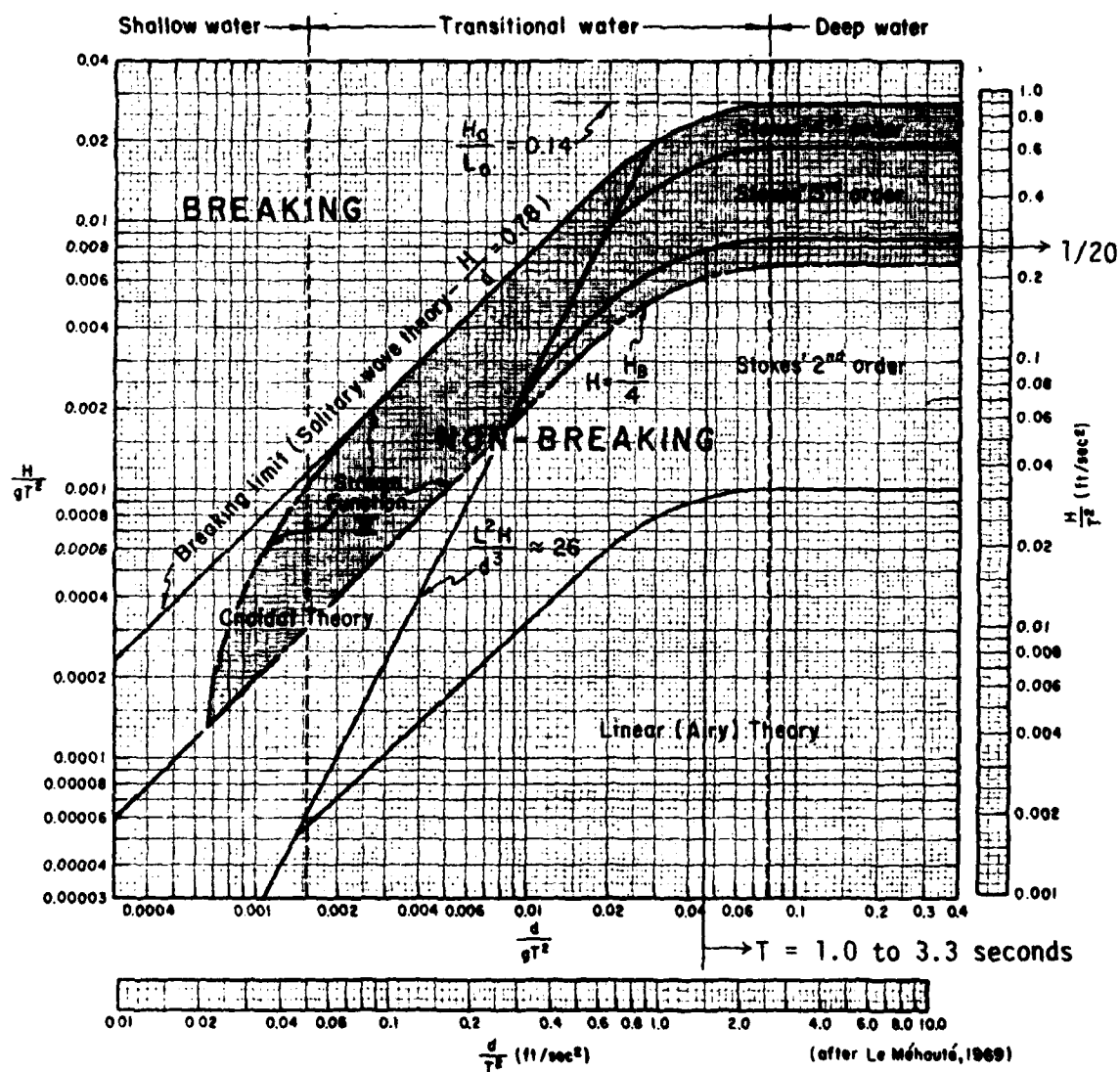

FIGURE 5   Regions of Validity for Various Wave Theories
(from Shore Protection Manual, U.S. Army Corps
of Engineers)

and was therefore chosen for this study. Linear theory was used in preliminary work and gave almost identical results.

Wave Forces on Fixed Bodies

The force that a wave imparts on a fixed vertical pile was studied by Morison, et al. (1950) who proposed a semi-empirical formula for estimating the force per unit length f in the direction of the waves. This has become known as the Morison equation:

$$f = \frac{1}{2} \rho C_D D |u| u + \rho C_M \frac{\pi D^2}{4} \frac{\partial u}{\partial t} \tag{10}$$

where:

ρ = Density of the fluid
C_D = Drag coefficient
D = Diameter of the pile
u = Water particle velocity
C_M = Inertia coefficient
$\frac{\partial u}{\partial t}$ = Water particle acceleration

This equation applies for wave forces on cylindrical surface piercing piles whose diameters are small in comparison with the wave length.

The first term in the Morison equation is a nonlinear drag term as it is proportional to the square of the water particle velocity. The second term, being proportional to the water particle acceleration, is an inertia term which is 90 degrees out of phase with the drag term. The dominance of either of these terms is determined by the wave characteristics. If the wave height H is equal to or less than the pile diameter, then the drag force is negligible. As the wave height is increased, however, the drag force becomes increasingly important to a

point where the inertia term becomes negligible. For the waves used in this project, the drag force ranged from approximately 30 percent to 150 percent of the inertia force. This is within the range experienced by full-scale offshore structures during storm conditions and thus provides a good experimental basis for the study of wave forces.

The values for C_D and C_M to be used in the Morison equation have been studied by Keulegan and Carpenter (1958), Sarpkaya (1975), Chakrabarti (1975) and others. Because waves are of an oscillatory nature, the steady flow values of the hydrodynamic coefficients cannot be used. The American Petroleum Institute (1977), which summarizes current engineering practices for the offshore industry in the United States, recommends using a drag coefficient for circular cylinders in the range from 0.6 to 1.0 and an inertia coefficient in the range from 1.5 to 2.0.

The values for velocity and acceleration for the Morison equation are chosen from an appropriate wave theory as discussed in the previous section. Because these values decay with depth, the wave force distribution also decays with depth as shown in Figure 6, and the total wave force at any instant can be expressed by the integral equation:

$$F = \int_{z_1}^{z_2} f(z) \, dz \tag{11}$$

The total moment M about the seafloor (z=-h) exerted on that part of the pile may similarly be given by:

$$M = \int_{z_1}^{z_2} (z+h)f(z) \, dz \tag{12}$$

where z_1 and z_2 are the depths over which the integration is to be performed.

Wade and Dwyer (1975) reviewed 4 techniques presently used in the offshore industry for using Morison's equation to determine the wave force on an arbitrarily oriented cylinder. It was shown that these techniques could lead to as much as a 22 percent difference in computed base shear, lift force, and overturning moment. The least conservative of these methods was presented by Chakrabarti, et al., (1975) of Chicago Bridge and Iron Company. This form was adopted for use in the present work.

The above method involves resolving the water velocity and acceleration into components normal and tangential to the cylinder axis. The normal component of the wave force is then calculated using the Morison equation which can, in turn, be resolved into a three dimensional vector
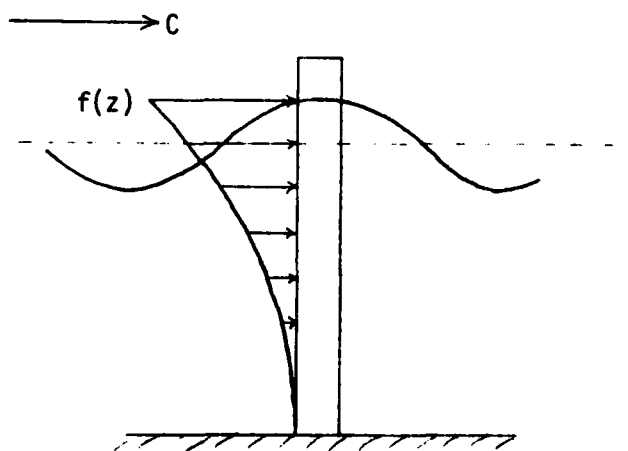
FIGURE 6 Wave Force Decay With Depth

for engineering application. The tangential force components are
ignored for engineering calculations because the coefficient of drag
due to skin friction was shown by Hoerner (1965) to be approximately
30 to 120 times smaller than the drag coefficient for transverse flow.

Because of the importance of these equations to the present study,
they are summarized below. Referring to Figure 7 and assuming a wave
propagating in the +x direction, the resulting water motion will have
horizontal and vertical velocities u and w and corresponding accelera-
tions of a_x and a_z. With polar coordinates θ and ϕ defining the
orientation of the cylinder axis, the magnitude of the water velocity
normal to the cylinder axis is given by:

$$v^2 = [u^2 + w^2 - (c_x u + c_z w)^2] \tag{13}$$
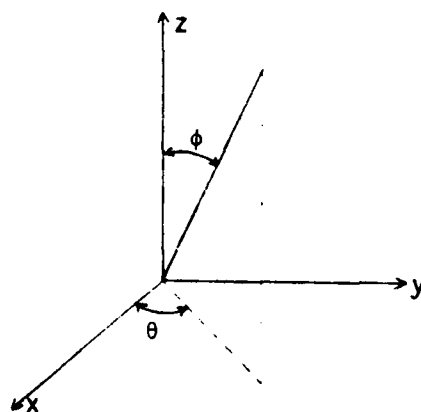
FIGURE 7   Member Axis Orientation

and its components in the x, y, and z directions are given, respectively, by:

$$u_n = u - c_x(c_x u + c_z w)$$

$$v_n = -c_y (c_x u + c_z w)$$

$$w_n = w - c_z(c_x u + c_z w)$$

(14)

where:

$$c_x = \sin\phi \cos\theta$$

$$c_y = \sin\phi \sin\theta$$

$$c_z = \cos\phi$$

(15)

The components of the normal water acceleration in the x, y, and z directions are denoted by a_{nx}, a_{ny}, and a_{nz} and similarly given by differentiations of the components of equation (14).

With these relations, the force per unit of cylinder length acting in the x, y, and z directions is given, respectively, by the generalized Morison equations:

$$f_x = \frac{1}{2}\rho\, C_D D\nu u_n + \rho C_M \frac{\pi D^2}{4} a_{nx}$$

$$f_y = \frac{1}{2}\rho\, C_D D\nu v_n + \rho C_M \frac{\pi D^2}{4} a_{ny}$$

$$f_z = \frac{1}{2}\rho\, C_D D\nu w_n + \rho C_M \frac{\pi D^2}{4} a_{nz}$$

(16)

For a small member such as a horizontal cross bracing on a structure, where the water motion does not vary appreciably over the member,

average values of u, w, a_x, and a_z may be used in the above equations and the total force on the member described simply by:

$$F_x = f_x\ell \qquad\qquad F_y = f_y\ell \qquad\qquad F_z = f_z\ell \qquad (17)$$

where ℓ denotes the length of the member. In the more general case where the water velocities and accelerations do vary appreciably over the length of the member, the total force must be calculated from the relations:

$$F_x = \int_s f_x ds \qquad F_y = \int_s f_y ds \qquad F_z = \int_s f_z ds \qquad (18)$$

where s denotes the distance along the member axis, and the limits on the integrals are chosen so as to include all of the pile on which the wave force acts. The total moments about the seafloor may also be calculated using Chakrabarti's formulation similarly adapted to equation (12).

Computerized Wave Force Determination

For deep water waves, such as those used in this study, where the velocity profile is changing rapidly with depth, it is important that the above equations be evaluated using a numerical integration technique. For the case where an offshore platform is in sufficiently shallow water so that the design wave may be considered a shallow water wave, the analysis may be simplified to the more approximate approach of equation (17) without incurring large errors. Using this approach on the test structure of the present study, however, yielded as much as 100 percent difference from the more exact numerical integration technique ultimately employed.

A computer based three dimensional mathematical model was developed using Chakrabarti's formulation for arbitrarily oriented members and Stokes' 2nd order wave theory. Computer tests were done to determine the maximum step size which could be used for a given wave to insure the numerical integration scheme remained within 2.0 percent of the exact integrated value. Input parameters included:

f = Wave frequency (Hz)
H = Wave height (ft)
α = Tower orientation (degrees)
C_M = Drag coefficient
C_D = Inertia coefficient
h = Still water level (ft)

The program considered phasing distances of incremental member length as a function of tower orientation. Similar consideration was given to moment-arm distances as well as incremental member orientation and depth. Extensive 'debugging' was done to validate this model which is the basis for all regular wave force data presented in this report. Step sizes ranged from 0.50 inches to 3.0 inches and computer run time required between 80 and 160 seconds per run. Each run calculated the wave force over 1 wave period.

The input parameters were based on the individual experimental runs. Wave heights were within ± 5.0 percent of those required for waves of 1/20 slope. One exception to this was the wave height for the 0.3 Hz waves which were generally 15 percent below the wave height required for 1/20 slope. The still-water level which changed 3.60 inches (1.9 percent) between the 2 phases of testing was determined to theoretically cause as much as a 6 percent error in computed base shear, lift force, and overturning moment. In the borderline case of deep water, this is

not surprising due to the sensitivity of the wave equations. Tank temperature variation was negligible, therefore the density of the water was assumed constant.

Individual experimental data points in this report represent the average of the peak values for each run. An experimental error analysis is given in Appendix C.

Results and Discussion

The results of the regular wave study are presented in Figures 8 through 19 and are from experimental runs using the previously mentioned waves for structure orientations of 0 degrees, 30 degrees, and 45 degrees. The results of a rotational study are also shown using 0.5 Hz waves of 0.99 feet average height.

A range of theoretical results was calculated using the above mentioned computer program based on a drag coefficient range of 0.6 to 1.0 and inertia coefficient range of 1.5 to 2.0. This theoretical band defines the range of the American Petroleum Institute (API) recommended standards and is indicated by the shaded region of each plot.

The results of the 0 degrees structure orientation study as shown in Figures 8, 9, and 10 indicate that experimental values of base shear force, lift force, and overturning moment fall within the theoretical limits defined by API recommended hydrodynamic coefficients for frequencies ranging between 0.3 Hz and 0.7 Hz. For the higher frequencies ranging from 0.7 Hz to 1.0 Hz, however, the experimental values consistently lie above the theoretical band. This may be due to member

phasing relationships as the wave lengths become increasingly shorter or
to the extreme variability of the drag and inertia coefficients at low
values of water particle velocity as reported by Sarpkaya (1976).
Reviewing the data points along an entire curve, it can be seen that
the position within the theoretical limits is not constant. When
reviewed on a run-by-run basis for the 3 figures, however, there exists
a consistency in the position of this point in relation to the theore-
tical limits. This may be considered the result of uniform experimental
error for the 3 measurements or more likely, the result of variation of
actual drag and inertia coefficients.

Essentially identical results are indicated by Figures 11 through 16
which present the results of regular wave studies for structure orienta-
tions of 30 and 45 degrees. Not only do the experimental values follow
the same general curve, but these points for a given frequency can be
found to lie in very similar positions within the theoretical limits.

This is shown more clearly by plotting the results for the rotation
study as shown in Figures 17, 18, and 19. The theoretical values were
calculated over the rotation range using a 0.5 Hz wave of 0.99 feet in
height. Actual corresponding wave heights ranged from 0.97 feet to
1.00 feet, and the experimental data points may be considered constant
within experimental error. The slight variation of theoretical values
from 0 to 45 degrees (1.8 percent for base shear force, 10 percent for
lift force, and 1.8 percent for overturning moment may be due to the
result of a slightly non-uniform velocity profile acting across the
entire structure for the given wave. If this is true, replacing the
0.5 Hz wave, which has a corresponding wave length of 20.5 feet with a

0.4 Hz wave, of wave length 32.0 feet, would be expected to yield more consistent theoretical values over the rotation range of the structure. Using an identical wave of 0.4 Hz and 1.64 feet in height and assuming a constant water depth, the variation in computed values over the rotation range was found to be 0.05 percent for base shear force, 0.07 percent for lift force, and 0.05 percent for overturning moment, thus substantiating this explanation.

The consistency of the theoretical results for the rotation study is strictly a consequence of Chakrabarti's formulation for computing wave forces. This would not necessarily be true for other methods such as those based on the presented area and volume of a structural member. Hence, the invariance of the experimental results with rotation tend to substantiate Chakrabarti's approach to wave force determination on arbitrarily oriented structural members.

Although Figures 17, 18, and 19 indicate that proper hydrodynamic coefficients should be chosen towards the lower limits of the recommended API values, similar plots at 0.3 Hz would indicate near mean values to be appropriate. Other plots at 0.8 Hz or 0.9 Hz would indicate that values at the upper limits or even above the recommended API values would be appropriate. Hence, although the API values for the hydrodynamic coefficients are generally adequate below 0.8 Hz for the test structure, actual drag and inertia coefficient values appear to have strict dependence upon some value associated with frequency of the water waves.
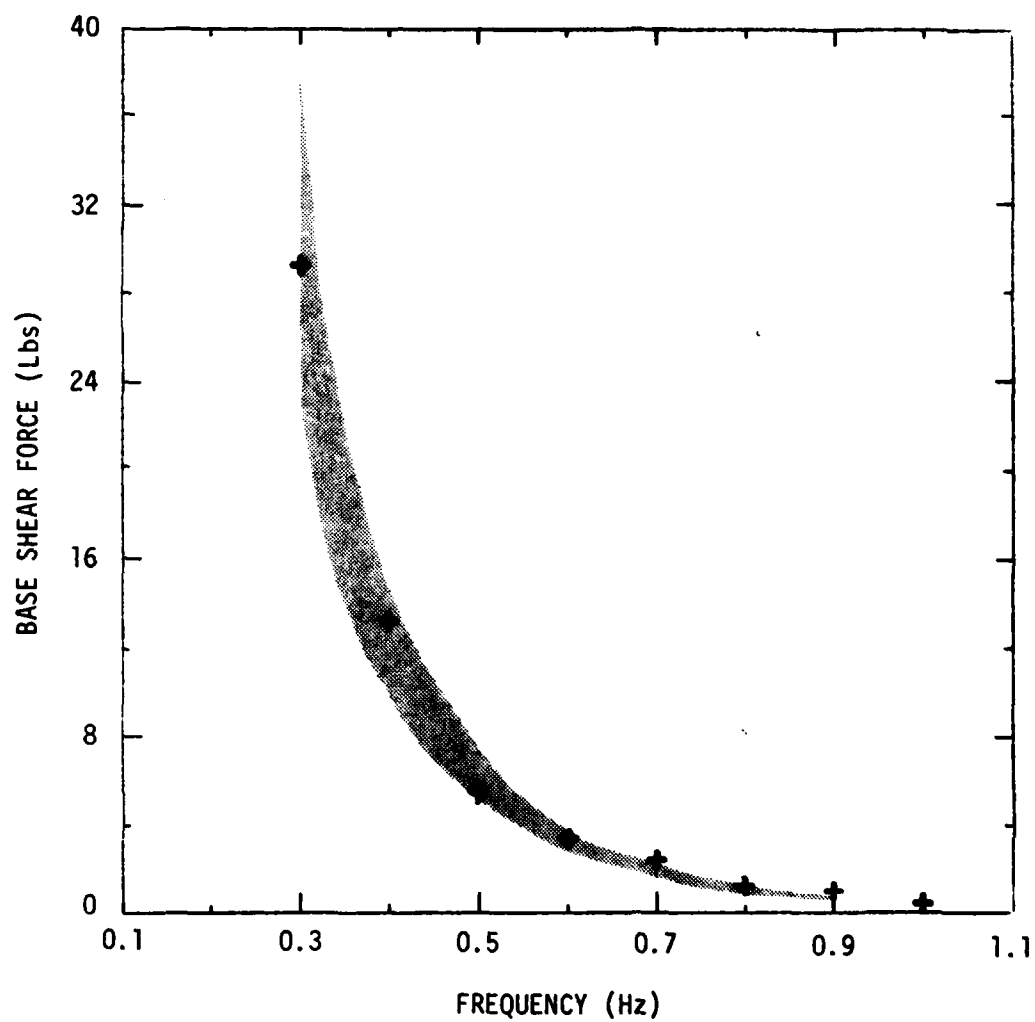
FIGURE 8   TOTAL BASE SHEAR FORCE
STRUCTURE ORIENTATION - ZERO DEGREES
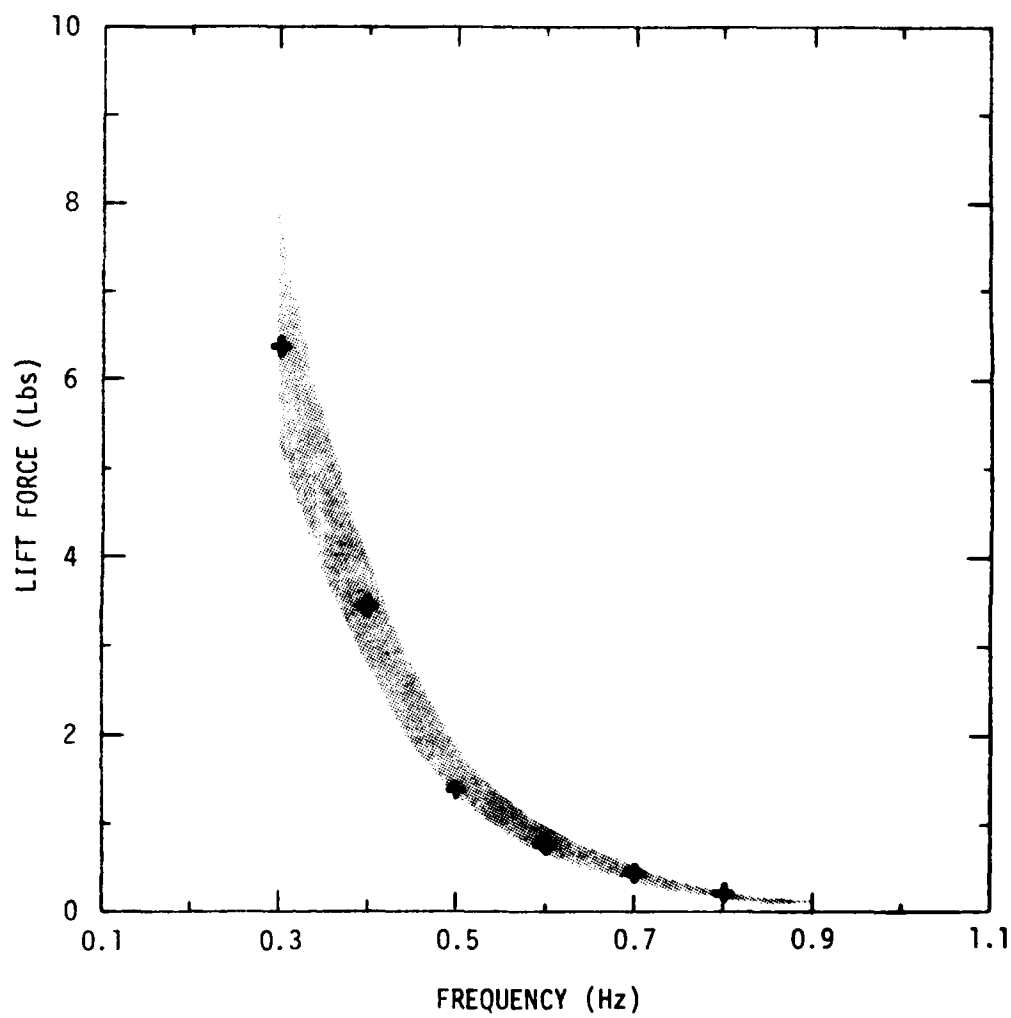
FIGURE 9   TOTAL LIFT FORCE
            STRUCTURE ORIENTATION - ZERO DEGREES
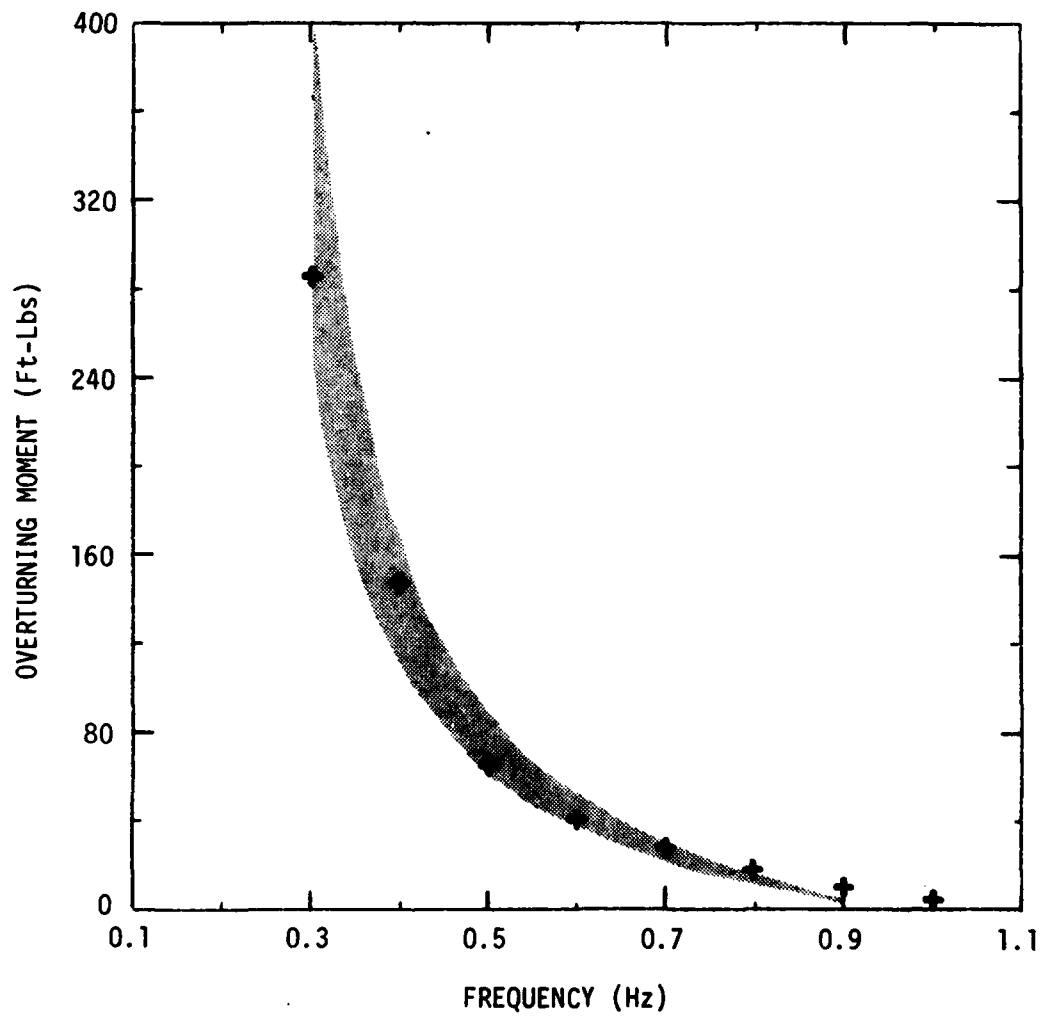
FIGURE 10   TOTAL OVERTURNING MOMENT
STRUCTURE ORIENTATION - ZERO DEGREES
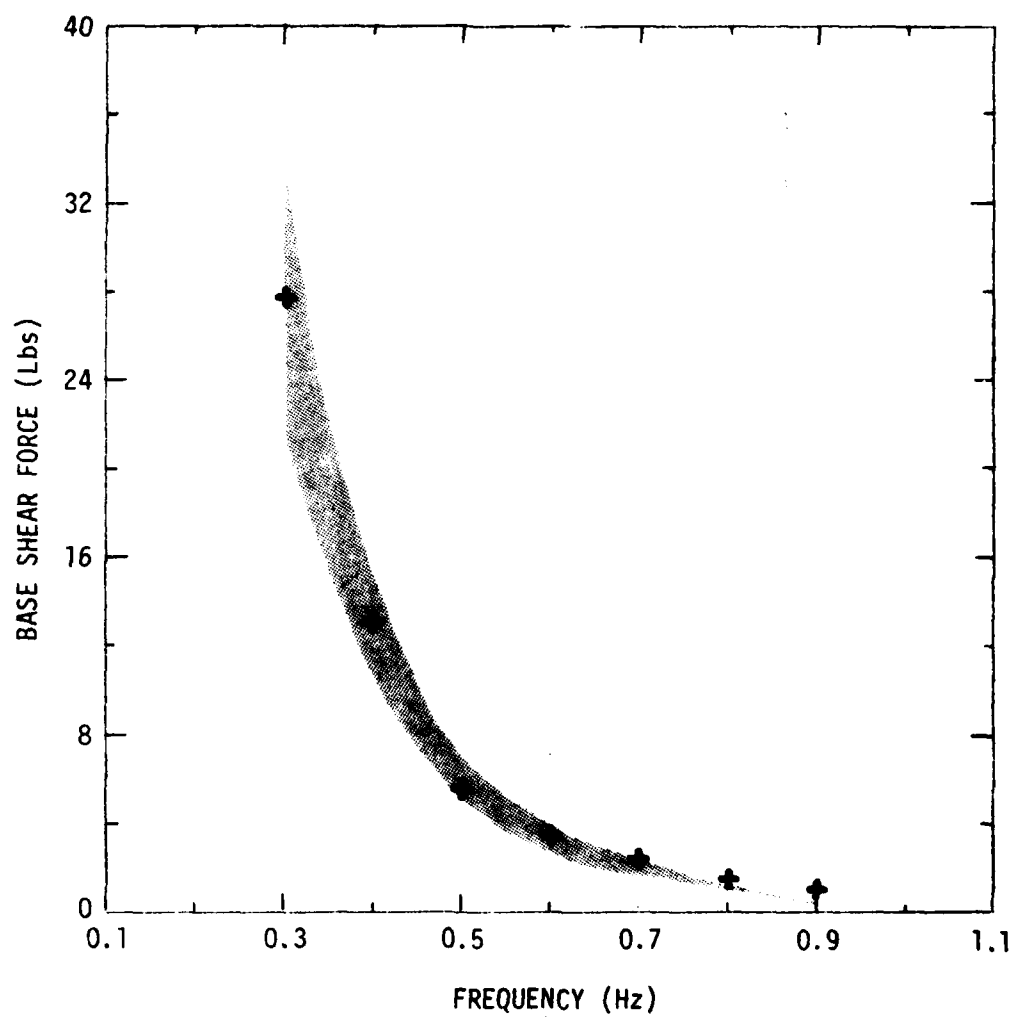
FIGURE 11   TOTAL BASE SHEAR FORCE
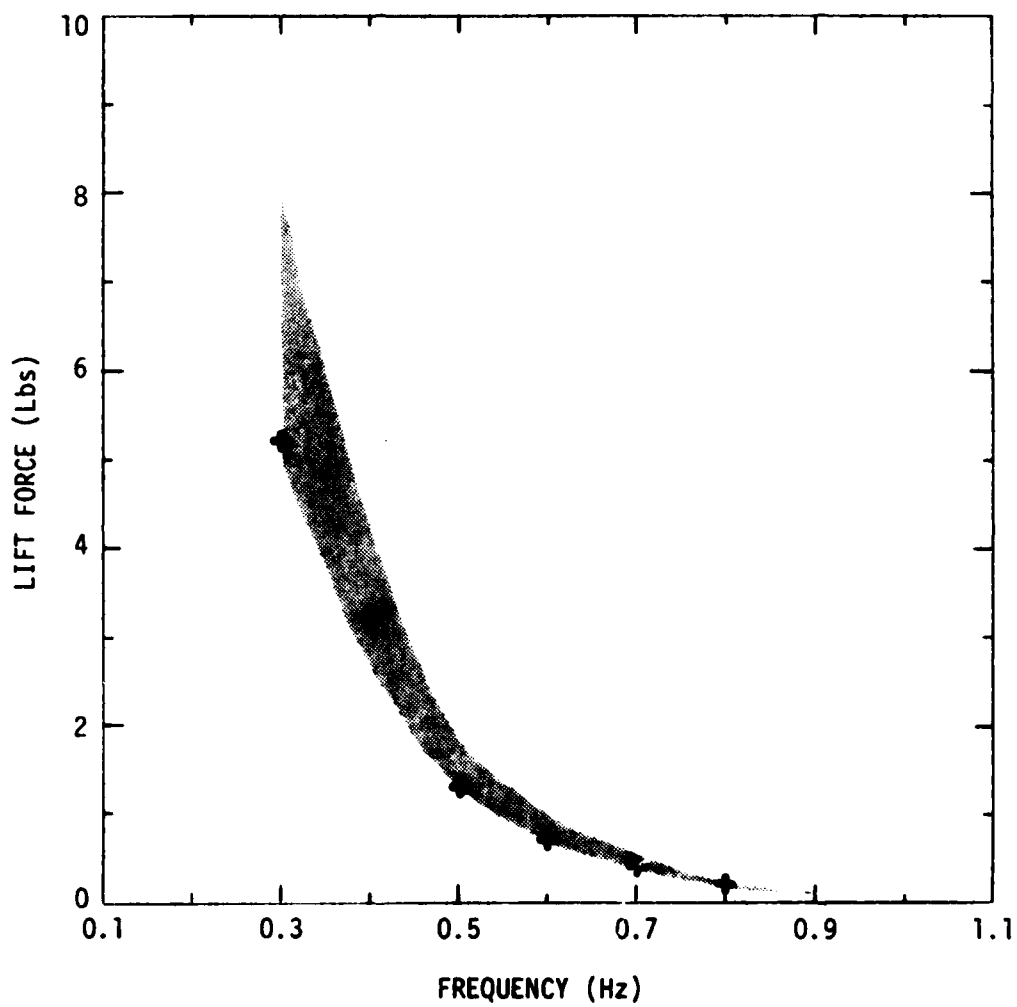   STRUCTURE ORIENTATION - THIRTY DEGREES

FIGURE 12   TOTAL LIFT FORCE
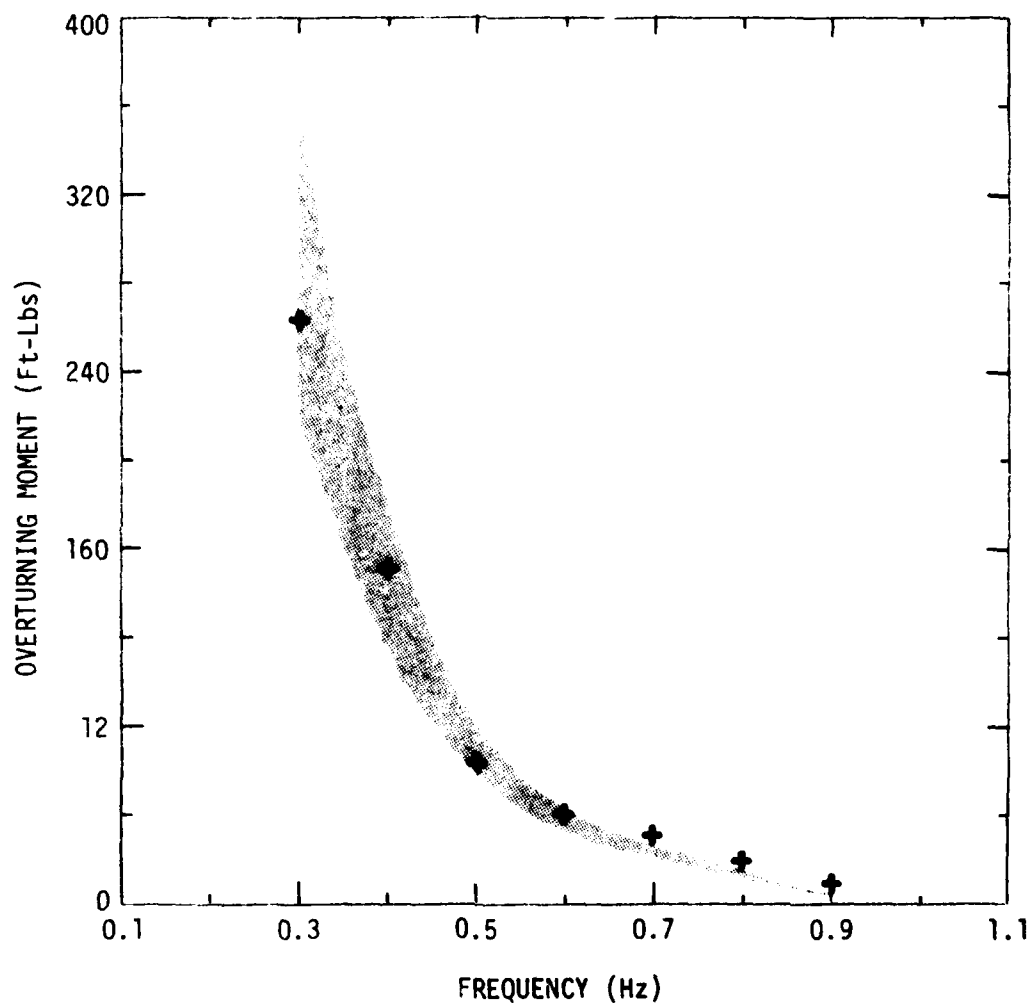STRUCTURE ORIENTATION - THIRTY DEGREES

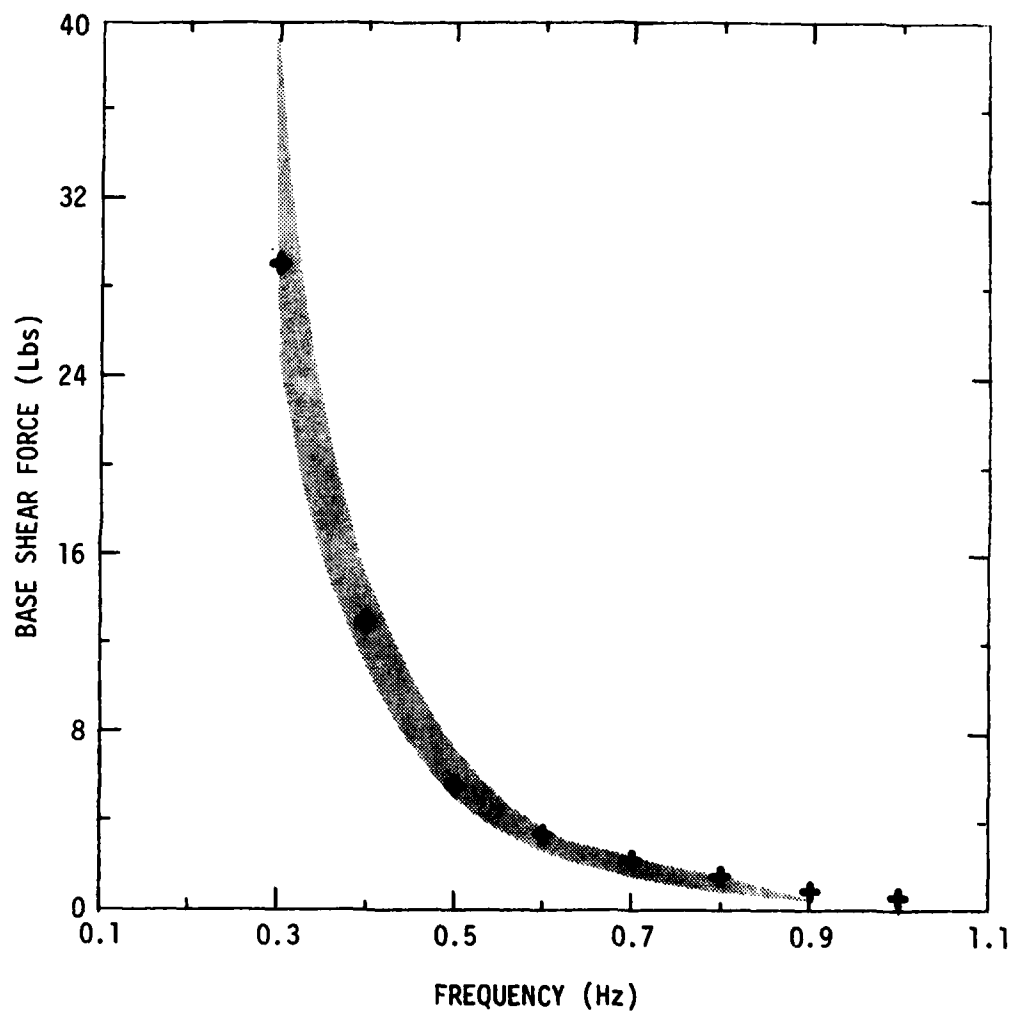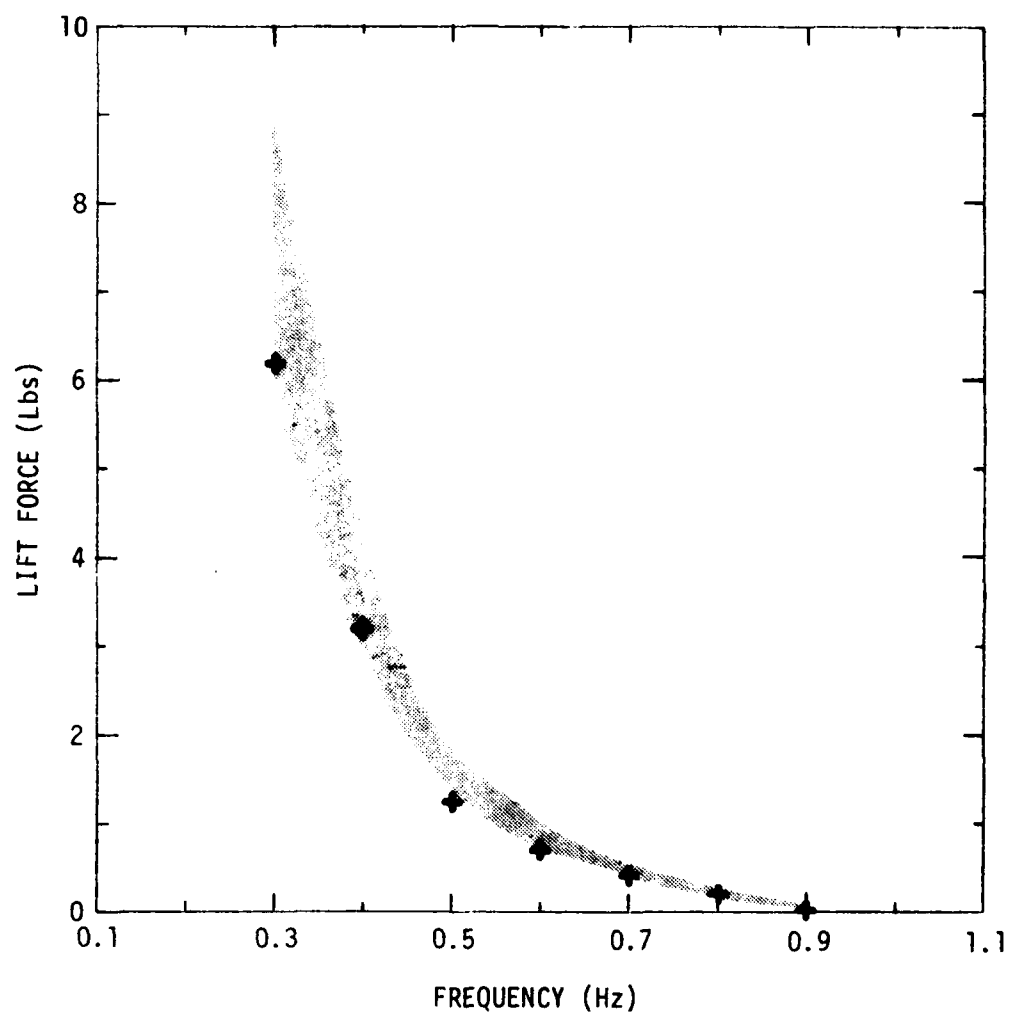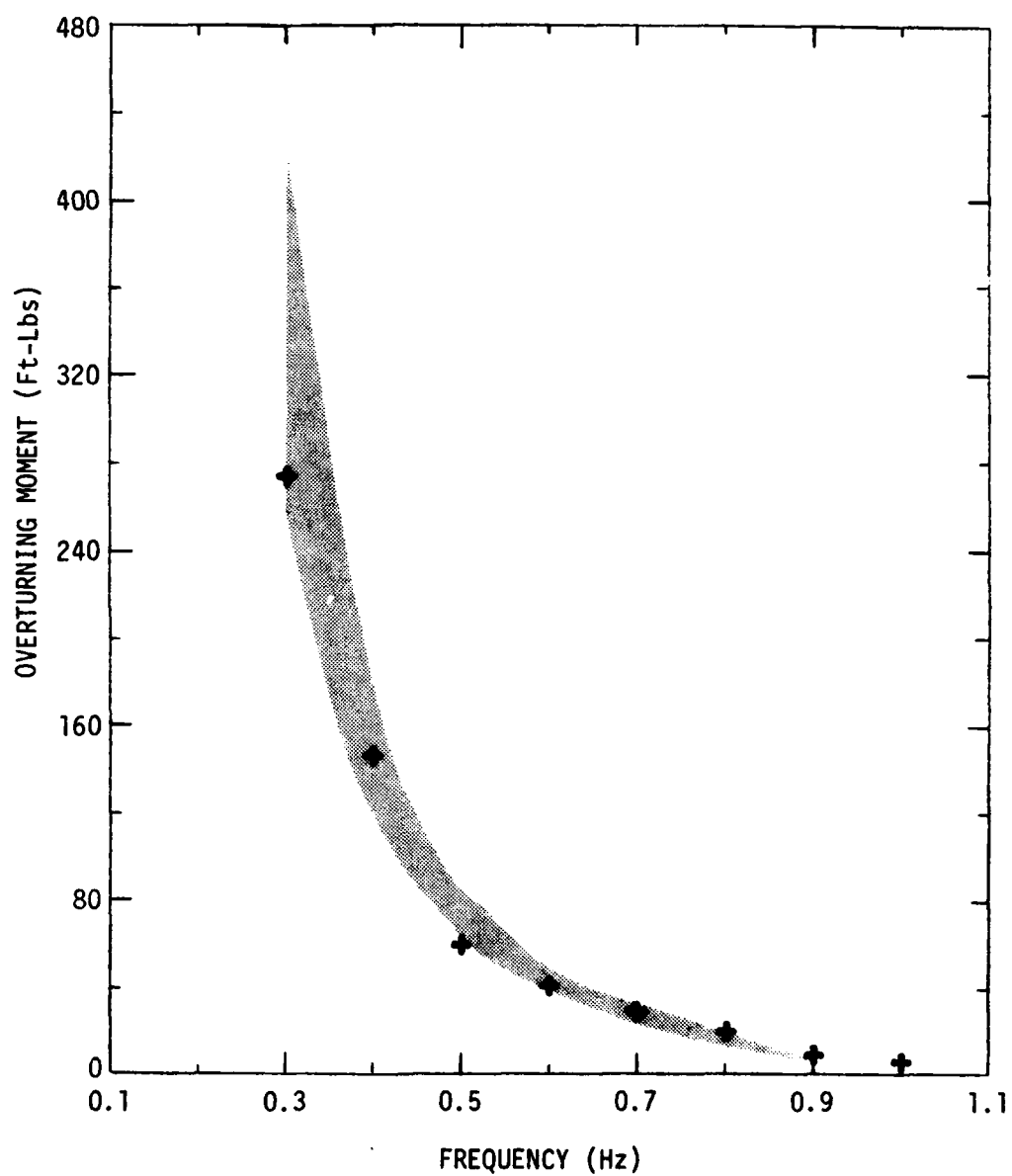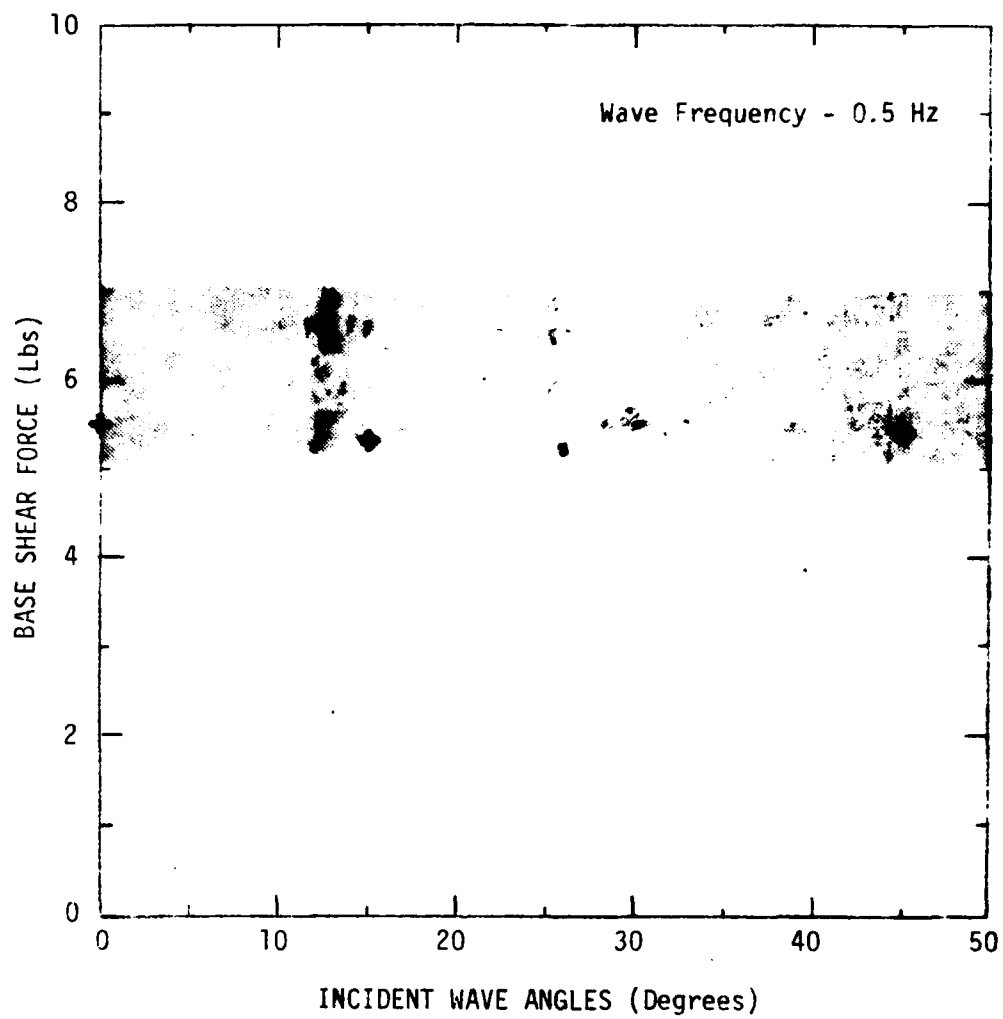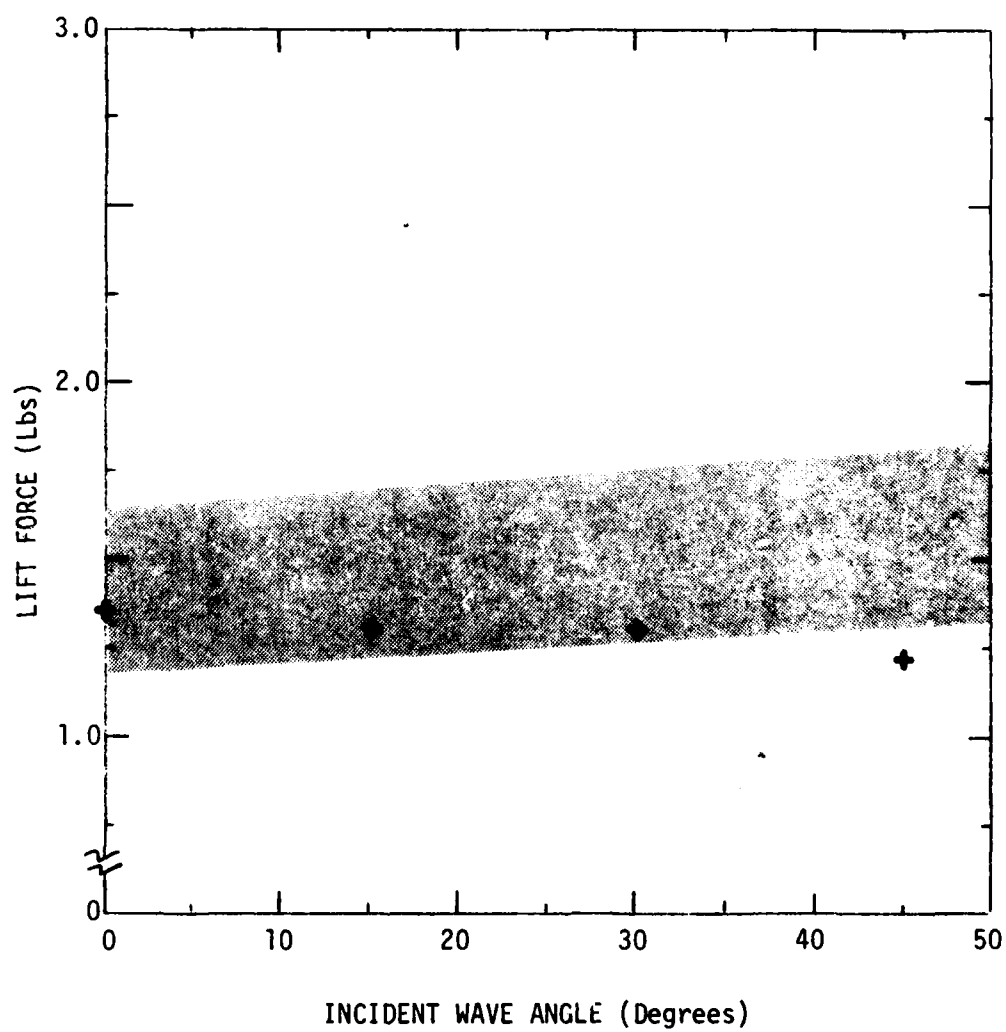FIGURE 13   TOTAL OVERTURNING MOMENT
STRUCTURE ORIENTATION - THIRTY DEGREES

FIGURE 14   TOTAL BASE SHEAR FORCE
            STRUCTURE ORIENTATION - FORTY-FIVE DEGREES

FIGURE 15   TOTAL LIFT FORCE
             STRUCTURE ORIENTATION - FORTY-FIVE DEGREES

FIGURE 16   TOTAL OVERTURNING MOMENT
STRUCTURE ORIENTATION - FORTY-FIVE DEGREES

FIGURE 17   TOTAL BASE SHEAR FORCE AS A FUNCTION OF
STRUCTURE ORIENTATION

FIGURE 18 TOTAL LIFT FORCE AS A FUNCTION OF STRUCTURE
ORIENTATION
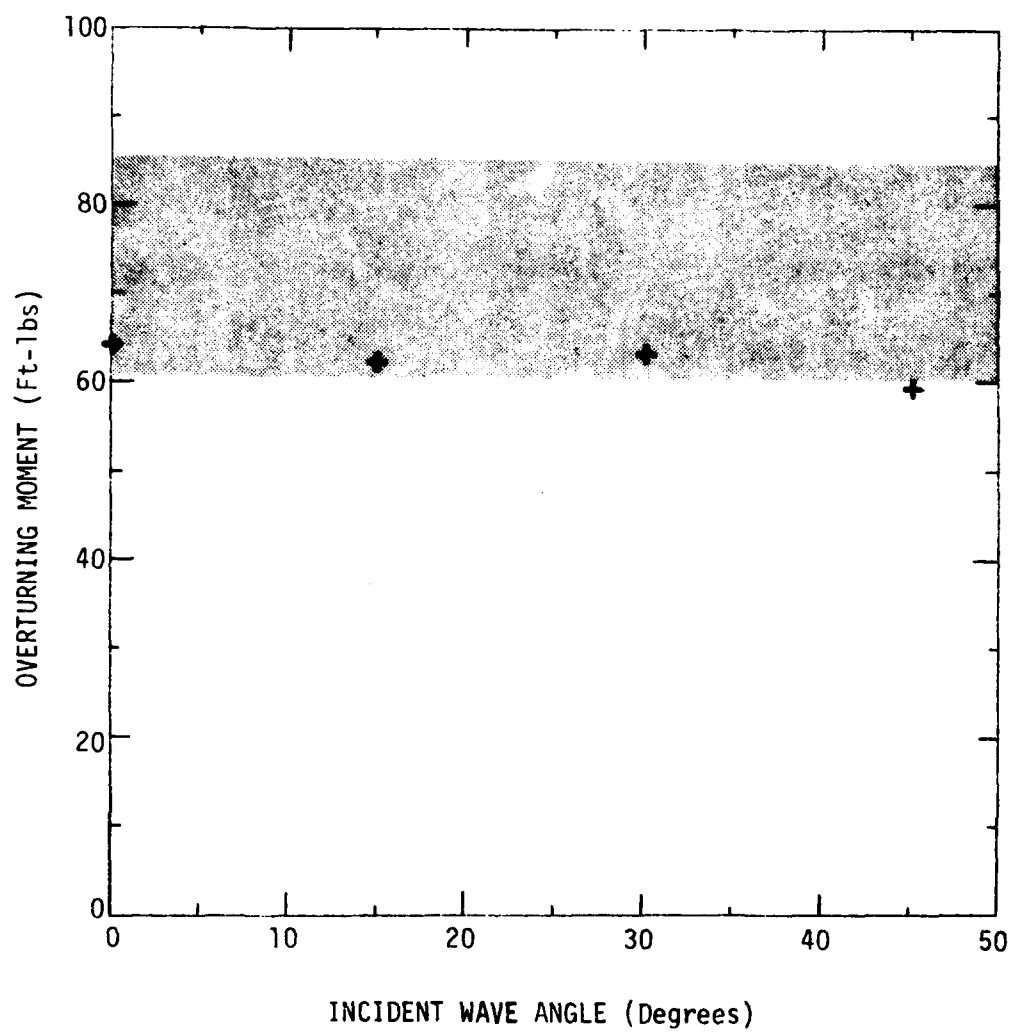
FIGURE 19   TOTAL OVERTURNING MOMENT AS A FUNCTION OF
STRUCTURE ORIENTATION

SECTION II: IRREGULAR WAVE STUDY

Advancing the wave force analysis a step further, irregular waves may be used to represent the random nature of the oceans. A typical wave trace of an ocean wave is shown in Figure 20, and because of their random nature, the characteristics of these waves are most easily handled by statistics.

The simplest and most widely-used description of irregular waves neglects finite-amplitude effects and uses linear theory. It assumes that the surface deflection η from the still-water level at any point can be represented by the random sum of waves of variable amplitude and random phase such that:

$$\eta = \sum_n A_n \cos(k_n x - \omega_n t + \varepsilon_n) \qquad (19)$$

where:

A = Wave amplitude equal $\frac{H}{2}$
k = Wave number
ω = Angular frequency
ε = Phase angle

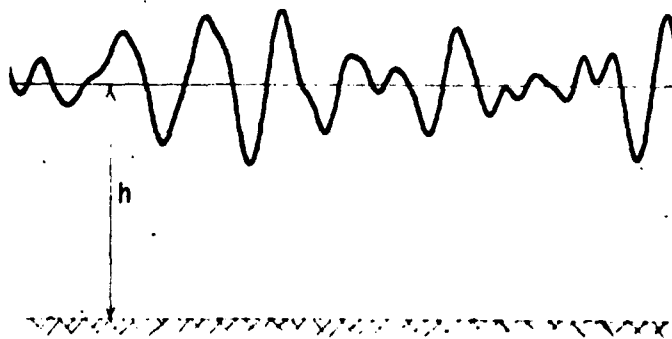with the subscript indicating the value of the nth wave.

FIGURE 20 Irregular Wave Trace

The phase angle ϵ_n in equation (19) is assumed to be distributed uniformly over the interval 0 to 2π so that any one value is as likely to occur as any other. The amplitude A_n associated with wave frequencies between ω_n and $\omega_n + \Delta\omega$ is further assumed expressible as:

$$\frac{1}{2}A_n^2 = S_n \Delta\omega \qquad (20)$$

where S_n is the energy or amplitude spectrum and represents the wave energy distribution over the frequency interval.

For each wave component of equation (19), the associated horizontal and vertical velocities of the water may be determined from linear theory. Assuming the waves are all propagating in the same direction, the horizontal water particle velocity u and the vertical water particle velocity w are given at any position x,z and time t by:

$$u = \sum \omega_n A_n \frac{\cosh k_n(h+z)}{\sinh k_n h} \cos(k_n x - \omega_n t + \epsilon_n) \qquad (21)$$

$$w = \sum \omega_n A_n \frac{\sinh k_n(h+z)}{\sinh k_n h} \sin(k_n x - \omega_n t + \epsilon_n) \qquad (22)$$

where x is the phasing distance, z is measured positive upward from the still-water level and k_n is related to ω_n for deep water by:

$$\omega_n^2 = g k_n \qquad (23)$$

Numerous theoretical approaches have been proposed to describe the energy spectrum of random sea states based on a combination of theoretical reasoning and empirical data. The spectrum used in this report was proposed by Bretschneider in 1959. This is a 2 parameter spectrum

based on H_S and f_m which may be written as:

$$S_n = \frac{1.25}{4} \frac{f_m^4}{f^5} H_S^2 e^{-\frac{5}{4}(\frac{f_m}{f})^4} \tag{24}$$

where H_S is the significant wave height, defined as the average of the highest 1/3 waves, and f_m is the frequency of peak energy.

Experimental Wave Generation

Individual wave height components $H(f)$ must be defined at descrete intervals of frequency so the spectrum may be developed by computer wave generation. The values of $H(f)$ are a function of the repeat period which is simply defined as the time interval before the spectrum begins to repeat itself. The relation is:

$$H(f) = [8S_n \Delta f]^{\frac{1}{2}} \tag{25}$$

where Δf is the reciprocal of the repeat period. The Bretschneider spectrum was chosen for this project because both the significant wave height and frequency of peak energy may be specified.

Five Bretschneider spectra were defined on the computer with a peak energy frequency of 0.4 Hz and a significant wave height range of 0.5 feet to 1.50 feet in 0.25 feet increments. Individual wave components were defined between 0.3 Hz and 1.0 Hz in 0.05 Hz increments. Criteria for choosing these values included keeping the peak energy frequency high enough to assume deep water while low enough to accomodate significant wave heights up to the 1.5 foot range. A plot of the computer defined spectra is shown in Figure 21.

Wave Forces Arising from Irregular Waves

To determine theoretically the wave forces on a structure which
result from irregular waves, the Morison equation must be altered.
These forces may be studied using the energy spectrum described by
equation (20) provided the forces vary linearly with the wave ampli-
tudes. This necessitates restriction to linear wave theory in the
Morison equation and an approximate linearization of the drag term.
Borgman (1967) proposed on theoretical grounds a simple linearization
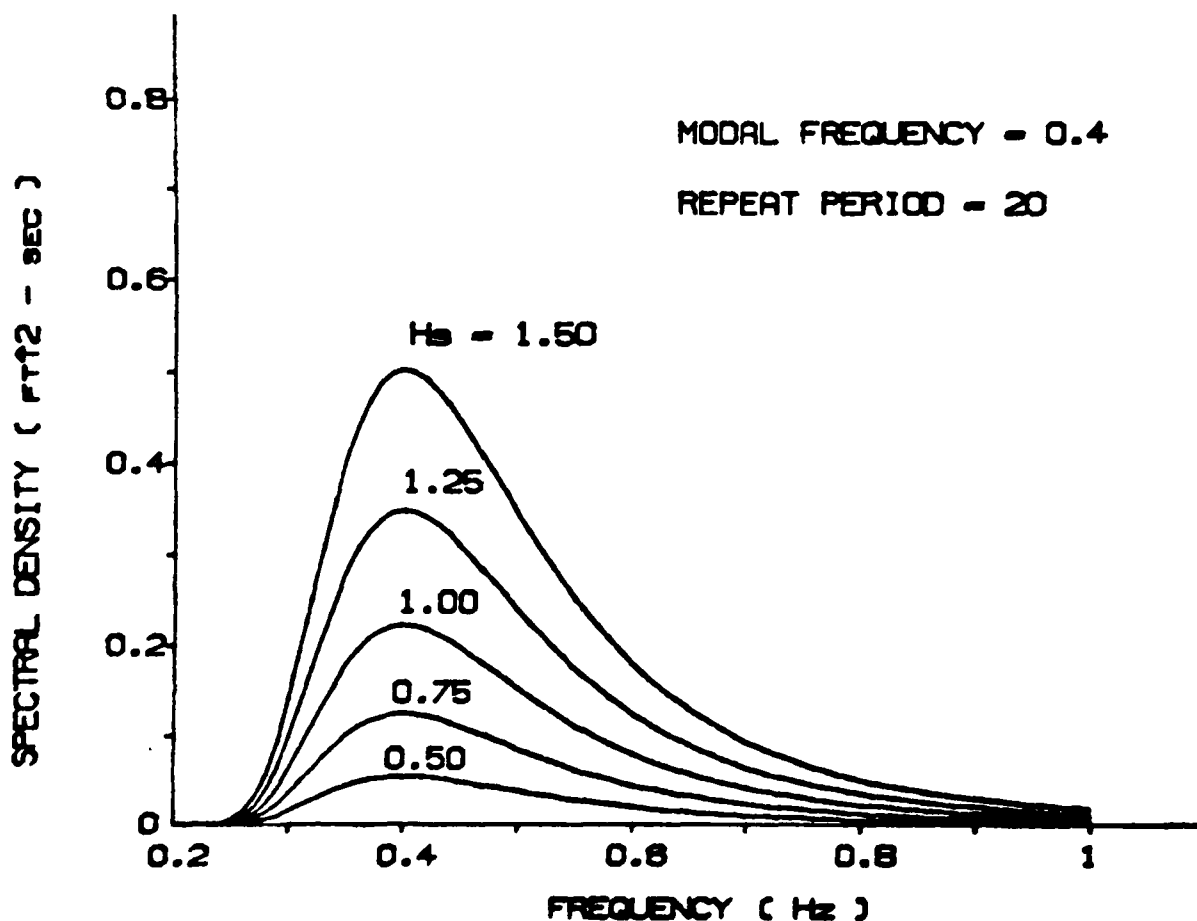
FIGURE 21   Computer Defined Bretschneider Spectra

in which the term $|u|u$ is replaced by $\sqrt{8/\pi}\, u_{rms}u$, where u_{rms} is the root-mean square of the horizontal water particle velocity. Borgman showed that this linearization represents the best linear estimate in a least-square sense.

The restrictions inherent in this approach include:

- only vertical piles may be used in modeling the structure;

- forces are only considered below the still-water level;

- no vertical velocity components may appear in the force

equation.

This last restriction precludes the use of a modified Chakrabarti formulation for irregular wave force determination with Borgman's approach.

Using this approximation, the Morison equation becomes expressible for irregular waves as:

$$f = \sum_n \frac{2}{\pi} \rho C_D D u_{rms} u + \sum_n \rho C_M \frac{\pi D^2}{4} \frac{\partial u}{\partial t} \tag{26}$$

where u_{rms} is dependent upon depth and is determined from integration of S_n by the relation:

$$U_{rms}^2 = \int_0^\infty [\omega \frac{\cosh\, k(h+z)}{\sinh\, kh}]^2 S_n\, d\omega \tag{27}$$

Further using the wave energy spectrum, the force spectrum S_f of the structure may be expressed as:

$$S_F = T_F^2\, S_n \tag{28}$$

where T_F is the transfer function relating S_F and S_n and is equal to the maximum force experienced by the structure for unit amplitude waves at specified frequencies of S_n.

Similarly from equation (28), the total moment spectrum S_M of the structure may be expressed as:

$$S_M = T_M^2 S_\eta \qquad (29)$$

where T_M is the transfer function relating S_η with S_M.

Theoretical Calculations

The restriction of the Borgman method for treating random wave forces required the test structure to be modeled using vertical circular cylinders. Representative areas and volumes of the horizontal and diagonal members were lumped at 10 points along each pile. An integration scheme for determining forces and moments based on presented area and volume was developed which numerically integrated along the length of the piles and accounted for phasing relationships.

As a check on the accuracy of this idealized description, the model was used in a regular wave computer study and the maximum computed wave force compared with that found using the more exact model employed earlier in the regular wave study. The results varied from -5 percent to -95 percent for unit amplitude waves and frequencies ranging from 0.3 Hz to 0.9 Hz. It should be recalled that the total force of the structure using a statistical analysis depends upon u_{rms}, which is dependent upon the entire bandwidth.

To improve upon the idealized structural description, a correction procedure was developed which made the error of the maximum structure force for unit amplitude waves uniformly small over the bandwidth while

remaining within restrictions imposed by the Borgman analysis. The computer program SMEARTEK determined, by iteration, the necessary correction values of lumped areas and volumes based on velocity profile and phasing considerations. These values were then implemented into the previously mentioned regular wave study and the results indicated the simplified model now differed only by a maximum -18 percent for 1 point with all other values within ±5 percent. The results are shown in Figure 22. This 'smeared' model, when used with sufficiently large irregular wave height components to induce drag force dependency, provided a good basis for experimentally determining the applicability of Borgman's analysis.

Another application of the program SMEARTEK was to determine correcting values for regular waves of 1/20 slope over the frequency bandwidth. Using these values, the total base shear force and overturning moment were determined within 5 percent of those determined by Chakrabarti's formulation. For this application, the restriction to linear wave theory and force calculations only below the still-water level was no longer necessary, and values were obtained using only 5 percent to 10 percent of the total computer run time required for the more exact analysis. The results of the SMEARTEK correction for 1/20 slope waves are shown in Figure 23.

An additional computer program was developed to determine the force and overturning moment spectral densities at specified frequencies using the experimentally determined wave spectral density. This program was run for both corrected and uncorrected wave force models

using the Borgman analysis. Determination of u_{rms} at each incremental value of depth was determined by integration of the experimentally determined wave spectral density of S_η as given by equation (27) using the trapazoidal rule with a Δf of 0.05 Hz. The transfer-function calculation considered regular waves of unit amplitude and horizontal velocities u and u_{rms} consistent with the Borgman approximation. The actual value of the transfer function was simply the maximum value of force or moment on the idealized structure for individual frequency components.

Results and Discussion

A computer-defined Bretschneider spectrum with a significant wave height of 1.00 feet was developed in the Naval Academy's 380 foot Towing Tank. The experimentally determined wave spectrum S_η had a significant wave height of 1.01 feet and is shown in Figure 24. The experimental force spectrum S_F is shown in Figure 25 along with the theoretically determined force spectrum range using API recommended drag and inertia coefficients. The corresponding overturning moment spectrum S_M is shown in Figure 26. These figures indicate theoretical values using the uncorrected lumped area and volume technique for cross bracing. The same experimental values are shown in Figures 27 and 28 with the theoretical range indicating values determined using SMEARTEK correction values.

The results using the uncorrected idealized model indicate the experimental values lie toward the upper bounds of the theoretical range. The corrected structural model as indicated by Figures 27 and

28 shifted this range to higher values. This was expected due to the results of the theoretical regular wave tests run on this model. The degree to which the range was shifted varied from 21 percent at the lower frequencies up to 59 percent at 0.9 Hz. Even though the theoretical values at the upper frequency range increased more in a percentage sense as compared to the lower frequencies, the force and moment calculations above 0.6 Hz were not sensitive enough to reproduce the secondary 'hump' of the wave spectral density and experimental force spectral density which appeared between 0.6 Hz and 0.8 Hz. This corrected model appears to provide a better theoretical range for the experimentally determined values.

Because irregular wave analysis employs a statistical approach, the analysis is subject to errors arising from the following 3 sources:

- the mathematical approach suggested by Borgman;

- the spectral determination method;

- the idealized model development technique.

The overall agreement between theoretical and experimental spectral values can be considered within the above stated restrictions of the statistical analysis as well as any errors in experimental measurements. This indicates the Borgman method for approximating force and moment spectral densities by linearizing the drag term may be used with a degree of confidence in spectral density calculations of offshore platforms.
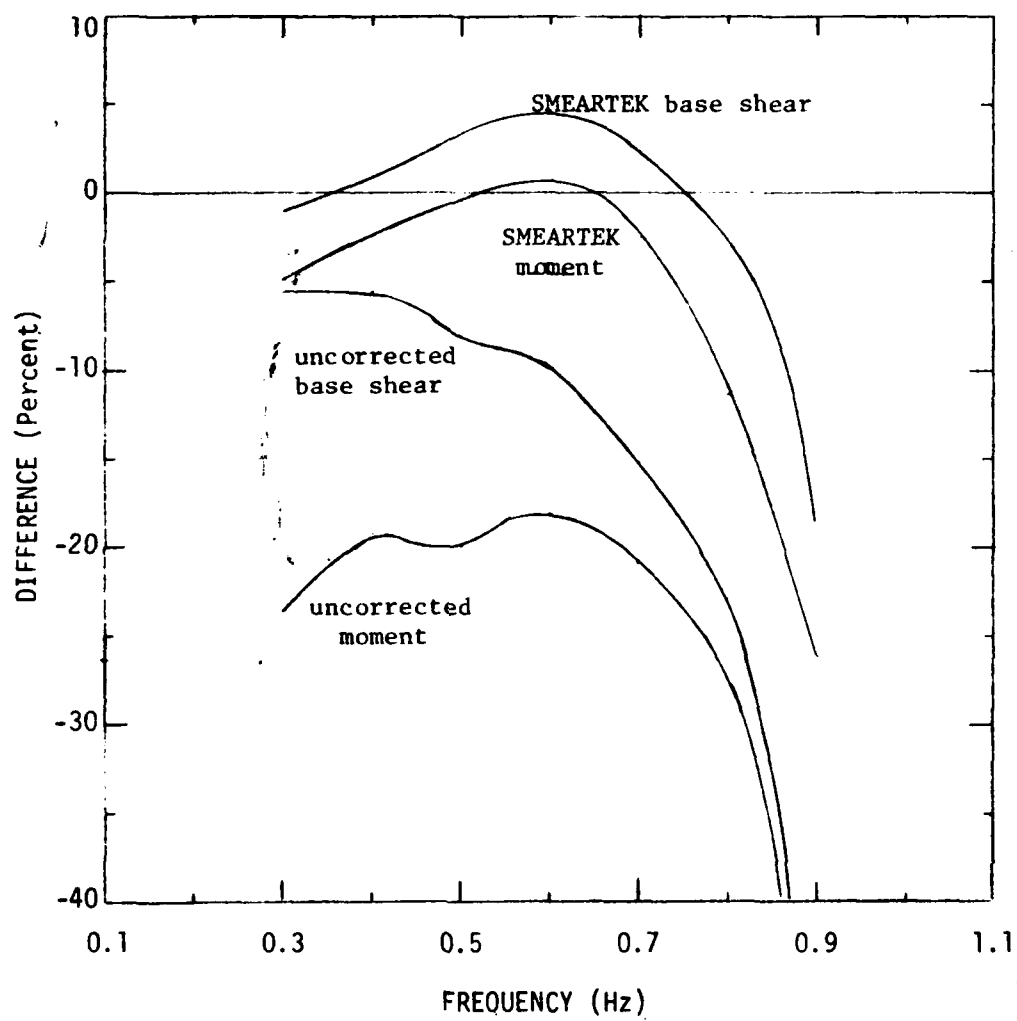
FIGURE 22   RESULTS OF SMEARTEK CORRECTION FOR
IRREGULAR WAVE ANALYSIS
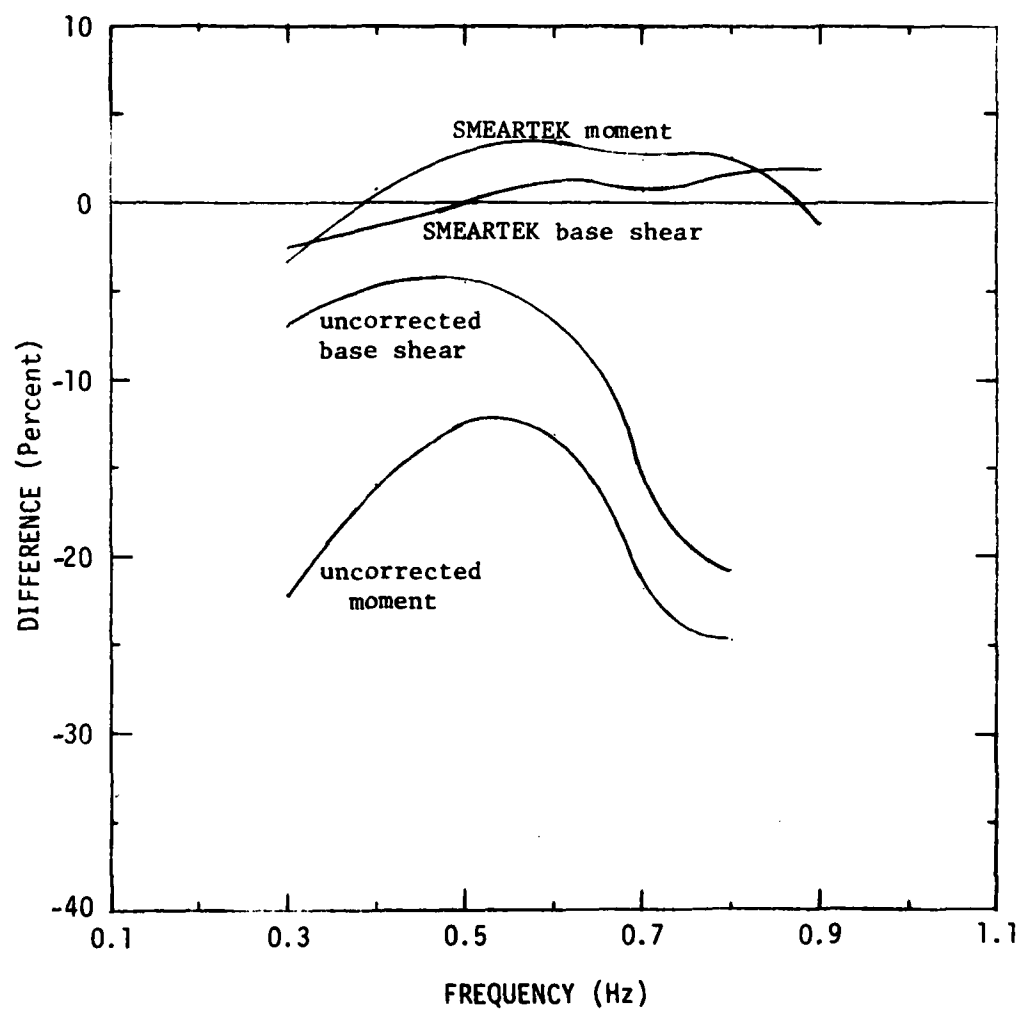
FIGURE 23 RESULTS OF SMEARTEK CORRECTION FOR
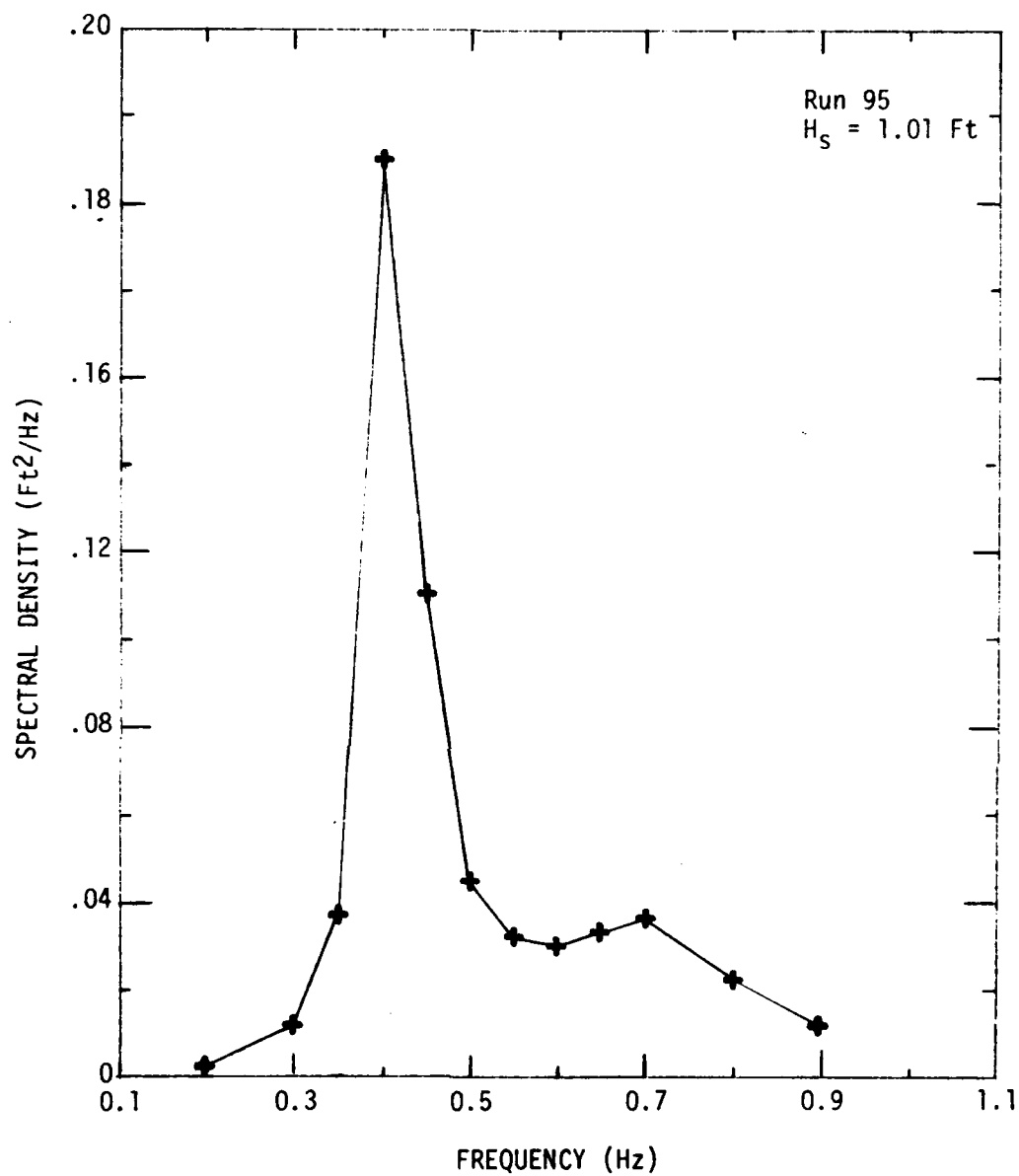REGULAR WAVES OF 1/20 SLOPE
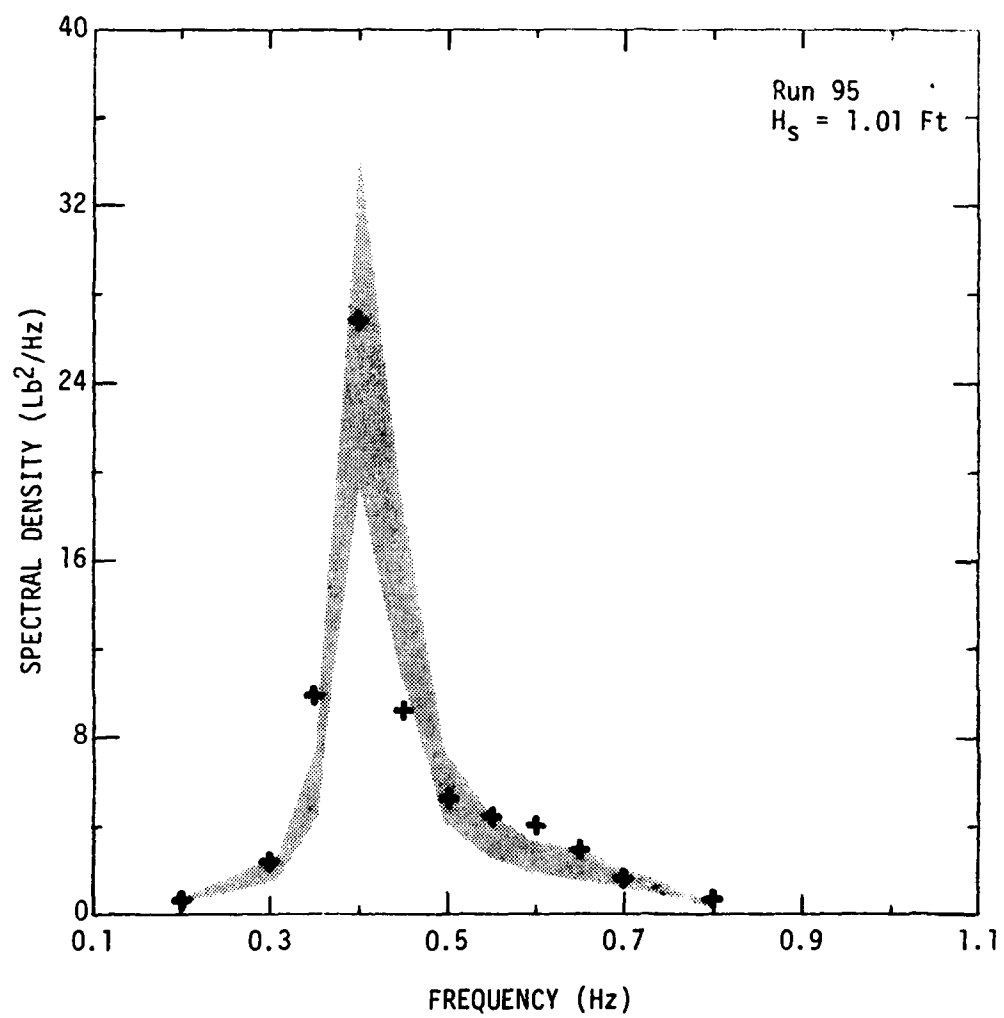
FIGURE 24   WAVE SPECTRAL DENSITY

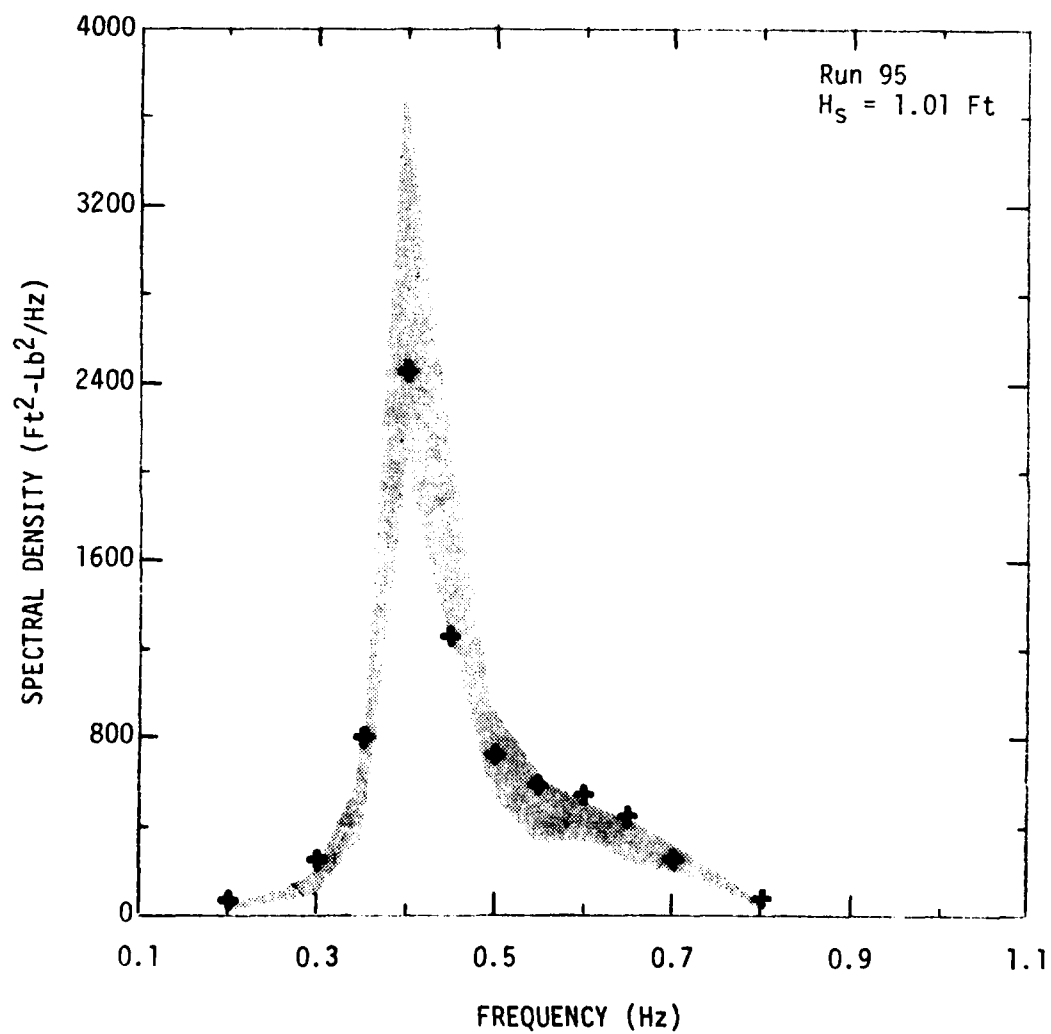FIGURE 25   TOTAL BASE SHEAR SPECTRAL DENSITY

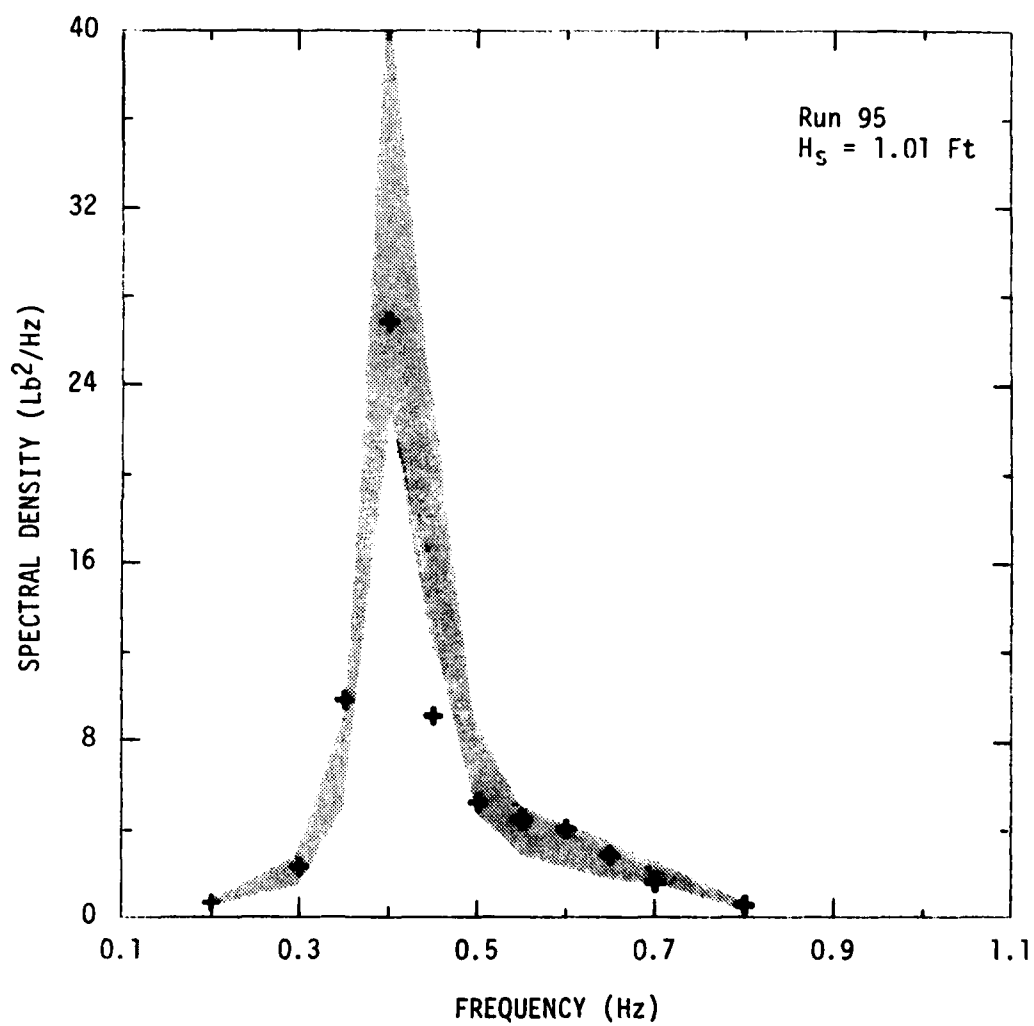FIGURE 26   TOTAL OVERTURNING MOMENT SPECTRAL DENSITY

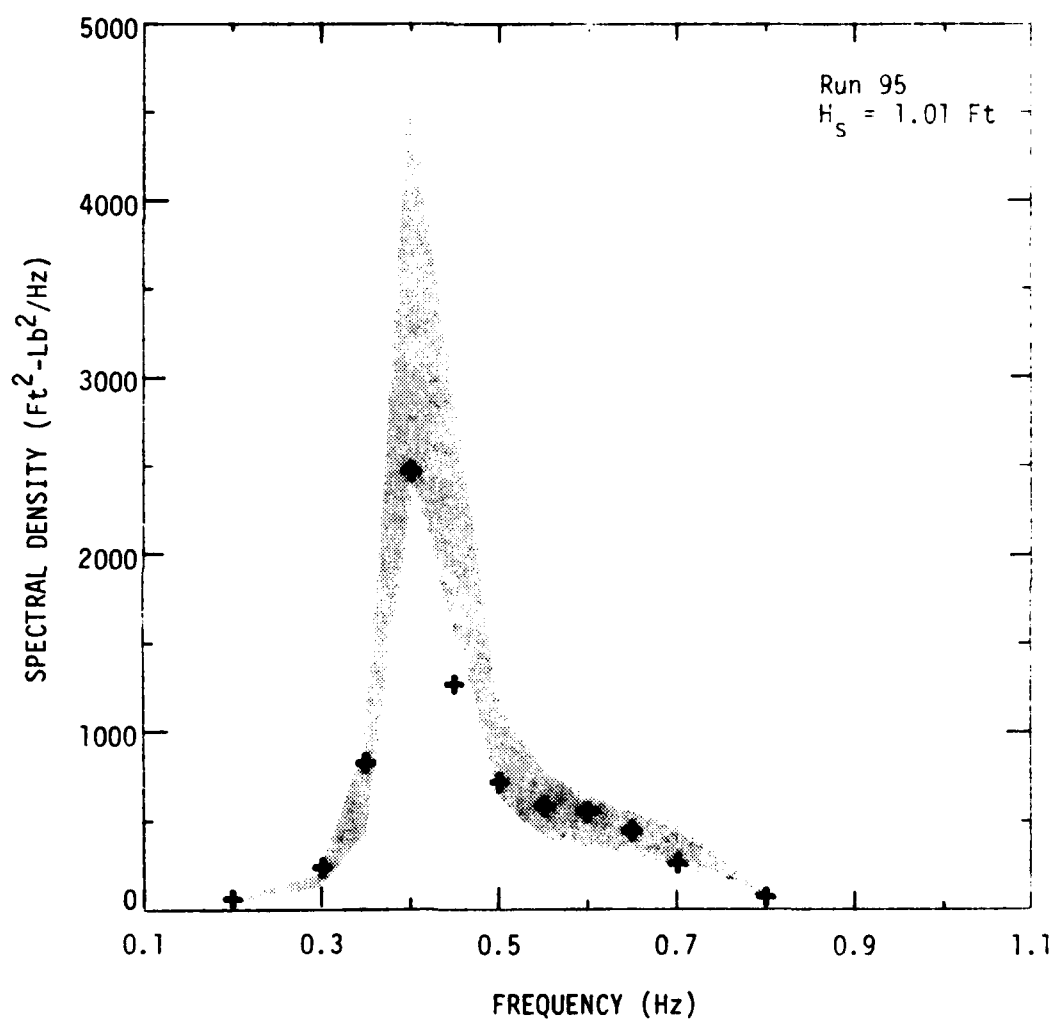FIGURE 27   TOTAL BASE SHEAR SPECTRAL DENSITY USING CORRECTED
STRUCTURAL MODEL

FIGURE 28   TOTAL OVERTURNING MOMENT SPECTRAL DENSITY
USING CORRECTED STRUCTURAL MODEL

SECTION III: STRUCTURAL RESPONSE STUDY

Offshore platforms consist of a complex network of individual members designed to resist the applied wind, wave, and current loadings. The response of the entire structure as well as individual member response is of primary importance. The analysis is carried out using structural matrix methods which have become practical for complex structure analysis with the introduction of the digital computer.

From strength of materials, the forces on a member are proportional to the member displacements and rotations in a frame analysis through proportionality constants which express the member's stiffness. If the member is considered in two dimensions, the forces and moments at each end may be related to the displacements and rotation of these end points by:

$$
\begin{Bmatrix} F_{1x} \\ F_{1y} \\ M_1 \\ F_{2x} \\ F_{2y} \\ M_2 \end{Bmatrix}
=
\begin{bmatrix}
\frac{EA}{\ell} & & & & & \\
0 & \frac{12EI}{\ell^3} & & \text{SYMMETRIC} & & \\
0 & \frac{-6EI}{\ell^2} & \frac{4EI}{\ell} & & & \\
\frac{-EA}{\ell} & 0 & 0 & \frac{EA}{\ell} & & \\
0 & \frac{-12EI}{\ell^3} & \frac{6EI}{\ell^2} & 0 & \frac{12EI}{\ell^3} & \\
0 & \frac{-6EI}{\ell^2} & \frac{2EI}{\ell} & 0 & \frac{6EI}{\ell^2} & \frac{4EI}{\ell}
\end{bmatrix}
\begin{Bmatrix} U_1 \\ V_1 \\ \Theta_1 \\ U_2 \\ V_2 \\ \Theta_2 \end{Bmatrix}
\tag{30}
$$

where:

E = Modulus of elasticity
I = Moment of inertia
A = Member cross sectional area
ℓ = Member length

If the same member is considered in three dimensions, a similar relation to equation (30) may be developed which includes axial and transverse loadings of the member and twisting and bending about 2 principle axes of the cross section. This necessitates that equation (30) be expanded to a twelfth order system of equations.

Considering the two dimensional case, equation (30) may be rewritten as:

$$\{F\} = [K] \{U\} \tag{31}$$

where the elements of $\{F\}$, $[K]$, and $\{U\}$ are given by the corresponding elements of equation (30). The matrix $[K]$ is referred to as the stiffness matrix of the member.

To allow for the specification of either moments at the joints or rotations of the joints, the structure is usually modeled as a rigid joint frame. This requires the joints to preserve the relative angular spacing of the attached members at the joints while undergoing loading. With rigid joints, all members connected at the joint will therefore suffer the same rotation at the joint as the joint itself.

Multi-member structures such as offshore platforms are analyzed in this manner using properly constructed matrices which reflect individual member connectivity, properties, and orientation. This method of structural analysis has become known as the direct stiffness method.

Regardless of the size of the structure, equation (31) always applies, the only difference being the size of the matrices. For example, the test structure shown in Figure 29a in two dimensions requires a 36th order matrix to reflect 2 degrees of translation and 1 degree of rotation at each joint. The same structure in three dimensions as shown in Figure 29b, however, requires a 144th order matrix to handle the 3 degrees of freedom translation and 3 degrees of freedom rotation which is necessary to describe the system.

Applying the proper boundary conditions to insure a determinate system and knowing the forces and moments at each joint, equation (31)
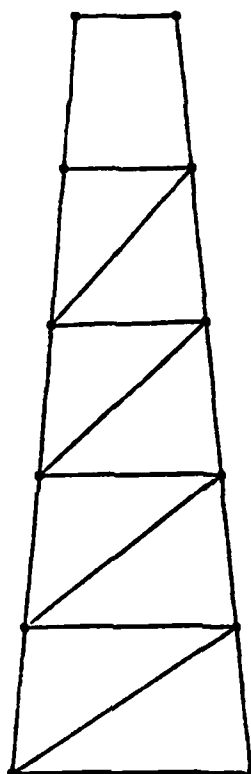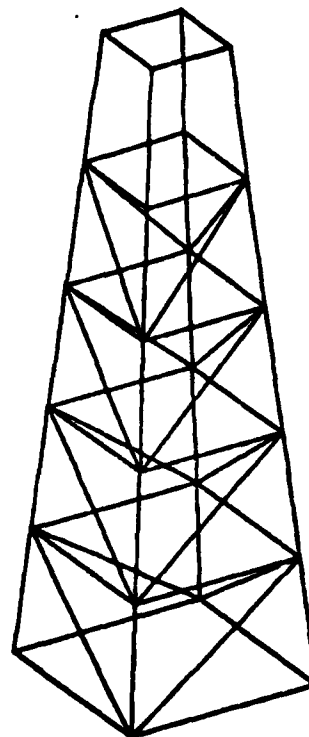
a. Two Dimensions   b. Three Dimensions

FIGURE 29 Computer Based Math Models

may be solved for the displacements and rotations through the relation:

$$\{U\} = [K]^{-1} \{F\} \tag{32}$$

where $[K]^{-1}$ is the inverse of the stiffness matrix or more commonly called the flexibility matrix.

Determination of the forces and moments on each member is accomplished through the use of an appropriate wave and force theory as described in previous sections. As a wave passes the structure, there are 2 cases of importance - the first being when the total force on the structure is at a maximum and the second being when the force on an individual member is at a maximum. Because the overall structure response as indicated by deck deflection is of interest in this project, only the first case was studied.

When the total structural force is at a maximum, individual member forces may be computed and modeled using 2 techniques. The first technique as shown in Figure 30a calculates the force on the member and distributes this load equally over the member. This load may then be computed into equivalent point loads and moments as shown in Figure 30b
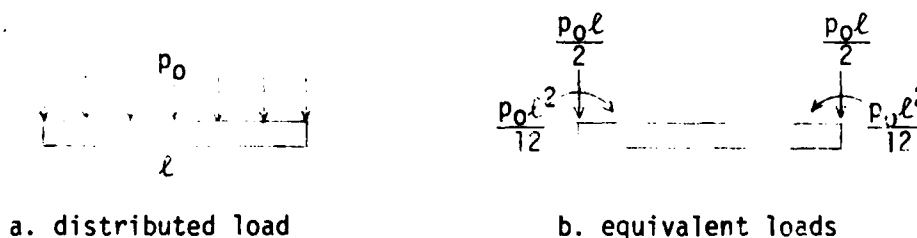

a. distributed load   b. equivalent loads

FIGURE 30   Distributed Load Technique

and applied at the end points. The second technique assumes a concentrated load acting on the member and similarly computes equivalent joint loads and moments as shown in Figures 31a and 31b.

Using a digital computer, equation (32) may be solved for the unknown displacements and rotations of each joint. These, in turn, may be used to determine the internal forces in each member from which the maximum stresses may be found from well established solid mechanics principles. For a complete discussion of structural analysis by the direct stiffness method see Willems and Lucas (1968).

Computer Solution

The matrices described by equation (31) were developed for a two dimensional model of the test structure and placed on the computer. The program used for the regular wave analysis was then adapted to use the concentrated load technique described above. The method of distributed loads was once again found undesirable due to the deep water velocity profiles of the experimental waves. The step size considerations remained the same as in the regular wave force analysis to insure accurate results.
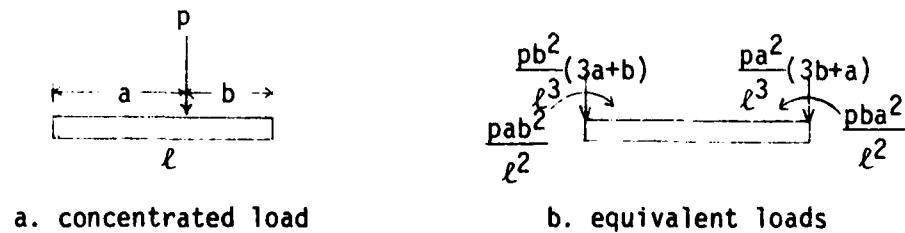
a. concentrated load   b. equivalent loads

FIGURE 31 Concentrated Load Technique

To verify the concentrated load technique used in this program, the results were compared with the regular wave force program. The maximum percentage difference for all encountered waves was 7.5 percent. This error could be attributed to the uncertainties of the technique for diagonal members normal to the waves.

The equivalent forces and moments at each joint found by this method were then used in the previously constructed matrices. The matrix equation was solved on the computer for individual joint displacements and rotations.

Frequency Analysis

As offshore structures move into deeper water, they tend to become more flexible and as a result the dynamic aspects of wave loadings become more important. The natural frequencies of these platforms can be excited if the frequency of the design wave or peak frequency of the design spectrum comes within range of the platform frequencies.

The design of the test model required 2 frequency considerations; the first was to have the fundamental response high enough to assume static wave loading and the second was to allow this response to be changed sufficiently using added deck weight to allow a study of dynamic loading effects.

Single Spring/Mass Model

Using the previously constructed matrices for the two dimensional structural analysis, a load evenly placed on the deck of the platform

will result in a given deck displacement such that the structure's effective spring constant K' may be calculated from the relation:

$$K' = \frac{F}{U} \tag{33}$$

where U is the deck displacement for the load F. Assuming a 1 degree of freedom spring/mass system, the first-mode natural frequency of the structure may be calculated from:

$$\omega_n = \sqrt{\frac{K'}{M'}} \tag{34}$$

where M' can be considered the effective mass of the structure given approximately by:

$$M' = M + \frac{1}{2}M_p + \frac{1}{2}M_v \tag{35}$$

where:

    M = Mass of the deck
    M_p= Mass of the support structure
    M_v= Mass of the displaced water

This method uses a simple lumped mass model which approximates for the mass of the structure and displaced water.

When the above method was applied to the two dimensional test model, the fundamental frequency response was found to be 4.66 Hz for a deck weight of 125 pounds.

Three Dimensional Analysis

The complexity of a frequency analysis for a three dimensional platform has lent itself to the development of computer codes to handle user

defined platforms. Modeling these structures as multi-degrees of freedom systems allows for a more accurate and complete frequency analysis.

The computer code 'GIFTS-IV' (Graphics oriented Interactive Finite element Time sharing System) was used to model the test structure as a three dimensional multi-degrees of freedom system for the calculation of 6 modal frequencies. 'GIFTS' was developed by Professor Hussein A. Kamel and Michael W. McCabe of the University of Arizona as a modular code for structural analysis. The structure to be analyzed must first be defined and may then be subjected to both static and transient load analyses as well as a frequency analysis. The test model was developed in three dimensions as shown in Figure 29b, and the first mode frequency analysis as described by equation (34) resulted in a response within 1 percent of the two dimensional model. This is not surprising due to the symmetry of the model. The front and rear faces contribute very little to the stiffness of the model for a force applied, say, to the positive x axis for a tower orientation of 0 degrees.

For the three dimensional analysis, 'GIFTS' lumps the masses of the members at each of the 24 connecting nodes, applies loads in the x, y, and z directions represented by a power series, and then uses a subspace iteration routine to converge on the frequency modes. This routine in three dimensions produced results which differed from the experimental values of the fundamental mode by 150 percent or more

(1.38 Hz predicted value versus 3.61 Hz experimental for 125 pounds deck weight). Using 'GIFTS' for the structure defined in two dimensions, however, yielded a fundamental response equal to that obtained by an equation (34) analysis. The 'GIFTS' frequency analysis in three dimensions indicated, however, that the first 3 modes of the structure would be almost identical. This corresponded to the experimentally observed cross-coupling of these modes.

Dynamic Response

Another structural consideration which is dependent upon both the frequency response of the structure as well as the wave force loading is dynamic response. Regular wave loading on an offshore structure can be considered an oscillatory forcing function of some angular frequency ω. Extending the single spring/mass model of the test structure to include a dashpot to account for damping, the amplitude of the deck deflection U as a function of $\frac{\omega}{\omega_n}$, where ω_n is the undamped natural frequency of the structure, may be expressed in nondimensional form as:

$$\frac{UK}{F_o} = \frac{1}{\sqrt{[1 - (\frac{\omega}{\omega_n})^2]^2 + [2\zeta(\frac{\omega}{\omega_n})]^2}} \tag{36}$$

where

ζ = Damping factor
K = Structure stiffness
F_o = Magnitude of forcing function

This technique is discussed by Thompson (1972) and the value of $\frac{UK}{F_o}$ has become known as the dynamic amplification factor.

The curve of the dynamic amplification factor for the test structure as a function of $\frac{\omega}{\omega_n}$ was generated on the computer. Because ζ is an experimentally determined parameter, ω_n was taken to be the experimental value instead of the theoretical value described by equation (34) for the sake of consistency.

Using the concentrated load technique described for structural analysis but lumping the forces at the deck and seafloor instead of at each joint will give the necessary F_o to solve equation (36) for deck displacements. The value of K in this case is the effective spring constant of the structure determined from equation (33).

Experimental Determination of the Fundamental Response

The first mode response was determined experimentally using a number of excitation techniques to assure repeatability. Accelerometers were mounted on the deck of the structure as well as the top horizontal cross members. A 'twang' test and impulse test were used for first mode response determination. In addition, the structure was pushed (on axis) and then released. All 3 methods gave identical results within the accuracy of the experiment and the average values, for the structure in water, along with the three dimensional theoretical response from equation (34). are shown in Figure 32.

In determining the frequency response of the structure, the effect of damping was assumed negligible. This may be checked using the method of logarithmic decrement as discussed by Thompson (1972). The damping ratio ζ was determined from an accelerometer trace to be 0.045, which

indicated that the frequency damping of the structure was in fact negligible ($\omega_d = 0.999\,\omega_n$). The additional damping due to the water was determined experimentally to be approximately 1.0 percent which did not contribute significantly to the frequency damping of the structure.

Two cases of deck weight were used during testing to meet the 2 criteria discussed earlier; 125 pounds and 1,330 pounds which gave respective experimental first mode responses of 3.61 Hz and 1.27 Hz.

Results and Discussion

A plot of the experimental frequency results (in water) as well as the results of a three dimensional equation (34) analysis were given in Figure 32. The experimental values are shown to range from 16 percent to 25 percent lower than the theoretical values. With the damping negligible, the most probable explanation lies with the method of theoretical analysis. The assumption of rigid joints used in determining the effective spring constant may model the structure too 'stiffly,' hence accounting for the lower experimental frequency values.

The results of the deck deflection calculations and corresponding experimental values indicated a similar error in the theoretical analysis. As shown in Figure 33, the experimental deck deflections differed by a factor of 2.6 up to as much as 4.0 above the theoretical values. The maximum possible dynamic amplification for this weight case was 4 percent and hence did not contribute significantly to these factors of error. Therefore, with the previously established

accuracy of wave force calculations as well as the accuracy of the two
dimensional versus three dimensional structure analysis, the possibility
of error within the assumption of rigid joints is further substan-
tiated.

The results of the dynamic amplification study as shown in
Figure 34 indicate the experimental values based on deck deflection
are in reasonable agreement with the dynamic amplification curve for
a structure damping ratio ζ of 0.045. These values were based on the
ratio of the deck deflection for 1/20 slope waves with a deck weight
of 125 pounds to those for 1/20 waves with a deck weight of 1,330
pounds. The error from the theoretical curve ranged from 1 percent
at 0.3 Hz up to 12 percent at 0.7 Hz.
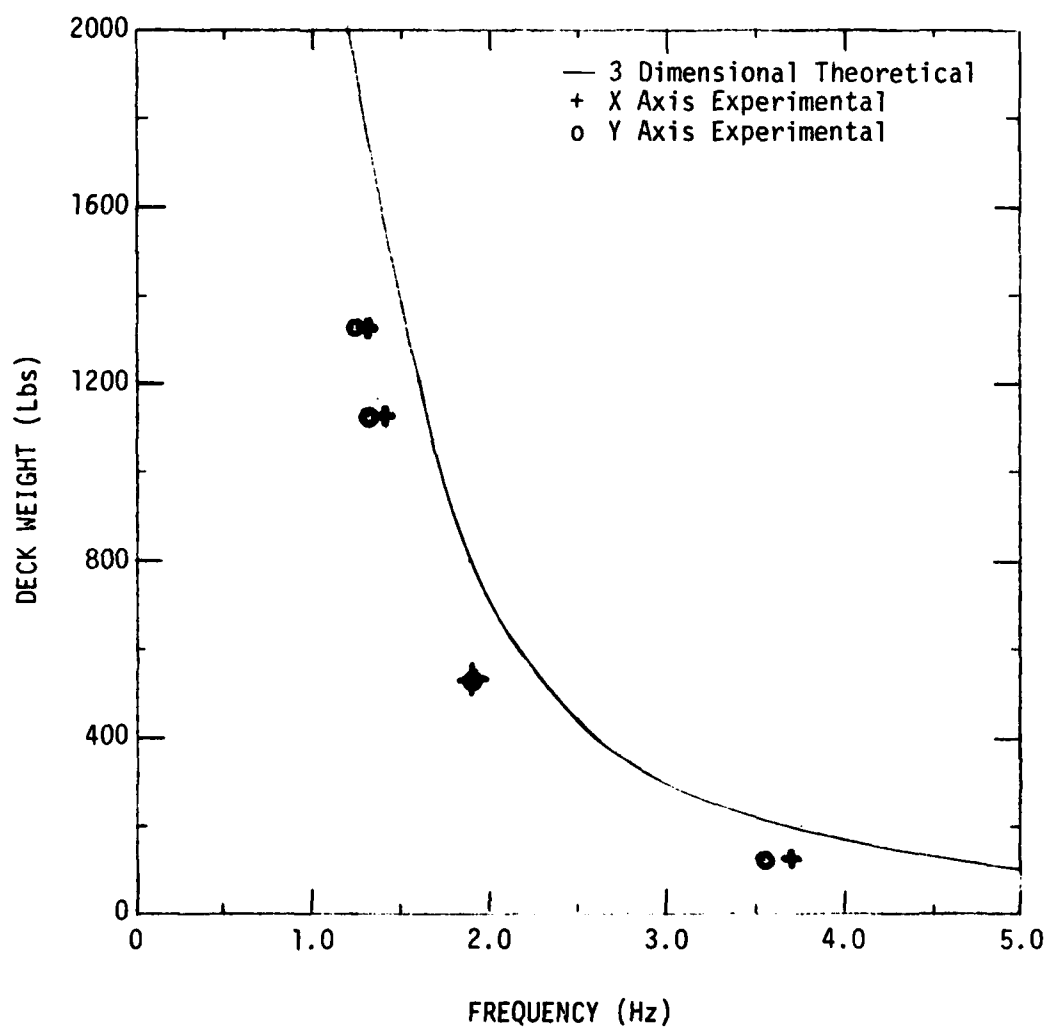
FIGURE 32   FIRST MODE NATURAL FREQUENCY COMPARISON
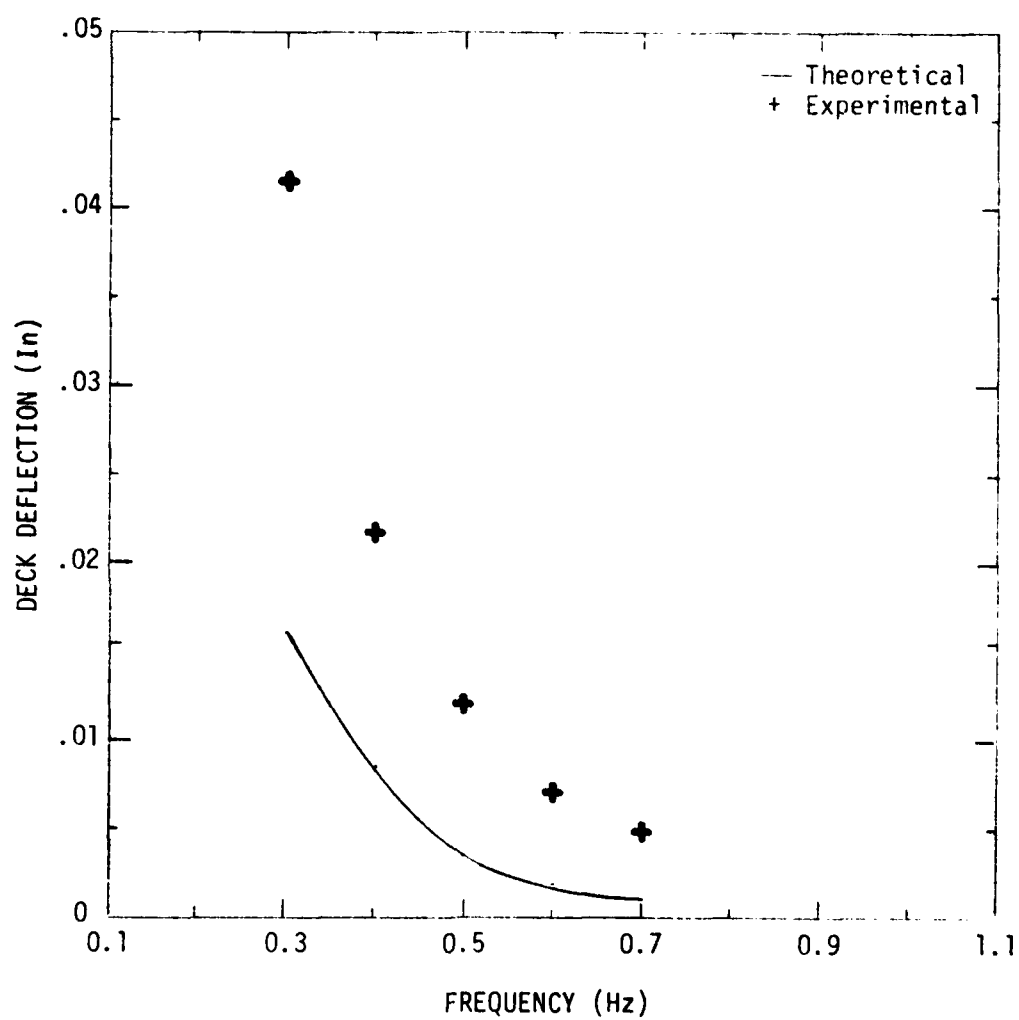
FIGURE 33   DECK DEFLECTION
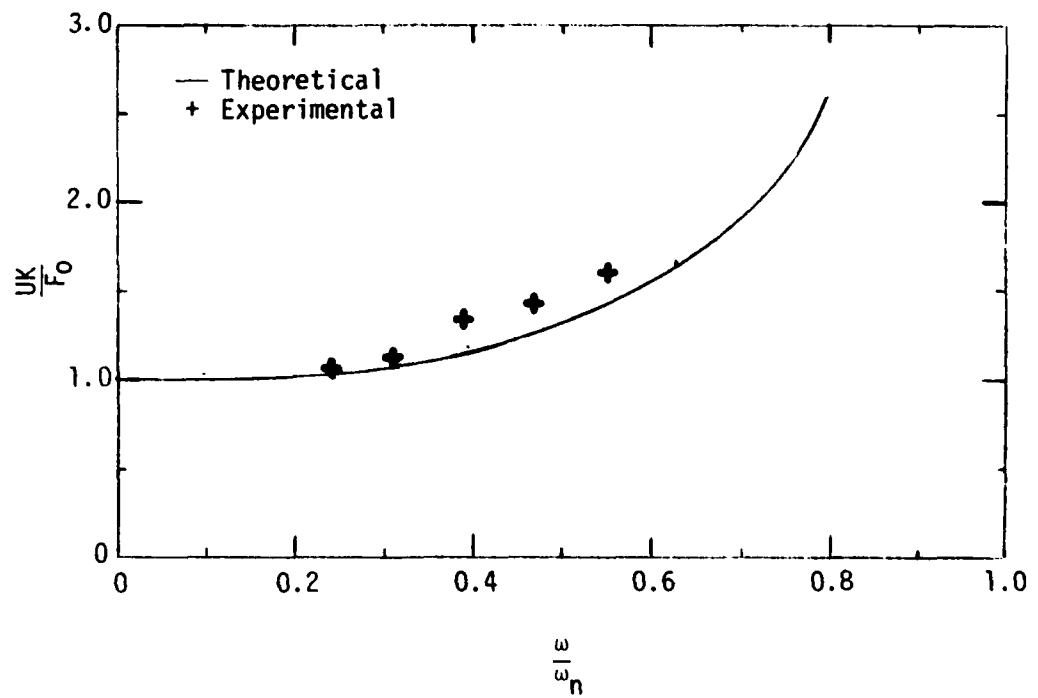
FIGURE 34   STRUCTURE DYNAMIC AMPLIFICATION

CONCLUSIONS

Based on the material presented in the above three sections, the following conclusions may be drawn:

● The regular wave study, which used deep water constant slope waves at various incident wave angles on the structure, indicated that force calculations based on consideration of the velocity and acceleration components normal to the individual members yielded uniformly good results when compared with experimental measurements for various structure orientations relative to the incident wave.

● As offshore structures continue to move into deeper water where even the longest design waves must be considered deep water waves, an approach such as the one used in this study should be considered which combines the above formulation for wave force analysis with an accurate numerical integration technique.

● The examination of the Borgman irregular wave force analysis indicated good agreement with experimentally determined values. This examination provided a better check on the linearization of the drag term than Borgman himself provided due to the significant wave height used in relation to the pile diameter. For a structure with significant cross bracing, an alternative approach to a simple lumped area and volume approximation of non-vertical members which accounts more

accurately for their wave force and moment contributions, appears to provide better spectral representation of the total force and moment on the structure.

● The American Petroleum Institute recommended range of values for the drag and inertia coefficients, 0.6 to 1.0 and 1.5 to 2.0, respectively, provided theoretical values which encompassed experimental values for wave frequencies below 0.8 Hz for the test structure. The regular wave study indicated a strict consistency in the relation of the experimental values to this theoretical range. This was concluded to be the result of the variation in values of drag and inertia coefficients for low values of frequency dependent parameters such as those discussed by Sarpkaya (1976) and Keulegan and Carpenter (1958). At the time of this report, theoretical force and moment calculations using values of drag and inertia coefficients based explicitly on encountered frequencies have not been determined.

● The results of the structural response study indicated that the joints of the test structure were overly restrained in the computer model which employed a rigid joint frame analysis for both frequency and deck deflection calculations.

ACKNOWLEDGEMENT

REFERENCES

API Recommended Practice for Planning, Designing, and Constructing Fixed Offshore Platforms, API RP 2A, American Petroleum Institute, Washington, November 1977.

Borgman, Leon E., "Spectral Analysis of Ocean Wave Forces on Piling," Journal of the Waterways and Harbors Division, American Society of Civil Engineers, pg. 129-156, May 1967.

Chakrabarti, S.K., W.A. Tam, and A.L. Wolbert, "Wave Forces on a Randomly Oriented Tube," Offshore Technology Conference Proceedings, pg. 433-441, 1975.

Chakrabarti, S.K., W.A. Tam, and A.L. Wolbert, "Total Forces on a Submerged Randomly Oriented Tube Due to Waves," Offshore Technology Conference Proceedings, pg. 723-740, 1976.

De, S.C., "Contributions to the Theory of Stokes' Waves," Proceedings of the Cambridge Philosophical Society, pg. 713-736, 1955.

Hoerner, S.F., Fluid-Dynamic Drag, published by the author, 1964.

Ippen, A.T., Estuary and Coastline Hydrodynamics, McGraw-Hill, New York, 1966.

Keulegan, G.H., and L.H. Carpenter, "Forces on Cylinders and Plates in an Oscillating Fluid," Journal of Research of the National Bureau of Standards, Vol. 60, No. 5, pg. 423-440, May 1958.

Kinsman, B., _Wind Waves_, Prentice-Hall, Inc., Englewood Cliffs, New Jersey, 1965.

McCormick, M.E., _Ocean Engineering Wave Mechanics_, John Wiley & Sons, Inc., New York, 1973.

Morison, J.R., M.P. O'Brien, J.W. Johnson, and S.A. Schaaf, "The Forces Exerted by Surface Waves on Piles," _Journal of Petroleum Technology_, American Institute of Mining Engineers, Vol. 189, pg. 149-154, 1950.

Sarpkaya, T., "Vortex Shedding and Resistance in Harmonic Flow About Smooth and Rough Circular Cylinders," _BOSS 76 Proceedings_, Vol. 1, pg. 220-235, 1976.

Sorensen, R.M., _Basic Coastal Engineering_, John Wiley & Sons, Inc., New York, 1978.

Stokes, G.G., "On the Theory of Oscillatory Waves," _Mathematical and Physical Papers_, Cambridge University Press, 1880.

Thompson, W.T., _Theory of Vibration with Applications_, Prentice-Hall, Inc., Englewood Cliffs, New Jersey, 1972.

U.S. Army Coastal Engineering Research Center, _Shore Protection Manual_, Vol. 1, 2, & 3, U.S. Government Printing Office, Washington, 1973.

Wade, B.G., and M. Dwyer, "On the Application of Morison's Equation to Fixed Offshore Platforms," _Offshore Technology Conference Proceedings_, pg. 1,181-1,190, 1976.

Wiegel, R.L., <u>Oceanographical Engineering</u>, Prentice-Hall, Inc., Englewood Cliffs, New Jersey, 1964.

Willems, N., and W.M. Lucas, <u>Matrix Analysis for Structural Engineers</u>, Prentice-Hall, Inc., Englewood Cliffs, New Jersey, 1968.

APPENDIX A

TEST STRUCTURE AND INSTRUMENTATION

TEST STRUCTURE AND INSTRUMENTATION

In addition to the specifications of the test structure which were
presented in the text of the report, material tests were conducted to
determine the best weld configuration and loss of yield strength due to
the tungsten inert gas (TIG) welding process. The results indicated a
butt-butt filet weld provided the best weld continuity while reducing
the yield strength approximately 50 percent to a value of 17,000 psi.
Corrosion tests were also completed which indicated a submergence time
of approximately 1 month would result in negligible corrosion of the
structure.

The instrumentation package chosen included 12 4-inch Hydronautics
variable-reluctance modular force gauges to measure forces, 4 Wesmar
high frequency sonic transducers to measure displacements, 2 MTS
resistance-type wave gauges to measure wave characteristics, and asso-
ciated equipment.

Three force gauges were used on each leg as shown in Figures A-1
and A-2 to allow the measurement of the force in the x, y, and z direc-
tions. Signals were processed through Hydronautics Multi-T signal condi-
tioning units and filtered through Ithaco filters at 10 Hz. A complex
design of multi-bearing/pivot connectors also shown in Figures A-1 and
A-2 was developed and built to allow the attachment of the structure to
the force gauges. This assembly allowed negligible pre-stressing of the

structure/gauge interface which could result from misalignment of the structure, base plate bending and/or thermal contraction. This system was necessary to resolve accurately the force gauge outputs into resultant forces and moments on the structure.

Deck deflection and rotation measurements were accomplished using high frequency sonic transducers in the configuration shown in Figure A-3. Signals were processed through Wesmar signal conditioning units and filtered through Ithaco filters at 10 Hz. The deck deflection signals were digitally manipulated to achieve x and y axis deflection and deck rotation. The high speed towing carriage was placed over the structure as shown in Figure 1 to act as the reference base for the deck deflection measurements as well as the relay point between the gauge signals and the computer.

FIGURE A-1 Structure - Gauge Interface

Wave characteristics were recorded using a resistance-type wave probe aligned at the leading edge of the structure (base level). This corresponded to the reference point used in theoretical calculations and allowed for phasing comparisons.
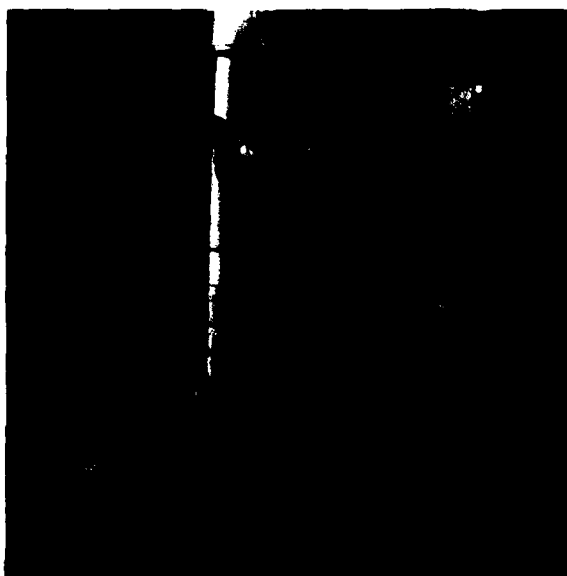
FIGURE A-2 Structure - Gauge Interface
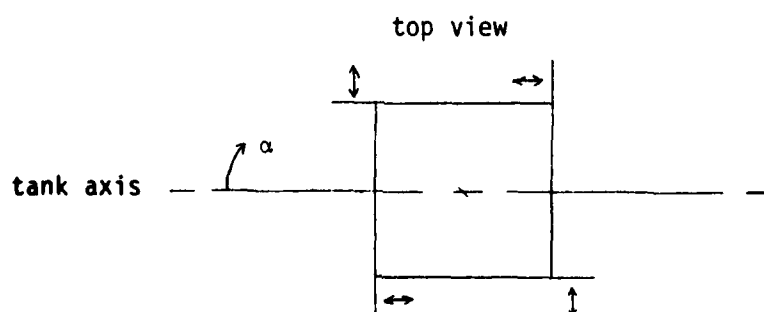
FIGURE A-3 Deck Deflection Measurement Schematic

APPENDIX B

SAMPLE EXPERIMENTAL DATA

SAMPLE EXPERIMENTAL DATA

Seventeen channels of data were acquired by the computer on each
test run. Of these, 12 channels were force data, 4 channels were
displacement data, and 1 channel was wave data. In addition to
this primary data, up to 8 channels were calculated by digital
manipulation of the primary data files. Values such as deck rotation
and torsional moment were found either too small to measure or gave
meaningless results and are not presented. The computed values pre-
sented in this report are limited to total base shear, lift force,
overturning moment, and x-axis deck deflection.

The sample data presented in this appendix is from both regular
and irregular wave test runs.

Regular Wave: Phase I   Run 21   0.4 Hz   1.56 ft
                              Structure Orientation - Zero Degrees

                Figure B-1   Wave   0.4 Hz   1.56 ft
                Figure B-2   X-axis force component on leg 'A'
                Figure B-3   Y-axis force component on leg 'A'
                Figure B-4   Z-axis force component on leg 'A'
                Figure B-5   X-axis deck deflection
                Figure B-6   Total base shear force
                Figure B-7   Total lift force
                Figure B-8   Total overturning moment

Irregular Wave Phase II   Run 95 f_m = 0.4 Hz   1.01 ft
                              Structure Orientation - Zero Degrees

                Figure B-9   Wave f_m = 0.4 Hz H_s = 1.01 ft
                Figure B-10   X-axis force component on leg 'A'
                Figure B-11   Y-axis force component on leg 'A'
                Figure B-12   Z-axis force component on leg 'A'

83
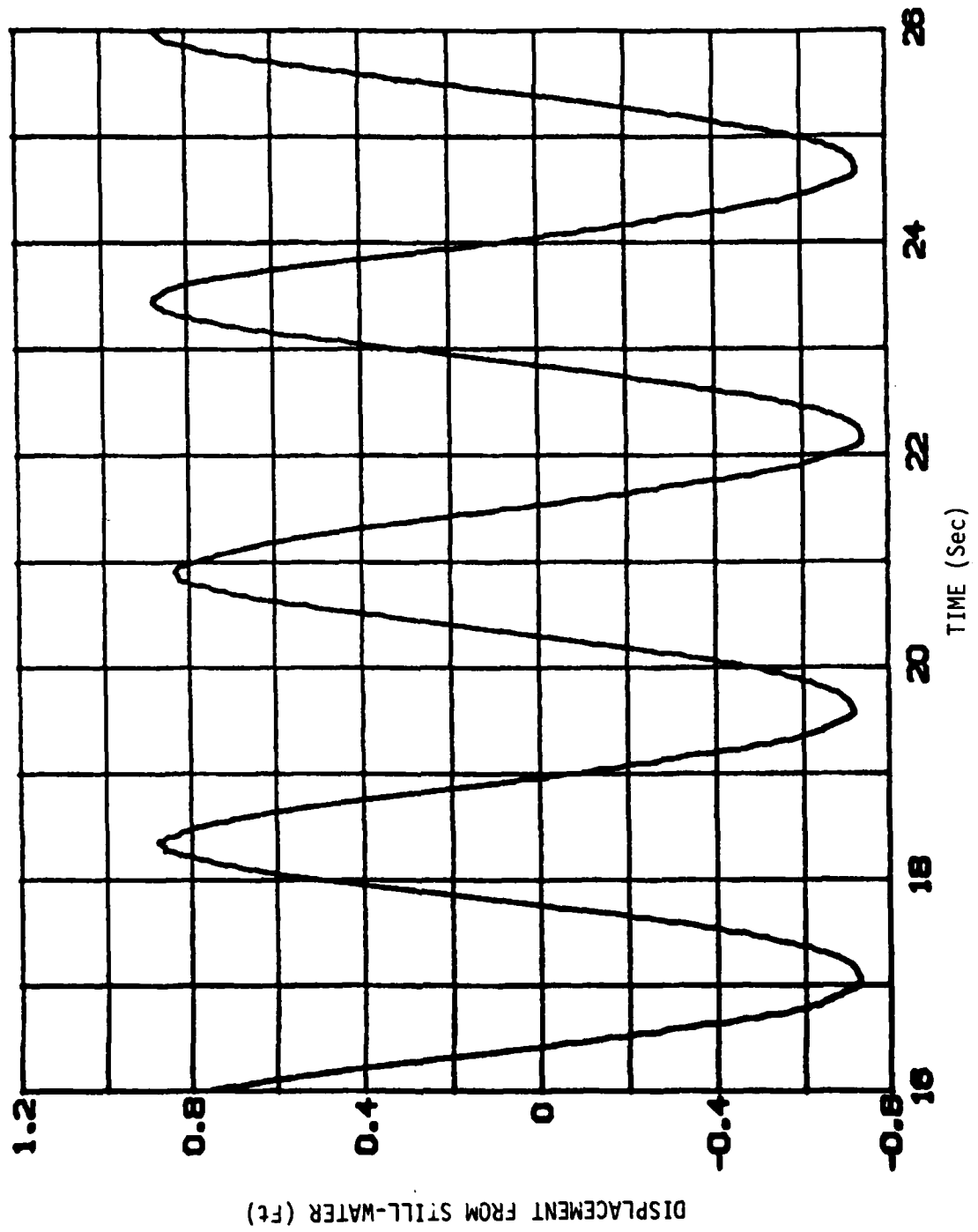
FIGURE B-1 WAVE 1.56 Ft 0.4 Hz
STRUCTURE ORIENTATION - ZERO DEGREES
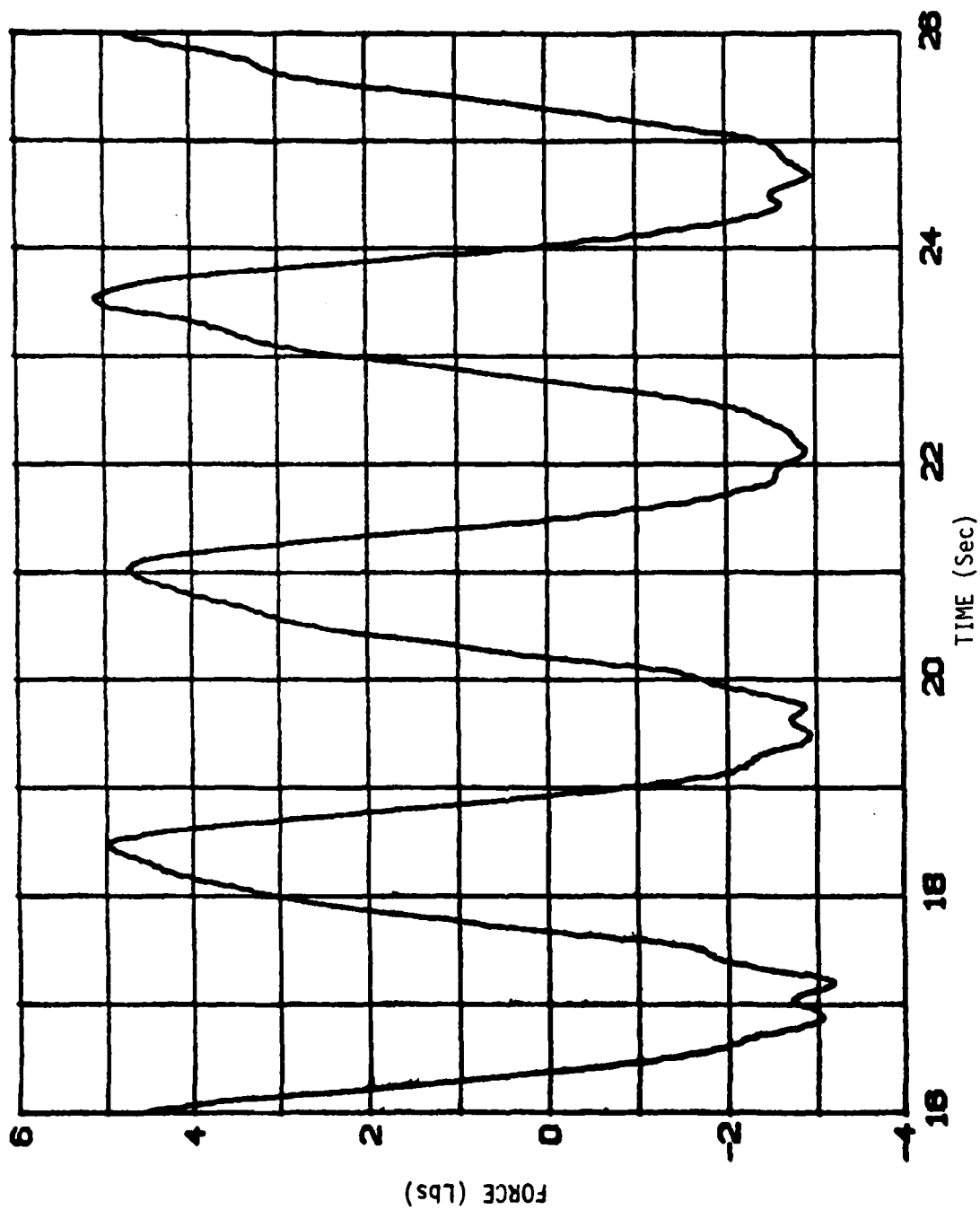
FIGURE B-2   X-AXIS FORCE COMPONENT ON LEG 'A'
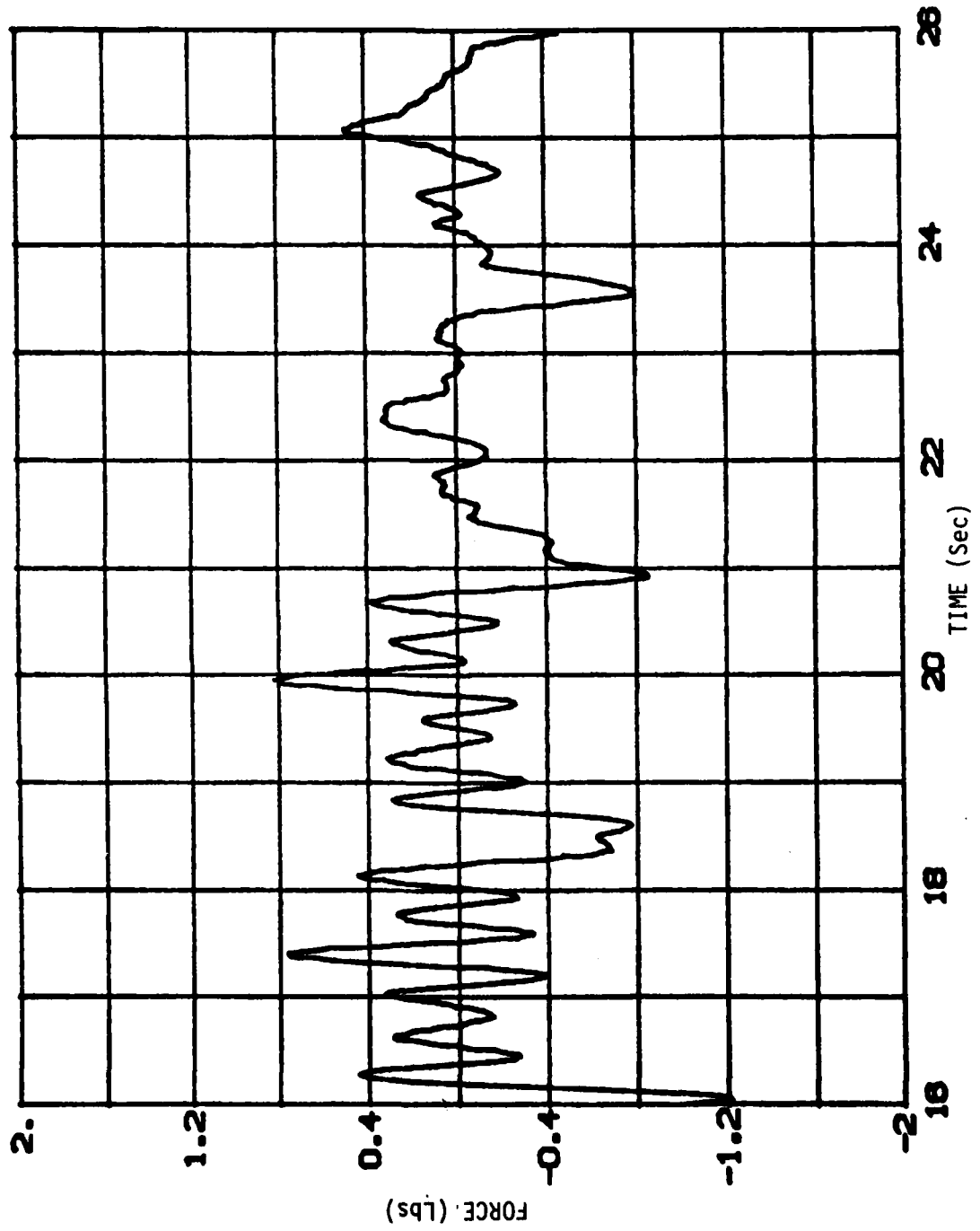STRUCTURE ORIENTATION - ZERO DEGREES

FIGURE B-3 Y-AXIS FORCE COMPONENT ON LEG 'A'
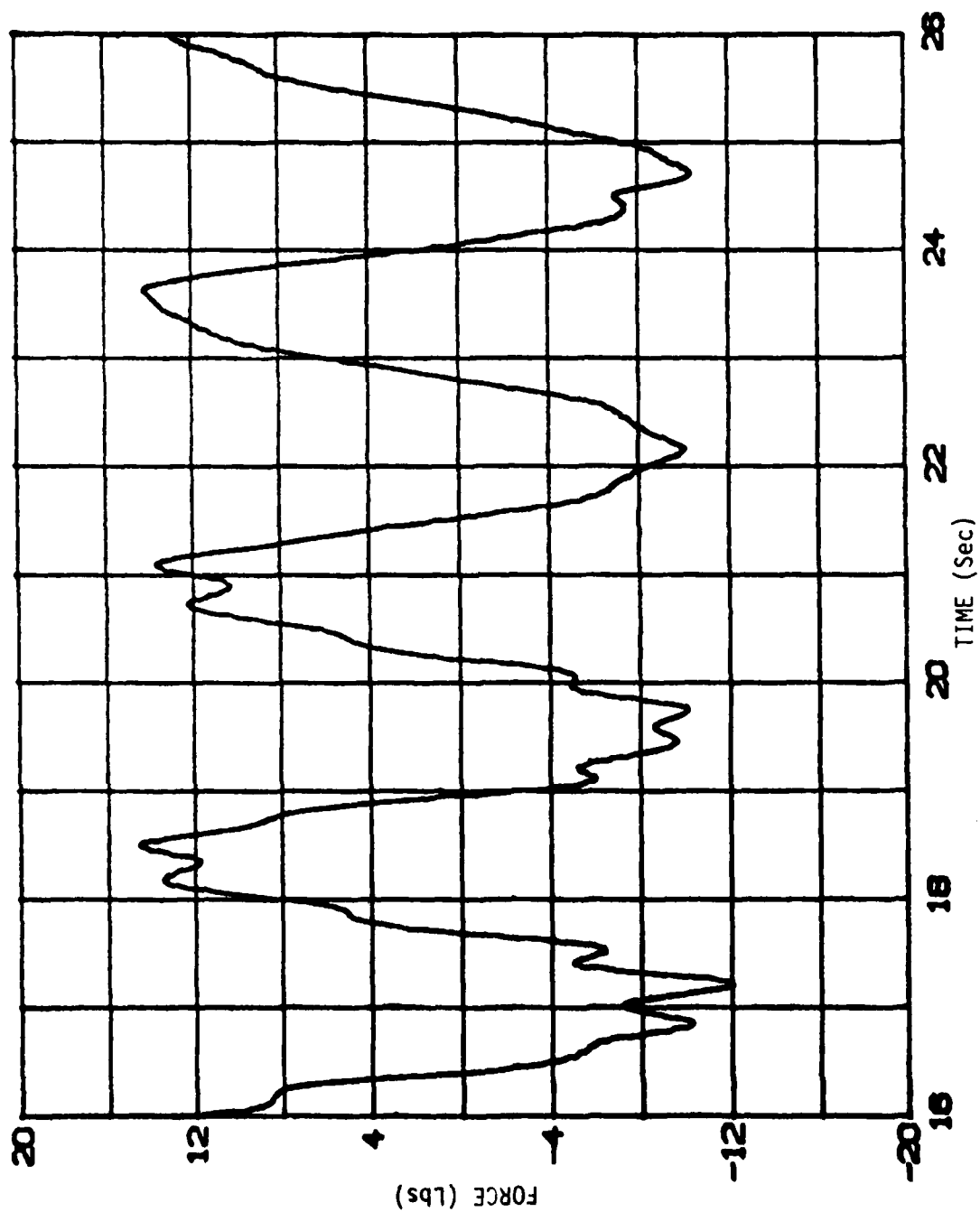STRUCTURE ORIENTATION - ZERO DEGREES

FIGURE B-4 Z-AXIS FORCE COMPONENT ON LEG 'A'
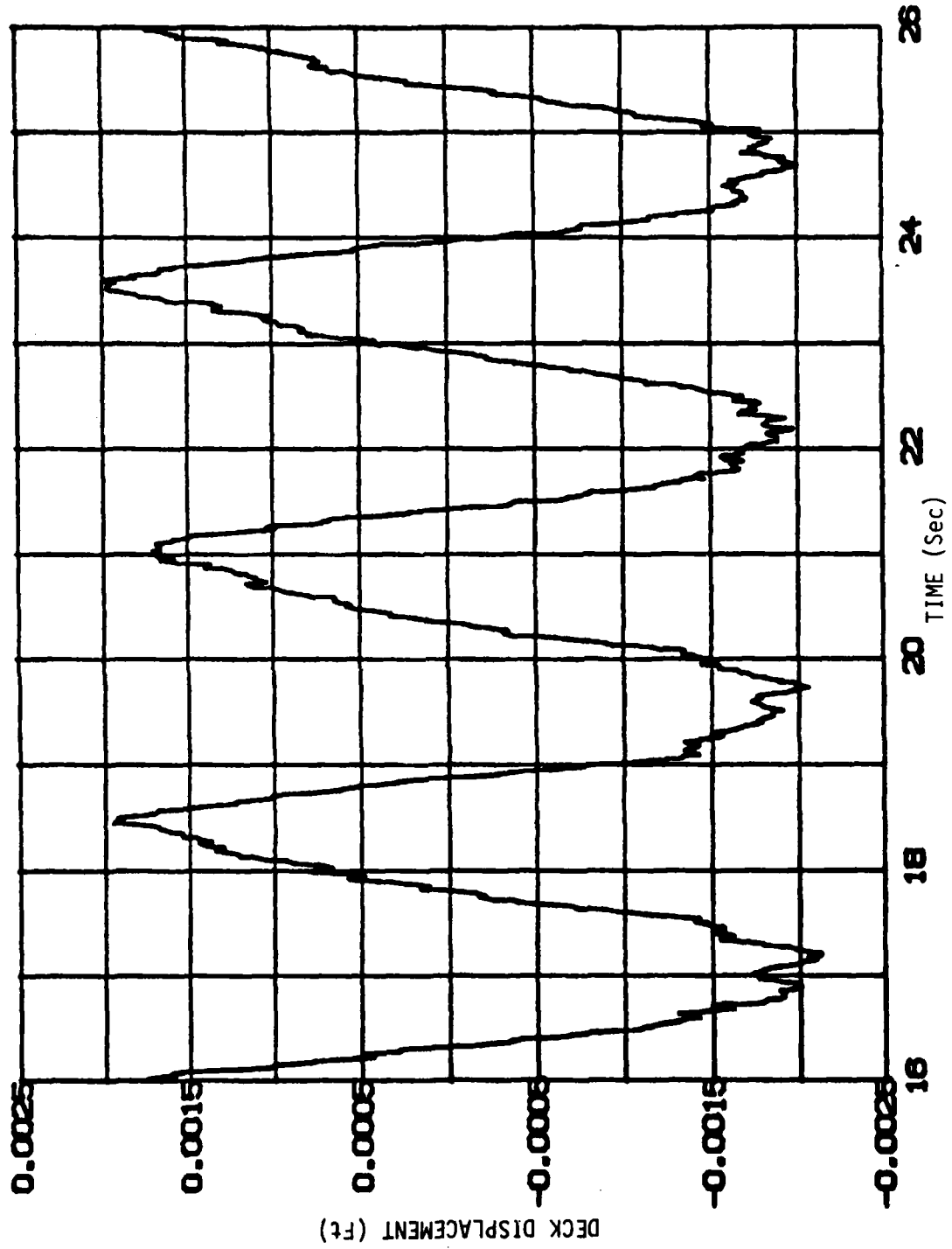STRUCTURE ORIENTATION - ZERO DEGREES

FIGURE B-5 X-AXIS DECK DEFLECTION
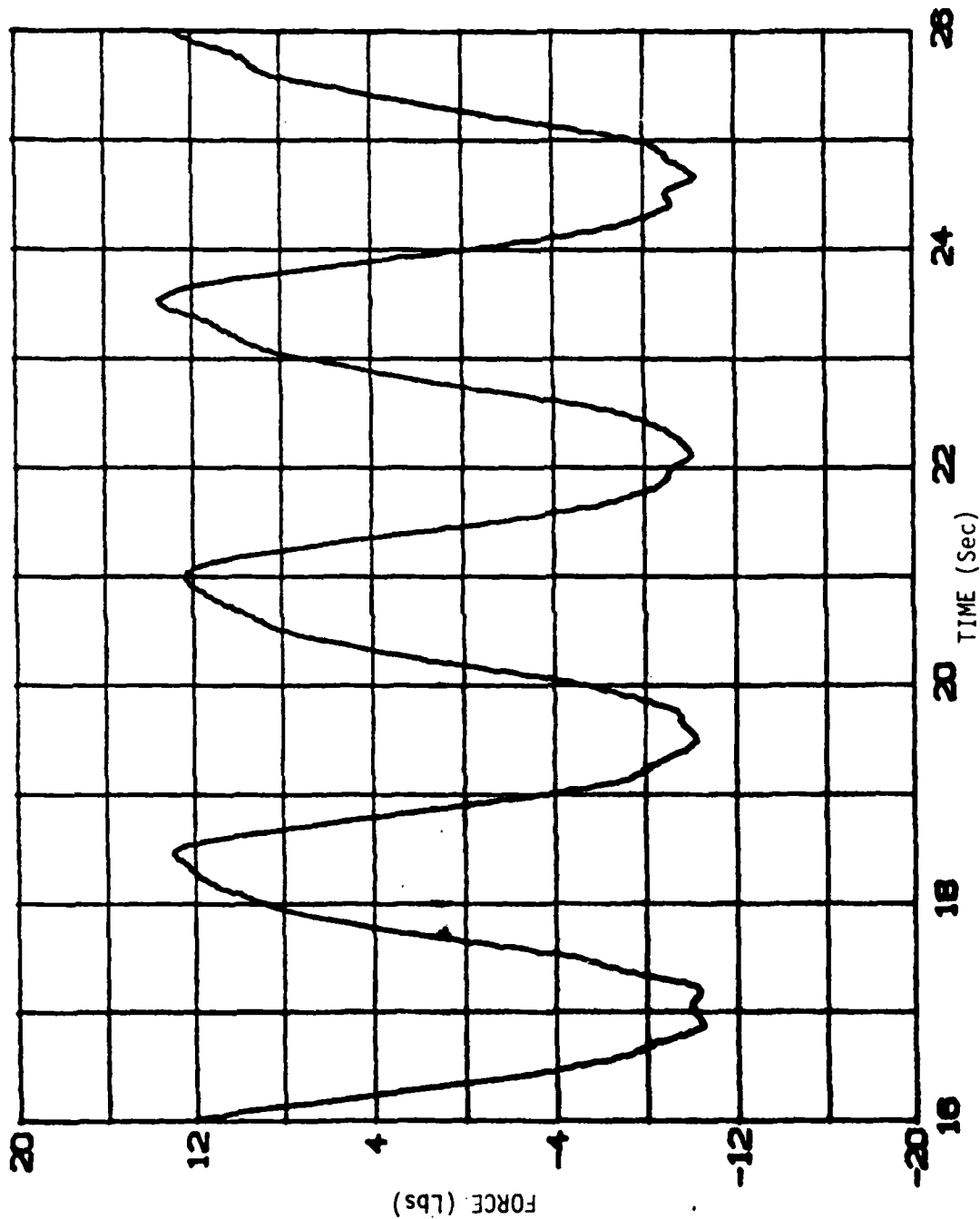STRUCTURE ORIENTATION - ZERO DEGREES

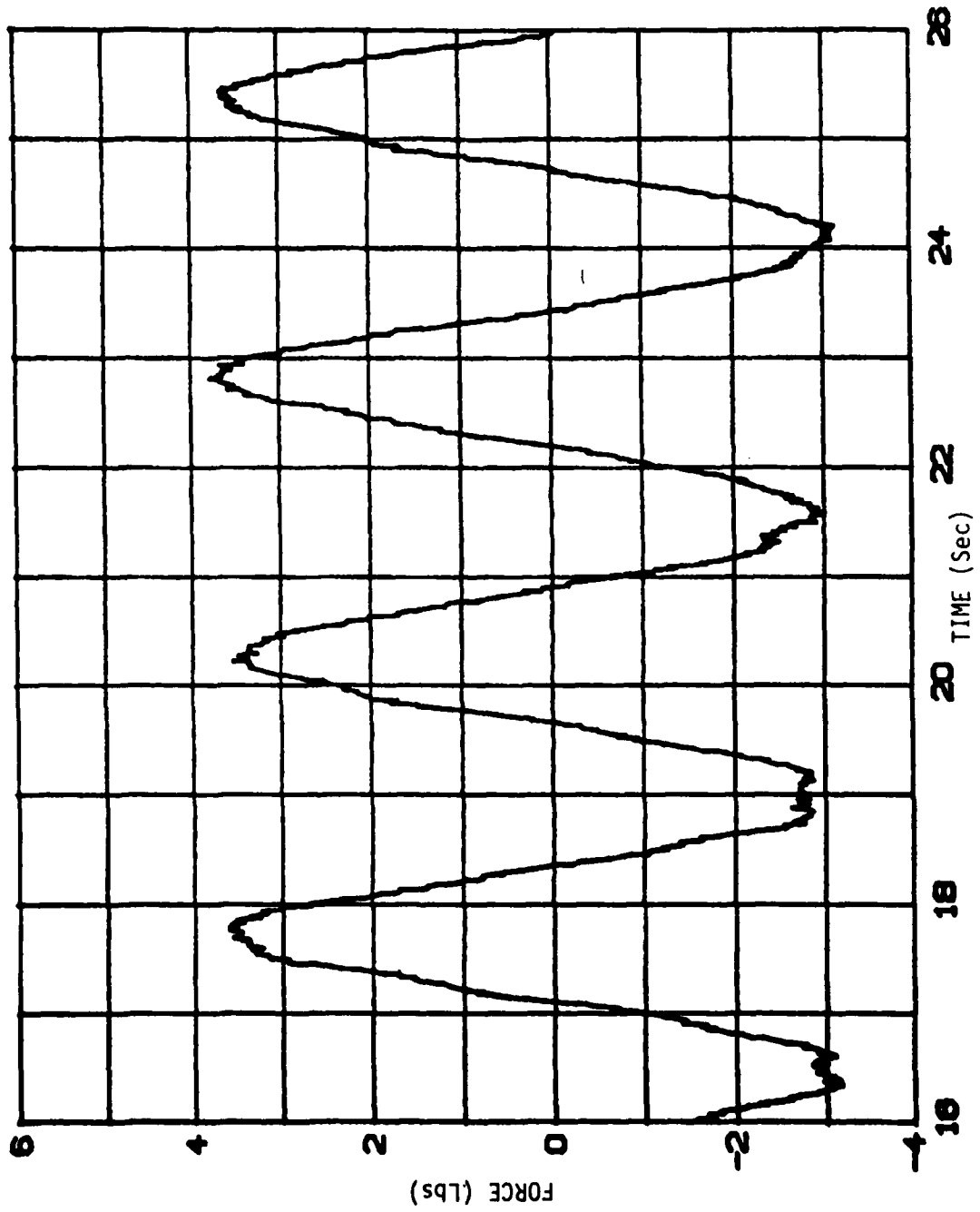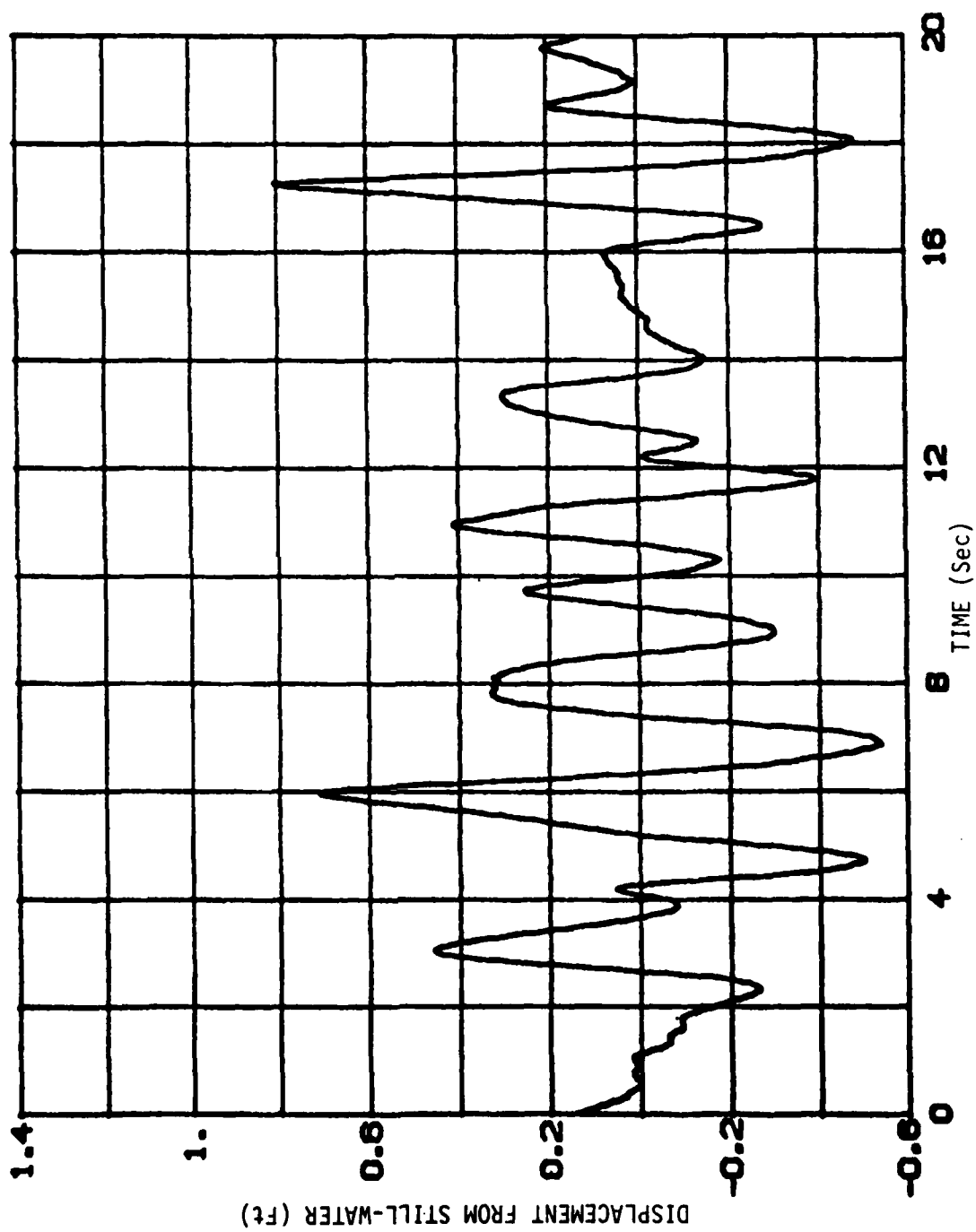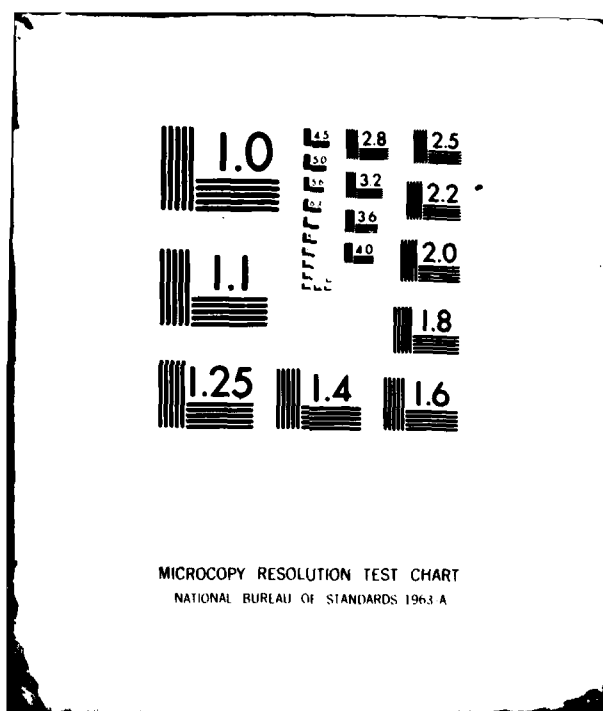FIGURE B-6 TOTAL BASE SHEAR FORCE
STRUCTURE ORIENTATION - ZERO DEGREES

FIGURE B-7   TOTAL LIFT FORCE
STRUCTURE ORIENTATION - ZERO DEGREES

FIGURE B-8   TOTAL OVERTURNING MOMENT
STRUCTURE ORIENTATION - ZERO DEGREES

FIGURE B-9 WAVE H_s = 1.01 Ft F_m = 0.4 Hz
STRUCTURE ORIENTATION - ZERO DEGREES
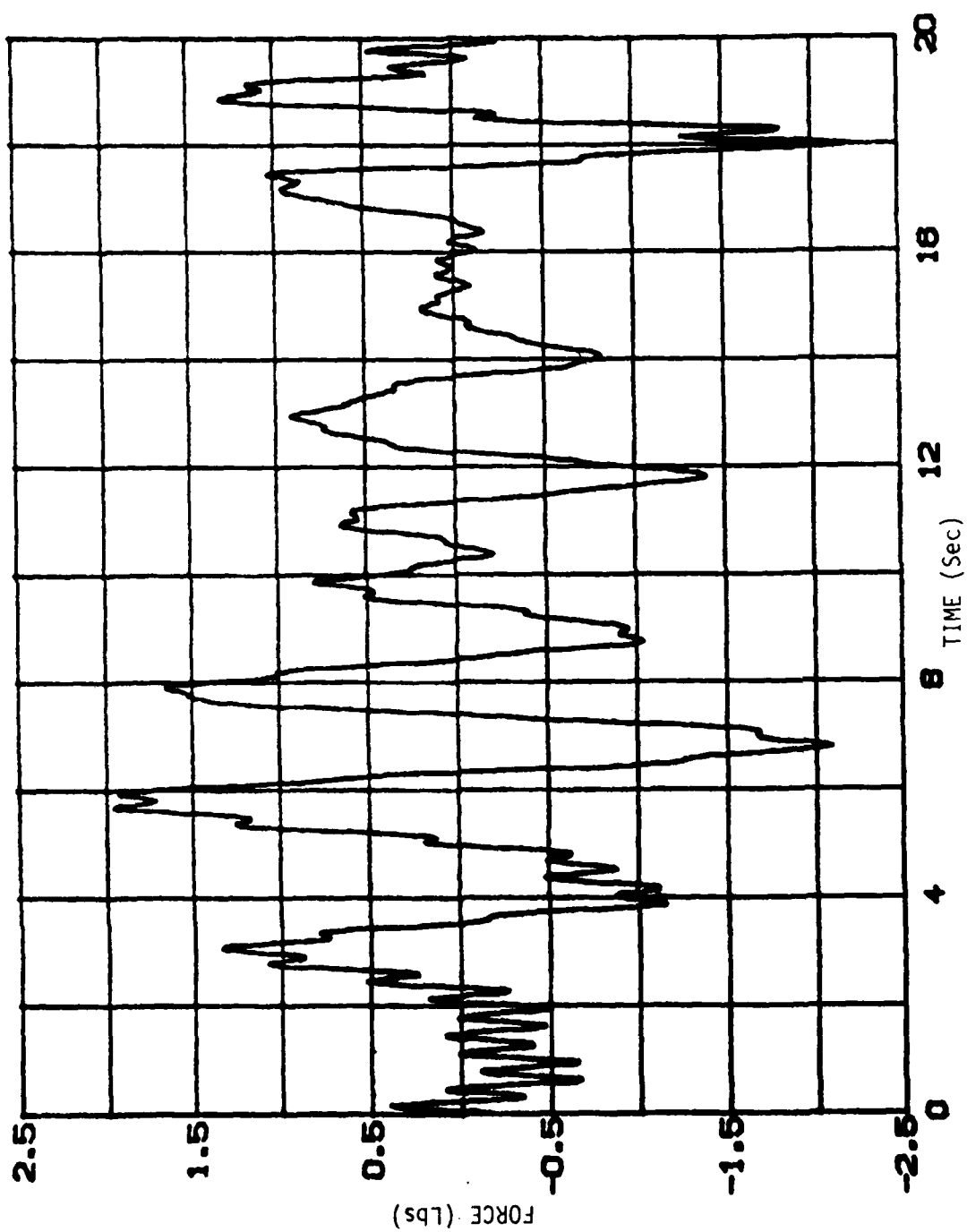
FIGURE B-10   X-AXIS FORCE COMPONENT ON LEG 'A'
STRUCTURE ORIENTATION - ZERO DEGREES

MICROCOPY RESOLUTION TEST CHART

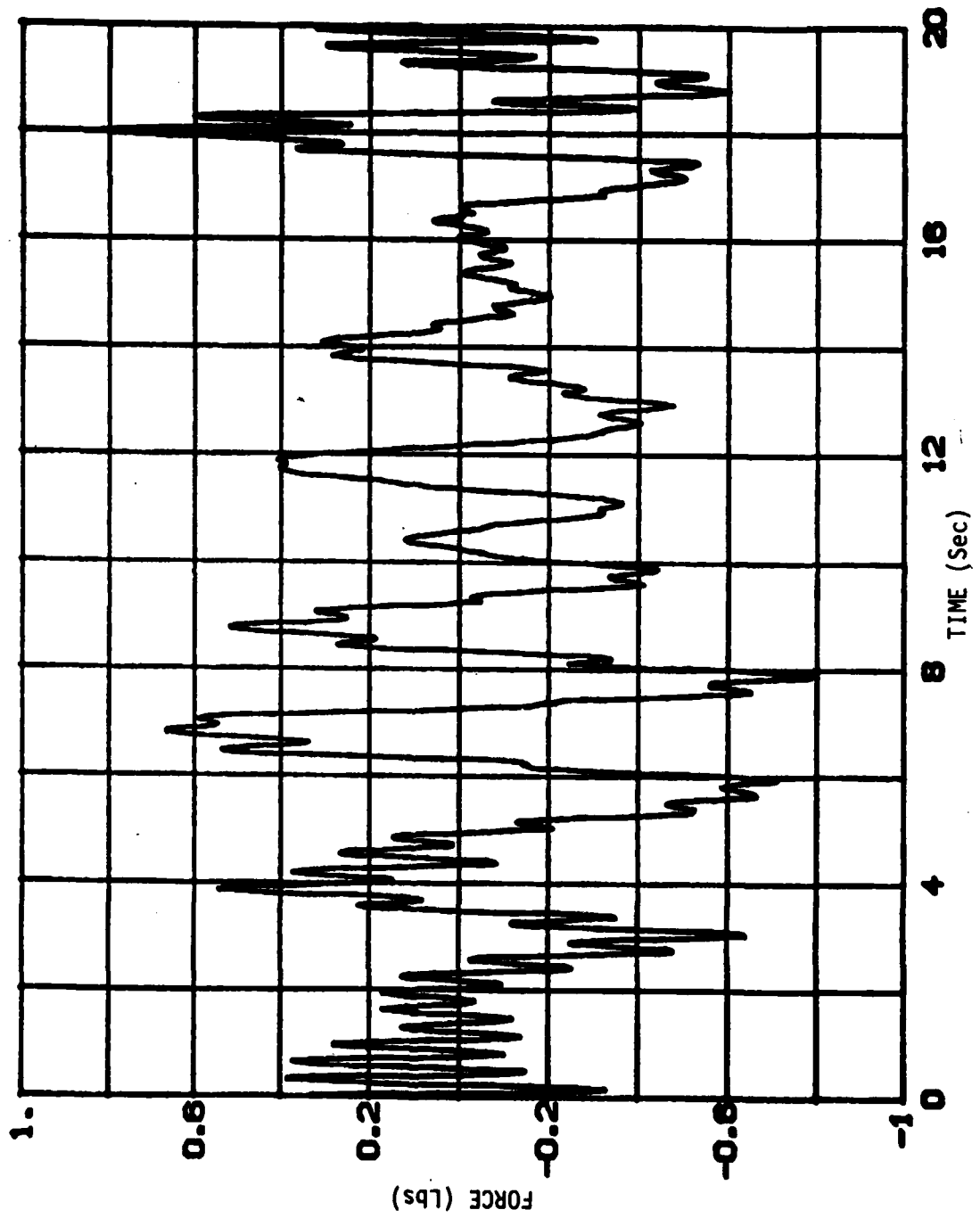NATIONAL BUREAU OF STANDARDS 1963 A

FIGURE B-11 Y-AXIS FORCE COMPONENT ON LEG 'A'
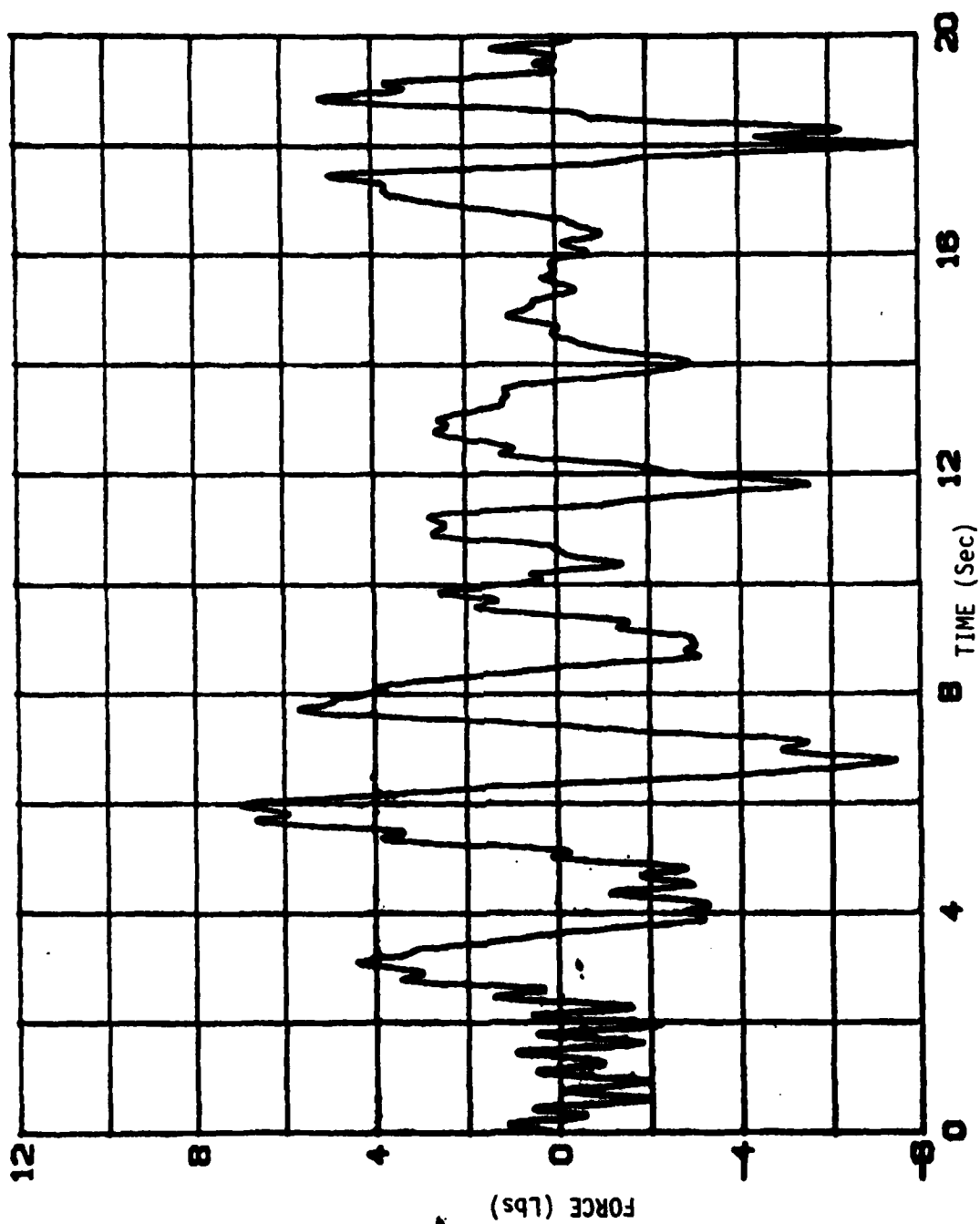STRUCTURE ORIENTATION - ZERO DEGREES

94

FIGURE B-12 Z-AXIS FORCE COMPONENT ON LEG 'A'
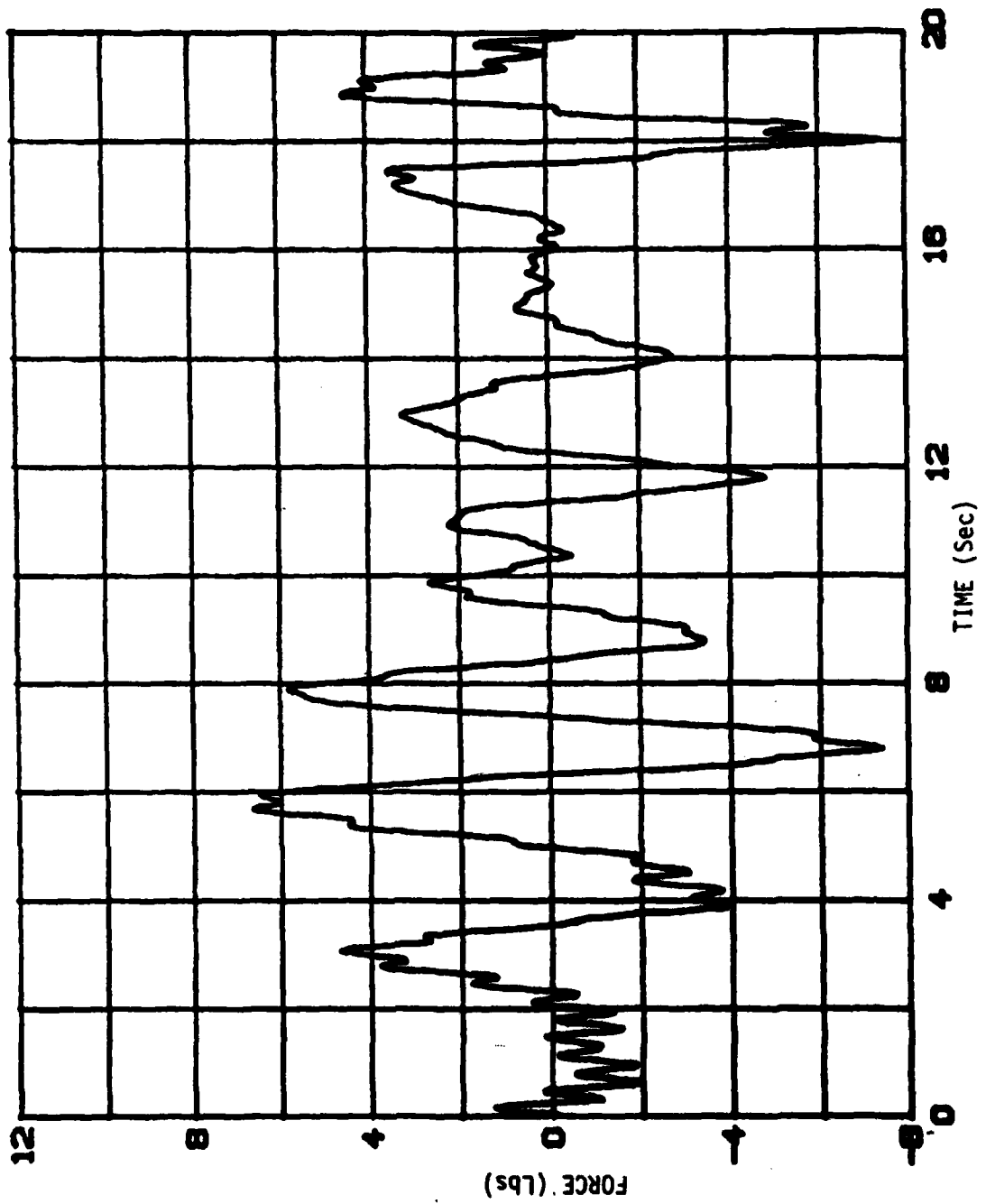STRUCTURE ORIENTATION - ZERO DEGREES

FIGURE B-13 TOTAL BASE SHEAR FORCE
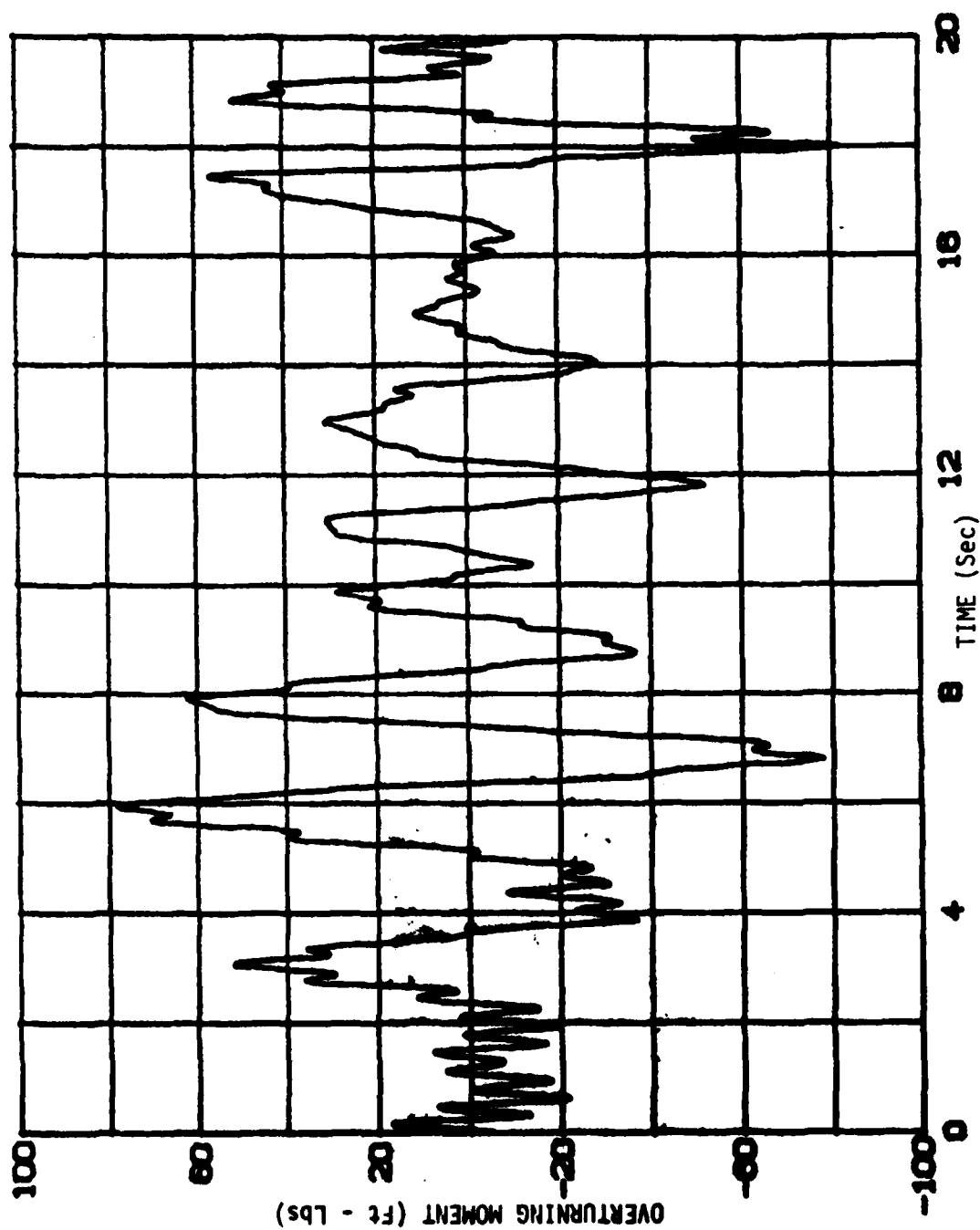STRUCTURE ORIENTATION - ZERO DEGREES

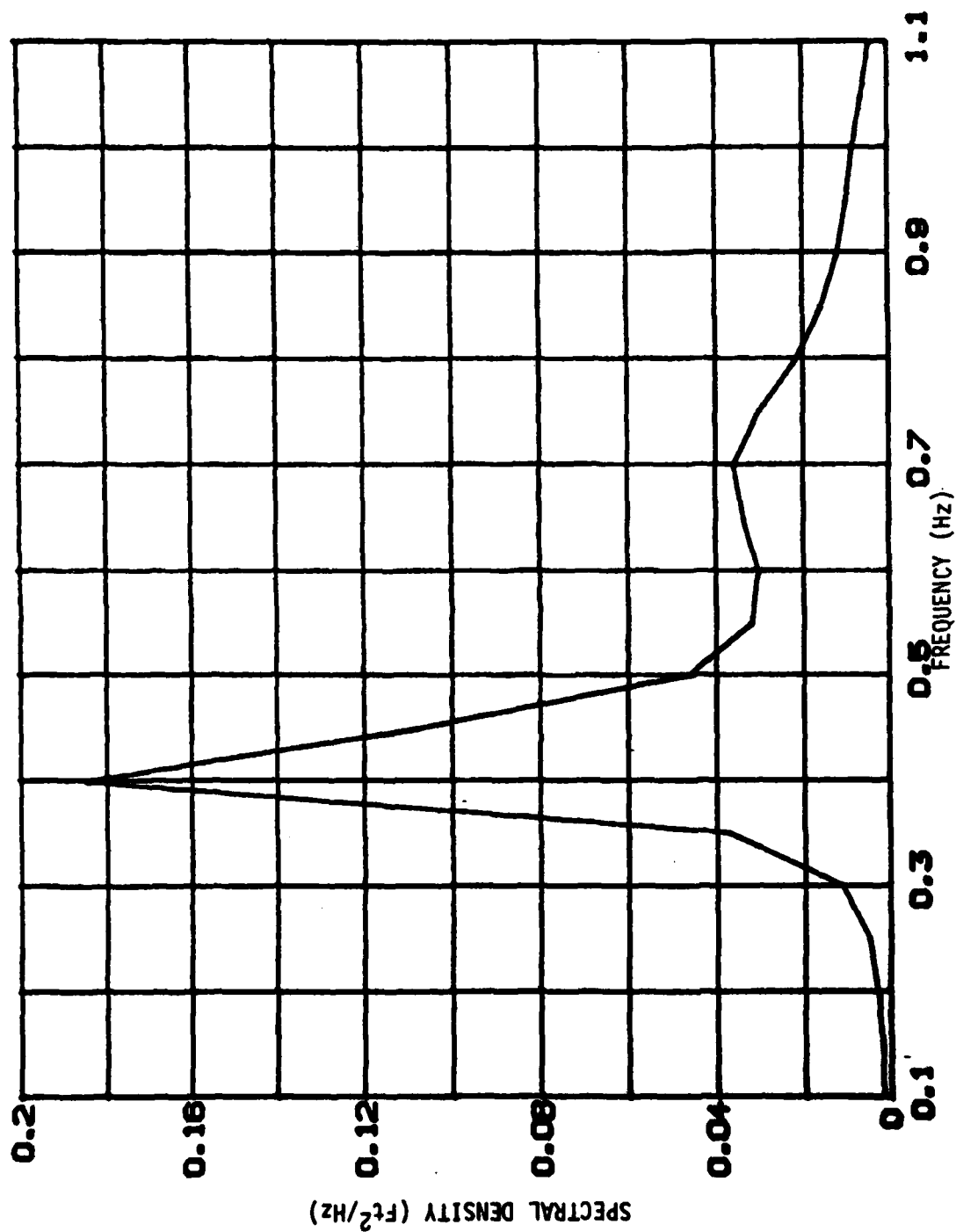FIGURE B-14 TOTAL OVERTURNING MOMENT
STRUCTURE ORIENTATION - ZERO DEGREES

FIGURE B-15 WAVE SPECTRAL DENSITY $H_s = 1.01$ Ft $F_m = 0.4$ Hz
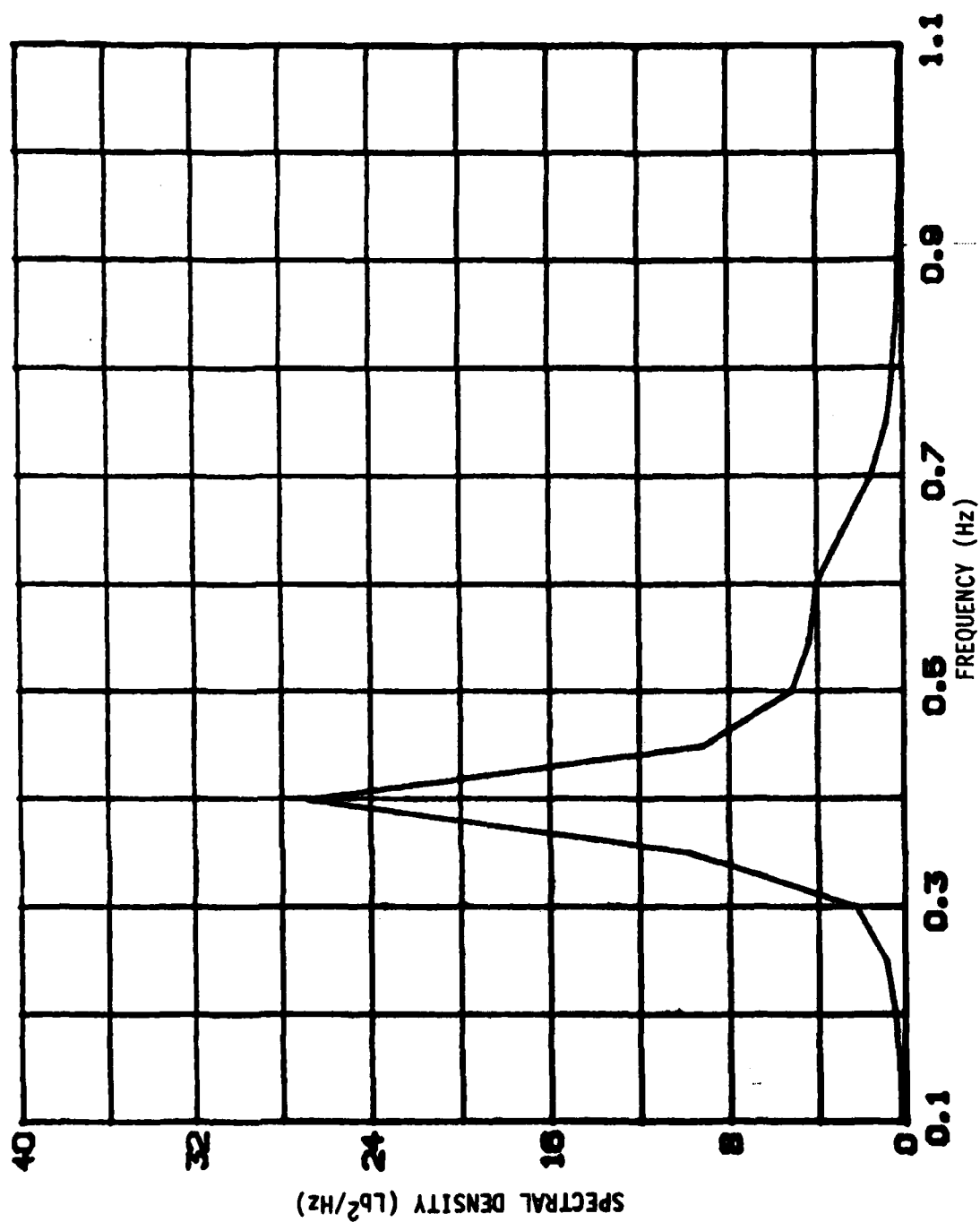STRUCTURE ORIENTATION - ZERO DEGREES

FIGURE B-16 TOTAL BASE SHEAR SPECTRAL DENSITY
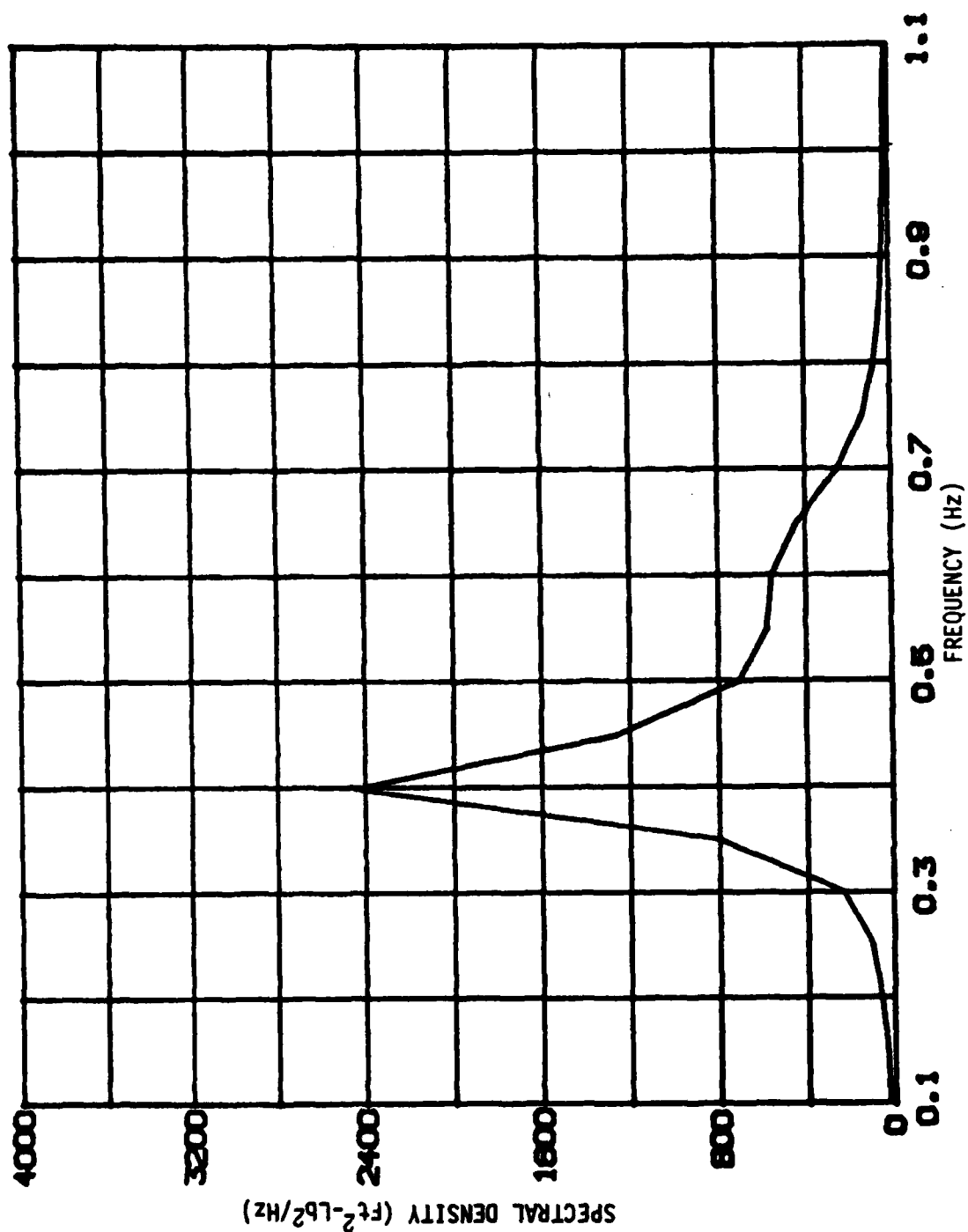STRUCTURE ORIENTATION - ZERO DEGREES

FIGURE B-17 TOTAL OVERTURNING MOMENT SPECTRAL DENSITY
STRUCTURE ORIENTATION - ZERO DEGREES

APPENDIX C
EXPERIMENTAL ERROR ANALYSIS

EXPERIMENTAL ERROR ANALYSIS

The purpose of this analysis is to identify and attempt to quantify those areas which effect the accuracy of the experimental results in this report.

Four areas can be identified which could contribute to experimental error:

- Model construction;

- Physical parameters;

- Measuring equipment/calibration;

- Data repeatability.

Model Construction

The construction accuracy of the 18 foot test structure was excellent. Dimensions were specified in the design within ± 1/64 inch with the desired construction accuracy at ± 1/4 inch. Measurements taken of the test structure after completion indicated all but 3 measurements were within specified limits. The 3 values outside this range were within ± 3/8 inch. These values were taken into consideration for the computer math models.

Physical Parameters

As discussed in the text of the report, the still-water level varied 3.60 inches. This was determined to vary the theoretical calculations

as much as 6 percent for a 0.3 Hz wave and as such was included as an input parameter for all theoretical calculations.

Tank temperature varied 7.8 degrees Fahrenheit, which had a negligible effect on water density and as such was not considered in theoretical calculations.

The effect of tank seiche on experimental accuracy was checked by running a 0.5 Hz wave of 0.79 feet for 2 minutes in the tank. The tank was allowed to settle for 15 minutes and a data acquisition was taken for all channels which indicated a natural tank period of approximately 32 seconds with a residual H_{rms} of 0.17 inches. The force blocks for all 3 axes indicated force levels well within the noise level of the signals. Hence, the effects of tank seiche on experimental values given in this report were considered negligible.

Measuring Equipment/Calibration

The electronic equipment used in this project was based on a voltage range of ±10 volts. All measuring equipment was calibrated before testing and signals were checked for mechanical zero on a daily basis. A check on the wave probe calibration was also done on a daily basis.

Although there were 2 types of measurements on the structure, deck deflection and forces, electronically they were similar. The following is a brief description of each piece of equipment in the signal path. Specific values not normally associated with the general equipment are given for the particular application in this study.

- Hydronautics Modular Force Gauges

These gauges utilize variable reluctance displacement transducers to accurately measure an applied load. The gauges convert the relative displacement of the parallel faces of the cube to generate an output voltage that is a linear function of the applied load. They are essentially insensitive to cross-axis loading. The gauges have a linearity of ± 0.25 percent of design load (250 pounds) and a corresponding hysterisis of 0.05 percent of the design deflection (.05 inches). The actual resolution of the gauge was 0.3 percent of the load.

- Wesmar LM4000 High Frequency Sonic Transducers

This system can be used for in-air range measurements from 2 to 7.5 inches with a resolution better than 0.5 percent of measured range. The linearity is better than 0.5% of the full scale measurement. The response time for the present study was 79.5 Hz with a half power beam width of 3 degrees.

- Ithaco 4120 Series Dual Low-pass Filters

These are precision active filters with phase and amplitude tracking between filters with the same setting within ± 4 degrees and ± 0.2 dB respectively. For this project, the filters can be considered to have had infinite resolution and essentially zero nonlinearity in the pass band.

- Hydronautics Multi-T Signal Conditioner Unit (SCU)

These are multi-transducer conditioners which incorporate the means to balance, establish polarity, excitation, calibration, and

to amplify signals from various transducers.

When used in the reluctance mode, the carrier frequency is 1000 Hz at 5.5 VRMS with an output linearity of ± 0.2 percent of full scale voltage.

- Preston 32 Channel A/D Converter

For the present study the A/D Converter had a 14 bit magnitude resolution capability which translated to an accuracy of 0.01 percent at ± (1/2 LSB) for 10 volts.

The overall result indicated that the measuring equipment could resolve the measurements within the accuracy of the calibration devices.

Force gauges were calibrated using precision weights accurate to within ± 0.5 percent. One pound increments were used up to ± 5 pounds and the calibration was extended to ± 20 pounds using 5 pound weights. Maximum individual force values were ± 10 pounds on x-axis gauges, ± 3 pounds on y-axis gauges, and ± 30 pounds on z-axis gauges. The sonic transducers were calibrated using 0.25 inch aluminum plates with an expected accuracy of ± 1.0 percent. The sonic calibrations were checked on a daily basis. The wave probe was also checked on a daily basis with typical accuracy being within 1.0 percent for a 12 inch span.

Data Repeatability

The data was checked for repeatability over the entire 60 second acquisition, with a representative 10 second sample being placed on magnetic tape. In addition, identical runs at 0.3 Hz with a structure

orientation of 0 degrees indicated a 2.7 percent difference in total

base shear force, 3.1 percent in lift force, and 2.6 percent in total

overturning moment.

APPENDIX D

COMPUTER PROGRAMS

COMPUTER PROGRAMS

This project resulted in the development of 35 computer programs, 31 by the author to handle all engineering computations and 4 by Mr. Gene Morgan and Mr. Lon Ward of the Applications Group, Academic Computing Center, to handle the transfer and digital manipulation of experimental data. In addition, 7 programs were adapted by Dr. John S. Kalme, Mathematics Department, from his earlier work on multi-channel time series data analysis for use in this study. Spectral calculations were done by fitting autoregressive schemes to time series data using the technique of a Fast Fourier Transform (FFT).